



SOME ELEMENTAL DISTRIBUTIONS  
BETWEEN COEXISTING  
FELDSPARS IN METAMORPHIC ROCKS.

by

D. Virgo, B.Sc.(Hons.)  
Department of Geology,  
University of Adelaide.  
1966.

Thesis submitted for Ph.D. degree

TABLE OF CONTENTS.

SUMMARY

ACKNOWLEDGMENTS

CHAPTER I. INTRODUCTION

- A. Background 1.
- B. Aims of the present investigation 4.
- C. Previous work 5.

CHAPTER II. DISTRIBUTION COEFFICIENTS

- A. Theoretical considerations 12.
- B. Distribution diagrams 14.

CHAPTER III. GEOLOGICAL SETTING: SELECTION AND

LOCATION OF SPECIMENS: AND MINERAL SEPARATION

- A. Introduction 16.
- B. Granulite-almandine-amphibolite facies 16.
- C. Local areas near Adelaide 21.
- D. Sample selection and suitability of specimens 23.
- E. Sampling and mineral selection 24.

CHAPTER IV. ANALYTICAL TECHNIQUES

- A. Wet chemical methods 26.
- B. X-ray fluorescent analysis 29.

CHAPTER V. DISTRIBUTION OF SODIUM

- A. Introduction 52.
- B. Relationship between sodium partition coefficients and metamorphic grade 52.

250804

C.	Experimental determination of cation exchange between coexisting feldspars.	59.
D.	The effect of environmental factors on the sodium distribution coefficients	61.
E.	Summary	69.
<u>CHAPTER VI. DISTRIBUTION OF BARIUM, RUBIDIUM AND CALCIUM</u>		
A.	Introduction	70.
B.	Relationship between the elemental partition coefficients and metamorphic grade	70.
C.	Barium partitioning	73.
D.	Rubidium partitioning	75.
E.	Calcium partitioning	76.
F.	Summary	77.
<u>CHAPTER VII. DISTRIBUTION OF STRONTIUM</u>		
A.	Relationship between the strontium distribution and metamorphic grade	78.
B.	Factors responsible for the observed systematic changes in $Kd_{SrF}$	84.
C.	Discussion	88.
D.	Strontium partitioning in terms of the feldspar structures and atomic properties	96.
E.	Summary	99.
<u>BIBLIOGRAPHY</u>		101.

APPENDIX I

A 1.

List of mineralogical compositions of all rock samples from which the coexisting feldspars used in this investigation have been extracted.

APPENDIX II

A 4.

Comparison of Ca, Sr, and Ba results from X-ray spectrographic, wet chemical and optical spectrographic techniques.

APPENDIX III

A 8.

Basic X-ray spectrographic equipment.

APPENDIX IV

A 9.

Instrumental conditions for analyses of feldspars by X-ray spectrography.

APPENDIX V

A 10.

Measurement of mass absorption coefficients using the Compton scattering technique

APPENDIX VI

A 12.

Coexisting feldspar compositions in terms of elemental concentrations (weight percent) and theoretical components (weight and molecular percents).

APPENDIX VII

A 26.

Mass-absorption coefficient measurements of K-feldspars and Plagioclases.



APPENDIX VIII

A 28.

Coexisting feldspar compositions recalculated from data given in Appendix VI in terms of Or and Ab end-members for the K-feldspar and Ab and An end-members for the plagioclases.

LIST OF TABLES

		After page
Table 1	Albite component in coexisting feldspars of high grade metamorphites derived from illitic clays, with deduced distribution coefficients and corresponding temperature ranges (Winkler, 1961).	6
Table 2	Coexisting feldspar compositions and deduced $Kd_{Ab}$ values as determined experimentally by Yoder, Stewart and Smith (1957).	8
Table 3	Accuracy of alkali analyses using flame photometer.	27
Table 4	Precision of alkali analyses in unknown feldspar samples using flame photometer.	27
Table 5	Estimates of relative deviation for $K_2O$ and $Na_2O$ at the concentration levels found in the writer's feldspar samples.	28
Table 6	I and $I_0$ intensity measurements in mass absorption determinations for K-feldspars and Plagioclases.	40
Table 7	Mass absorption coefficient measurements ( $A_2$ ) at different $I_0$ values ( $\lambda = SrK\alpha$ ).	41

Table 8	Replicate determinations of the mass absorption coefficient ( $A_2$ ) using different weight's of powder and different slides ( $\lambda = \text{SrK}\alpha$ ).	41
Table 9	Measurement of mass absorption coefficients at two wavelengths: $\lambda = \text{SrK}\alpha$ and $\lambda = \text{RbK}\alpha$ .	41
Table 10	Counting strategy for Rb and Sr, Ba and Ca intensity measurements for both K-feldspars and Plagioclases.	41
Table 11	Recommended values of Rb and Sr for standards used to analyse G1 and W1, and the resultant values on G1 and W1 using the writer's technique discussed in the text.	42
Table 12	Data used to construct the calibration curve for plagioclase feldspars.	48
Table 13	Results of method of additions, applied to Feldspars 17263 and 16949.	50
Table 14	Data used to construct the calibration curve for K-feldspars.	50
Table 15	Results of some cation exchange experiments designed to test the Barth geothermometer.	59
Table 16	Chemical and modal analyses of samples of granulites and gneisses from Ceylon.	64

Table 17	Correlation of rock and feldspar compositions from the Ceylon area.	65
Table 18	Chemical and modal analyses of samples of least altered gneiss from the Adirondack lowlands, New York.	65
Table 19	Correlation of rock and feldspar compositions from the Adirondack lowlands area.	65
Table 20	K/Rb and Ba/Rb ratios of K-feldspars from the Broken Hill area.	82
Tables 21 - 29 are in Appendix VIII p. A 28 - A 36.		

## SUMMARY

Forty seven pairs of coexisting feldspars have been extracted from metamorphic rocks with the aim of testing major and minor element distributions according to the Nernst distribution law, determining the factors affecting the partitioning and to evaluate the usefulness of these distribution coefficients as indicators of relative metamorphic grade. To carry out these aims rocks from six different areas have been studied in detail, most areas including at least two zones of metamorphism: in this way a range of metamorphic grade viz. middle almandine-amphibolite facies to various grades of granulite facies has been investigated. Major elements analysed include Na, K and Ca, and minor elements include Ba, Sr, Rb and Ca (in the K-feldspars)

The alkali elements have been analysed using conventional flame-photometric techniques and the remaining elements by X-ray spectrographic methods.

Elemental partitioning is discussed in terms of the distribution of the feldspar components albite, Sr-feldspar, etc. and by means of distribution diagrams (Roozeboom diagrams).

The distribution of albite between K-feldspar and plagioclase generally shows no obvious, simple relationship either with changes in metamorphic grade or within a single area of isofacial metamorphism (equal pressure temperature

conditions). The distribution coefficient however, appears to vary in a regular way with both feldspar compositions in isofacial rocks and also in non isofacial rocks in a particular area. This relationship is correlated with variations in the bulk chemistry of the rocks. Such conclusions are supported by experimental work. Reasons are discussed as well as departures from the general trends.

Anorthite partitioning takes a form similar to albite distribution and it is suggested that principally bulk composition effects are important.

Barium and rubidium feldspar, both strongly preferred by the K-feldspar phase are also not regularly partitioned between the coexisting feldspars and there is no correlation with metamorphic grade. Some peculiarities of both feldspar structures, in particular the K-Ba and K-Rb relationships, are considered important in explaining the partitioning.

Strontium feldspar, almost equally preferred by both the K-feldspar and plagioclase, shows an equilibrium partitioning in isofacial rocks. The partitioning can be described by the Nernst distribution equation and is of the type:

$$\frac{\text{Mol percent Sr-feldspar in the K-feldspar}}{\text{Mol percent Sr-feldspar in the Plagioclase}} = \text{constant.}$$

Over the range of metamorphic grade examined, continuous, systematic and significant changes in strontium partitioning occur such that with increasing grade strontium is

preferentially taken into the K-feldspar lattice. It is suggested that the changes in strontium partitioning are solely temperature dependent and some data from experimental work support this. The observed partitioning is explained in terms of the temperature dependence of both feldspar structures and thermal expansion of the strontium ion.

This thesis contains no material which has been accepted for the award of any other degree or diploma in any University; nor, to the best of my belief, does the thesis contain any material previously published or written by another person, except where due reference is made in the text of the thesis.

D. Virgo.

Signed



### ACKNOWLEDGMENTS.

The framework of this project was initially suggested to the author by Dr. K. S. Heier, Department of Geophysics and Geochemistry, Australian National University.

The writer expresses his gratitude to Dr. K. Norrish, C.S.I.R.O. Soils Division, Adelaide, for advice and instruction in the field of X-ray spectrography and also Mr. A. B. Timms of the Australian Mineral Development Laboratories, Adelaide, for assistance in the field of optical spectrographic analyses.

The writer has had fruitful discussions on various aspects of this project with Mr. P. G. Slade, Dr. R. L. Oliver, Dr. J. B. Jones, and Mr. R. Offler of the Department of Geology, University of Adelaide and Dr. K. S. Heier of the Department of Geophysics and Geochemistry, Australian National University.

Drs. R. L. Oliver and J. L. Talbot have read and criticised the whole manuscript.

Rock samples have been kindly supplied to the author by Mr. R. Offler, and Drs. R. L. Oliver, K. J. Mills, A. J. White and R. A. Binns.

The author also wishes to acknowledge his wife, J. A. Virgo for typing of the thesis, drafting of many of the figures, bibliographic assistance and continual encouragement.

This work has been carried out during the tenure of an

Adelaide University Research Grant and also a Commonwealth  
Post-graduate Scholarship.

**INTRODUCTION.**



#### A. BACKGROUND.

Element distributions between coexisting rock forming silicates have been studied in experimental systems at liquidus and sub solidus temperatures: for example, Bowen and Schairer (1935) have determined olivine - clinopyroxene tie lines in the range 1100 - 1300°C at atmospheric pressure; Yoder, Stewart and Smith (1957) determined coexisting K-feldspar and plagioclase compositions in equilibrium with a liquid and a gas phase at temperatures 720 and 770°C and 5000 bars pressure and Orville (1962) located tie lines between K-feldspar - alkali chloride solutions in the range 350 - 700°C at 2000 bars pressure. Within the present writer's department Mr. P. Slade is working on coexisting K-feldspar and plagioclase compositions in equilibrium with a liquid phase in the range 520 - 850°C at 1000 bars pressure.

In natural environments the compositions of coexisting phases in igneous and metamorphic rocks have received much attention in the last decade and have resulted in valuable demonstrations of chemical equilibrium between mineral phases which has otherwise been inferred from textural equilibrium (Zen 1963). From theoretical considerations it is noted that:

- (a) minor element partitioning should be more sensitive to the attainment of equilibrium involving coexisting mineral phases.

- (b) elemental distribution coefficients are correlated with variations of the physical variables pressure and temperature.

Comparatively little work in metamorphic rock systems has been directed to both these theoretical implications. Research work of this nature should provide more reliable indicators of metamorphic grade than the more commonly used isograds based upon single minerals and polymorphic transitions (Atherton 1965).

Detailed investigations of trace element partitioning have so far been restricted mainly to isofacial metamorphic rocks and include the following: Howie (1955) examined coexisting K-feldspar - plagioclase, biotite - hornblende, hornblende - orthopyroxene, and ortho-clino pyroxenes with the object of finding trace element abundances in the minerals of each rock. Howie gave no interpretation of his results.

Nickel (1954) gave trace element data for Co, Ni, Cr, Zr, Sc and V in pairs of hornblende - biotite and biotite - chlorite. An interpretation of the data was made in terms of relative electronegativities of the major and minor elements.

Kretz (1959) examined coexisting biotite, hornblende and garnet phases for the trace elements Sc, Y, Ba and Cr. A disequilibrium relationship found for these elements is

somewhat puzzling in view of the orderly distribution found for the major elements Fe, Mg, Ca, Mn and Ti. It is reasonable however to suggest that the precision of the analytical methods is at fault.

Heier (1960) determined Ba, Rb, Sr, Cu, Pb and Li contents of coexisting feldspars in rocks of different metamorphic grades. Tentative conclusions from these data by Barth (1961) suggest a temperature dependence of Ba and Sr partitioning, (see further discussion p. 9).

Turekian and Phinney (1962) determined Ni, Co, Cr, Cu, Ba and Sr in coexisting biotite - garnet pairs. Their main conclusions were that rarely in samples of hand specimen size are chemical equilibrium distributions observed in metamorphic rocks and also the laws governing the inclusion of a trace element in different crystal lattices are more than those based on any single parameter such as ionic radius.

Moxham (1965) studied trace element partitioning between coexisting garnet and hornblende pairs and found that some elements (viz. Mn, V, Ni, Co, Cr, Sc and Ba) showed definite equilibrium relationships whilst for others (viz. Ti, Cu, Y and Sr) only a tendency towards regular distributions were shown. Some elements (viz. Mo, Zr, Ga, B and Sn) gave irregular partitioning patterns. A correlation between the value of the distribution coefficients of

minor elements with atomic properties was not apparent.

Albee (1965,b) analysed coexisting biotite - chlorite, chlorite - chloritoid, garnet - biotite, garnet - chlorite, and garnet - chloritoid mineral pairs for some trace elements. Albee suggests that Co, Ni, Cr and Zn partitioning approaches equilibrium, V, Ga and Sc indicate a lesser approach and Ba and Cu show a disequilibrium relationship. Tentatively it was also suggested that more precise analyses of Co and Cr and possibly Ni, V and Sc might provide useful parameters of temperature.

In view of the non finality of the investigations discussed above it is thought that a study of minor element distributions between coexisting mineral phases might be rewarding in terms of the relationship between minor element distribution coefficients and metamorphic grade provided analytical techniques of adequate precision are employed.

#### B. AIMS OF THE PRESENT INVESTIGATION.

To test the usefulness of distribution coefficients in metamorphic studies it is necessary that the mineral pairs occur over a wide range of metamorphic grade: coexisting potassium and plagioclase feldspars provide an excellent example. The present writer has therefore studied elemental distributions between coexisting feldspars from metamorphic rocks:

- (a) to determine which elements are regularly and which

are randomly distributed.

- (b) to outline the factors - chemical, structural and physical - that account for the observed partitioning.
- (c) to evaluate the usefulness of the distribution coefficients as indicators of metamorphic grade.

To accomplish these aims coexisting feldspars from rocks in different metamorphic zones were studied. Initially it was intended that rocks from a complete range of metamorphism viz. upper greenschist--almandine amphibolite--granulite facies would be studied. Despite several attempts it was not possible to obtain material representative of the upper greenschist and the lower part of the almandine amphibolite facies. The material examined in this study can be grouped in the following way:

- (a) rocks from both the upper almandine - amphibolite and granulite facies from Ceylon; Musgrave Range area, South Australia; and the Broken Hill area, New South Wales.
- (b) rocks from the sillimanite-almandine-muscovite and sillimanite-almandine orthoclase sub facies of the almandine amphibolite facies from areas near Adelaide, South Australia.

#### C. PREVIOUS WORK.

Barth (1956) postulated that the distribution of albite in coexisting feldspars from metamorphic and igneous rocks



provides a useful rock geothermometer. Barth correlated  $Kd_{Ab}^*$  against an empirically determined temperature scale over the range 350 - 1000°C. This geothermometer has been criticized by many authors (Dietrich, 1961, summarizes the major criticisms) and has resulted in only limited success in its application to natural environments (see discussion of data from Heier 1960, and Engel and Engel 1960, in Chapter V).

Barth's hypothesis has not been supported by experimental work. A brief discussion of some results from experimental work relating to the Barth geothermometer is given:

- (a) Winkler (1961) using silicate bearing powders (prepared from illitic clays at temperatures above 600°C and at  $P_{H_2O}$  pressure of 2000 bars) at 2000 bars  $P_{H_2O}$  and in the temperature range 620 - 720°C determined coexisting feldspar compositions and  $Kd_{Ab}$  values (Table 1) for three different metamorphites which differ compositionally only in the  $Na_2O$  content. Winkler deduced from these data that in each of the metamorphites the  $Kd_{Ab}$  does not show any variation over the investigated temperature range and the different  $Kd_{Ab}$  values in the three metamorphites are related to different soda contents. It is obvious then that bulk composition

---

\* See Chapter II, p. 12

Table 1. Albite component in coexisting feldspars of high grade metamorphites, derived from illitic clays, with deduced distribution coefficients and corresponding temperature ranges. (Winkler, 1961).

Ab - component (mol %)		$K_{d_{Ab}}$	Temperature °C	Bulk Na <sub>2</sub> O weight %
K-feldspar	Plagioclase			
2.5	42	.06 ± .02	670, 675, 700	.43
8.5	68	.13 ± .02	650, 670, 700, 710, 720	1.36
19.0	75	.25 ± .02	620, 630, 650, 670	2.11

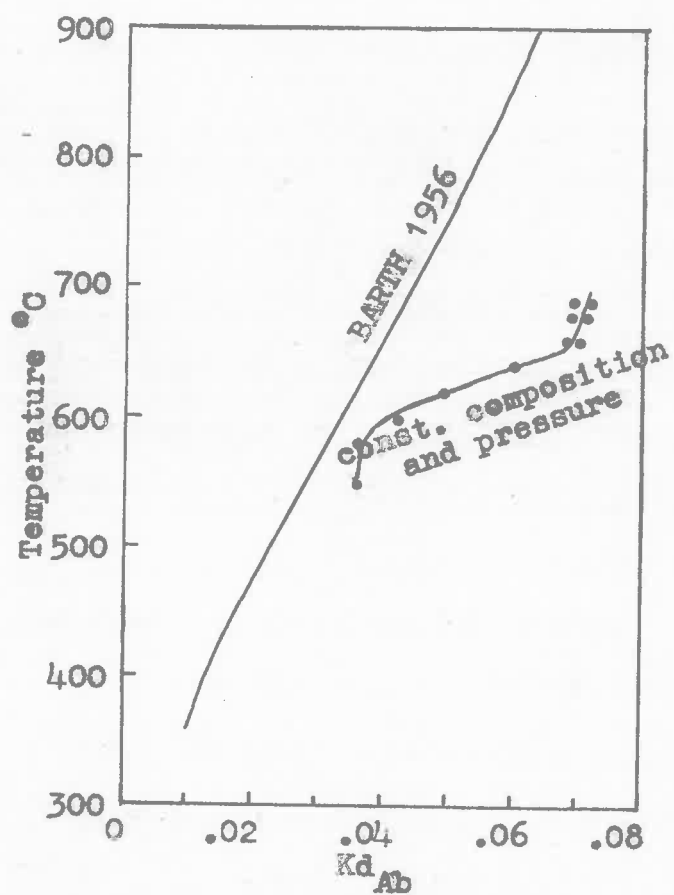
influences greatly the compositions of coexisting feldspars. Other data from Winkler (1961) shows that many of the major components in a rock may have some influence on the feldspar compositions. Winkler concluded that in view of the unknown complex inter-relationship of chemical variables which apparently govern sodium distribution between feldspars, feldspar compositions cannot give any indications of temperature of recrystallization.

- (b) Steuhl (1960) has determined the composition of coexisting feldspars in a paragneiss at  $P_{H_2O} = 2000$  bars and in the temperature range  $550 - 700^{\circ}C$ . The results of this work are compared graphically in Figure 1 with Barth's (1956) curve. It is evident that the variation of the albite distribution coefficient with temperature is obviously much more complicated than it would be if the Nernst distribution law\* is valid.
- (c) Orville (1962) reported the results of cation exchange reactions between a potassium feldspar phase and alkali - chloride solutions. The most important conclusions from this work are that only in the range  $Or_{96-85}$  for the K-feldspar composition are the tie lines constant for the K-feldspar - alkali-chloride system. By analogy a constant sodium distribution

---

\* See Chapter II, p. 12

FIGURE 1



Plot of  $Kd_{Ab}$  versus temperature of crystallization of the coexisting feldspars. Experimental data from Steuhl (1960) and their relationship to the curve proposed by Barth (1956).

coefficient in the K-feldspar - plagioclase system is suggested (Orville op. cit. p. 340). This contrasts markedly with the ideal compositional limits imposed by Barth (1956) for the K-feldspar phase viz.  $Or_{90-70}$ . In a series of experiments at different bulk compositions and at temperatures of 500, 600 and 700°C,  $Kd_{Ab}$  values certainly change with temperature in accordance with Barth's hypothesis but there is considerable overlap of  $Kd_{Ab}$  values at different temperatures.

- (d) Yoder, Stewart and Smith (1957) determined the compositions of coexisting K-feldspar and plagioclase in equilibrium with a liquid and a gas phase (Table 2) at  $P_{H_2O} = 5000$  bars and at 720 and 770°C respectively. It is apparent from Table 2 that although the distribution coefficient shows a temperature dependence it is reverse to that given by Barth's curve. Some explanation for this is evident from the experimentally determined Ab-Or and Ab-An systems (Yoder et al., op. cit. Figures 36 and 37). Yoder's experiments were carried out at physical conditions such that feldspar compositions fall on the solidus surface and are in equilibrium with liquid compositions on the liquidus surface. In these cases a decrease in temperature will result in an increase of the Ab content of both the K-feldspar and the plagioclase (hence the change

Table 2. Coexisting feldspar compositions and deduced  $Kd_{Ab}$  values as determined experimentally by Yoder, Stewart and Smith (1957).

Temperature °C	Feldspar component	K-feldspar	Plagioclase	$Kd_{Ab}$
770	Or	92.50	3.75	.138
	An	1.87	56.25	
	Ab	5.63	40.00	
720	Or	78.75	3.75	.264
	An	1.25	22.50	
	Ab	20.00	73.75	

in the feldspar compositions in Table 2). At sub solidus temperatures and at the same  $P_{H_2O}$  value, the feldspar compositions may change in accordance with Barth's hypothesis since the feldspar compositions will now move down the solvus dome with decreasing temperature. It follows therefore that at  $P_{H_2O} = 5000$  bars the relationship between  $Kd_{Ab}$  and temperature cannot be linear over the range  $350 - 1000^{\circ}C$  (Barth's temperature scale). It is likely that under most physical conditions of regional metamorphism, recrystallization of coexisting feldspars will take place under sub solidus conditions and thus the lower part of Barth's curve is applicable.

- (e) Some work has been commenced in the writer's laboratory by Mr. P. Slade concerned with testing the relationship between temperature and elemental distribution coefficients in coexisting feldspars. This work is discussed in Chapters V and VII.

The application of sodium distribution coefficients to isofacial rocks and to rocks from different metamorphic zones within comparatively small areas should provide an adequate test of Barth's hypothesis in natural systems.

Some indications of trace element distributions between feldspars is obtained from the work of Heier (1960) and interpretations by Barth (1961). Barth (op. cit.)

postulated concomitant changes in the distribution of Ca, Sr and Ba with temperature as shown in Figure 2. Barth writes:

"Although it must be emphasized that some of the temperature calculations are rather uncertain, that the number of chemical determinations are small, and that the individual plots allow lines to be drawn slightly curved in different directions the trend is unmistakable. For Ca, Sr, Ba and Na there is a clear and regular increase of the distribution coefficient with temperature".

Also from Barth's work it is indicated that certain elements viz. Li, Cu, Pb and Rb do not show any regular distribution between the feldspars. Barth gave an explanation for this on the basis of DeVore's (1955) postulate that a trace element is not accepted in regular lattice positions until its concentration is large enough to control the environment of this site. Below this concentration level the trace elements do not replace a main element of similar size and remain in positions outside regular lattice sites. It is safe to assume however that Rb is located in K lattice positions in K-feldspars. The constancy of the K/Rb ratio in common rock types (e.g. Heier and Taylor 1959) as well as the change of this ratio under conditions of extreme fractionation in a direction predictable from crystal



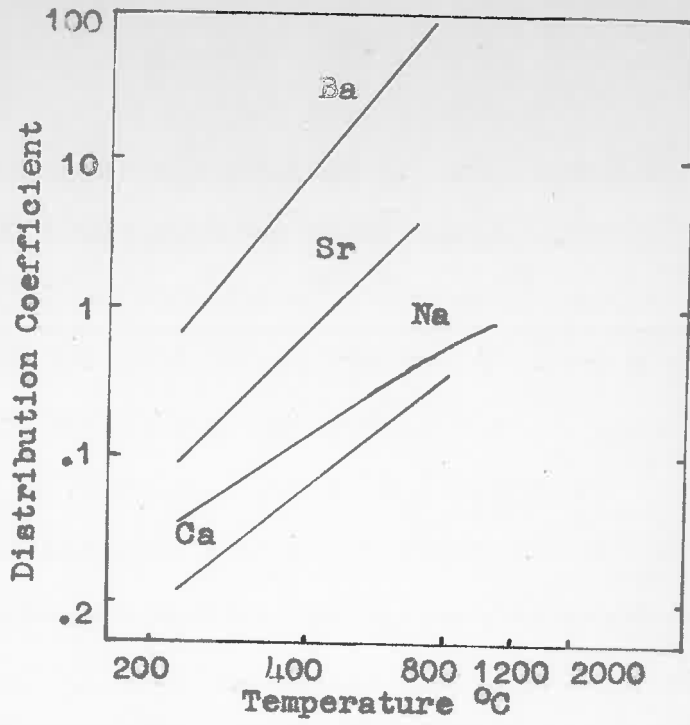


Fig. 2. Relation between temperature and the ratio of distribution of Na, Ca, Sr, and Ba between alkali feldspar and plagioclase (Barth, 1961).

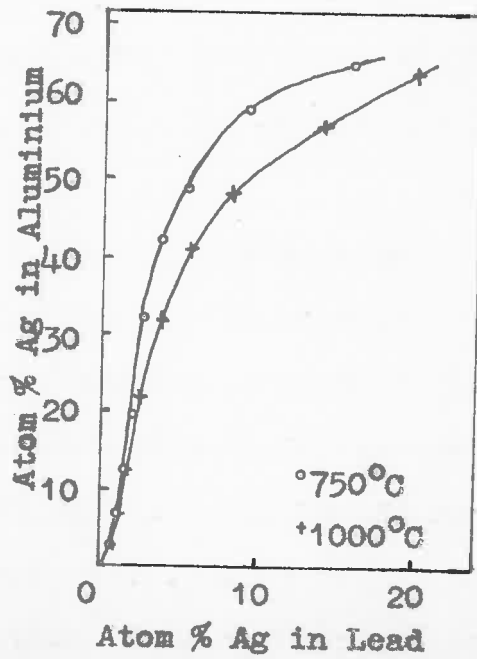


Fig. 3. Distribution of Ag between lead and aluminium (Lorentz and Erbe, 1929).

chemical reasoning suggests this. It cannot be so readily assumed that Rb is located in Na and/or Ca positions in the plagioclase since the size difference between the ions may be prohibitive. Nevertheless, because of the non finality of Heier's data concerning Rb distribution, and because of the suitability of Rb analyses by the writer's analytical methods, further investigations of this element are proposed.

In conclusion then because of the uncertainties about the location of Li, Cu, and Pb in the feldspar structure and from indications of Barth's work concerning Ba, Ca and Sr partitioning, the present writer considers that the following trace elements only are worthy of further investigation: Sr, Ba, Ca and Rb.

DISTRIBUTION COEFFICIENTS.

A. THEORETICAL CONSIDERATIONS.

The theory of elemental partitioning between coexisting phases has been adequately developed by various authors viz. Ramberg and DeVore (1951), Kretz (1959, 1961) and Mueller (1960, 1961) and requires little elaboration here.

The distribution of chemical species between coexisting feldspars can be considered as the partitioning of theoretical feldspar components, Na-feldspar, Sr-feldspar, etc. The Nernst distribution law indicates that at equilibrium the chemical potential of albite, for example, must be the same in both phases. The distribution coefficient can then be derived by introducing equations of the type:

$$\mu_{Ab}^{KF} = \mu_{Ab}^{\circ KF} + RT \ln \gamma_{Ab}^{KF} X_{Ab}^{KF}$$

where  $\mu_{Ab}^{KF}$  is the chemical potential of albite in the K-feldspar;  $\mu_{Ab}^{\circ KF}$  is the chemical potential of albite in K-feldspar in a standard state; R is the gas constant; T is the absolute temperature;  $\gamma_{Ab}^{KF}$  is the activity coefficient of  $X_{Ab}^{KF}$  and  $X_{Ab}^{KF}$  the mol. fraction of albite in the K-feldspar phase.

Then the distribution coefficient  $Kd_{Ab}$  is:

$$Kd_{Ab} = \frac{X_{Ab}^{KF}}{X_{Ab}^P} = \frac{\gamma_{Ab}^P}{\gamma_{Ab}^{KF}} e^{\left[ \frac{\mu_{Ab}^{\circ P} - \mu_{Ab}^{\circ KF}}{RT} \right]}$$

For ideal distributions and in the case of minor element partitioning the activity coefficients quotient should have

unit value and the distribution coefficient is constant at constant physical conditions.

Ramberg and DeVore (1951) deduced the following equations to show the dependence of  $K_d$  on pressure and temperature

$$K_{d_2} = K_{d_1} e^{\left[ \frac{\Delta V (P_2 - P_1)}{RT} \right]}$$

$$K_{d_2} = K_{d_1} e^{\left[ \frac{\Delta S (T_1 - T_2)}{RT_2} \right]}$$

where  $K_{d_2}$  and  $K_{d_1}$  are the distribution coefficients at the pressures  $P_1$  and  $P_2$  respectively or absolute temperatures  $T_1$  and  $T_2$  respectively;  $\Delta V$  is the partial molar volume change and  $\Delta S$  is the entropy change involved in the partitioning reaction.

Calculations of  $\Delta V$  for some mineral pairs (Ramberg and DeVore, op. cit.; Kretz, 1961; Albee, 1965a) indicated that  $\Delta V$  is a very small number and so to a first approximation the effect of pressure on partitioning can be safely ignored. Eugster (1955) determined experimentally the partitioning of trace quantities of Cs between a K-feldspar and a vapour phase and found that at 1000 and 2000 bars  $P_{H_2O} \frac{K_{d_{Cs}}}{K}$  was constant.

Temperature has long been assumed to be the main factor in affecting distribution coefficients and this also has been supported by experimental work. Bowen and Schairer (1935) showed that for clinopyroxene - olivine pairs  $K_{d_{Mg-silicate \text{ in olivine}}}$  changed from .61 to .82 in the  $\frac{Mg-silicate \text{ in Olivine}}{Mg-silicate \text{ in Pyroxene}}$

range 1100 - 1300°C. Eugster (1955) found that  $K_d \frac{Cs}{K}$  between K-feldspar and a vapour phase changed from .48 - 1.2 in the range 500 - 800°C, (at higher temperatures more Cs is taken into the K-feldspar lattice). In natural systems major element partition coefficients have been correlated with temperature by several authors and include the work of Kretz (1961), Albee (1965a), Moxham (1965) and Binns (1962). Some similar tentative correlations concerned with trace element partitioning have previously been noted in Chapter I.

#### B. DISTRIBUTION DIAGRAMS

The present writer has found it convenient to express the distribution of elements in a graphical way using a Distribution or Roozeboom diagram (Kretz, 1959 p. 379). In these diagrams the atomic or molecular ratios of the partitioning element in each phase are plotted against each other.\* If there is an equilibrium distribution of the component between the phases (i.e. constant pressure, temperature conditions), the distribution of points will define a straight line if:

- (a) both phases are ideal for the partitioning element.
- (b) the partitioning element forms a dilute solid solution in both phases.

---

\* In this study the writer has used variables of the type:  
mol per cent albite, anorthite, Sr-feldspar, etc.

---

Such a regular relationship is a graphic expression of the Nernst distribution law. A completely random distribution may indicate lack of chemical equilibrium but deviations from a straight line may result also from other causes even if chemical equilibrium is attained. The effects of non-ideality of a partitioning element in either or both phases as shown in distribution diagrams are varied, [in particular see Kretz (1959, 1960) and Mueller (1960, 1961)]. Of course the test for equilibrium will only be valid within the limits of precision of the analytical technique.

In the present work variation of the distribution coefficient versus changes in physical variables is seen in distribution diagrams as a series of lines radiating from the origin. Diagrams used in this way are rarely known to the writer from metamorphic systems although in the field of metallurgy, Lorentz and Erbe (1929) showed that the distribution of Ag between Pb and Al is temperature dependent and expressed their results on a distribution diagram (Figure 3).

GEOLOGICAL SETTING: SELECTION AND LOCATION OF SPECIMENS;

AND MINERAL SEPARATION.



### A. INTRODUCTION.

In order to carry out this investigation material was selected from different areas to include a range of metamorphic grades (ideally from the upper greenschist to the granulite facies), each area covering two or more different metamorphic zones. The material selected can be grouped in the following way:

- (a) rocks from the almandine-amphibolite and granulite facies in Ceylon; Musgrave Range area, South Australia; Broken Hill area, New South Wales.
- (b) rocks from the sillimanite muscovite and sillimanite orthoclase sub facies of the almandine-amphibolite facies from several local areas near Adelaide, South Australia.

The reader is referred to the relevant publications for a detailed discussion of the geology in each area. Mineralogical compositions of all samples examined in this study are given in Appendix I and the location of all samples used in this investigation is shown in Figures 4 to 6 and 8 to 10.

### B. GRANULITE--ALMANDINE-AMPHIBOLITE FACIES.

In the Ceylon and Musgrave Range area the granulite facies rocks belong to the pyroxene granulite and hornblende granulite sub facies (Turner and Verhoogen, 1960). In addition in the Musgrave Range area, acidic assemblages occur which contain hornblende but in which either clino or

Figure 4.

Numbers used in this Figure correspond to the following specimen numbers.

1. 30829	11. 30581
2. 30674	12. 30638
3. 30652	13. 30639
4. 34504	14. 30230
5. 34611	15. 30637
6. 30726	16. 30640
7. 30573	17. 30840
8. 30577	18. 30847
9. 30575	19. 30838
10. 30543	20. 30553
	21. 34616
	22. 30855

Locations of samples 10 and 21 are not shown in Figure 4 but occur,  $15\frac{1}{2}$  miles W  $13^{\circ}$ N of Ernabella and 7 miles E of KenMore Park respectively.

Samples 1 - 9 refer to specimens from which coexisting feldspars have been extracted and chemically analysed by the writer.

Samples 10 - 22 refer to specimens from which coexisting clino and orthopyroxenes have been extracted and optical measurements made by A.F. Wilson (1960). These data are discussed in Chapter VII p.90 and Figure 47.

FIGURE 4 GEOLOGICAL SKETCH MAP OF THE EASTERN MUSGRAVE RANGES, SOUTH AUSTRALIA, SHOWING SPECIMEN LOCATIONS (Wilson 1954b).

 Charnockitic granulites (showing Strike & Dip direction)

 Intrusive granites

 Prominent Hills

Nos. correspond to specimen nos. as listed on the opposite p.

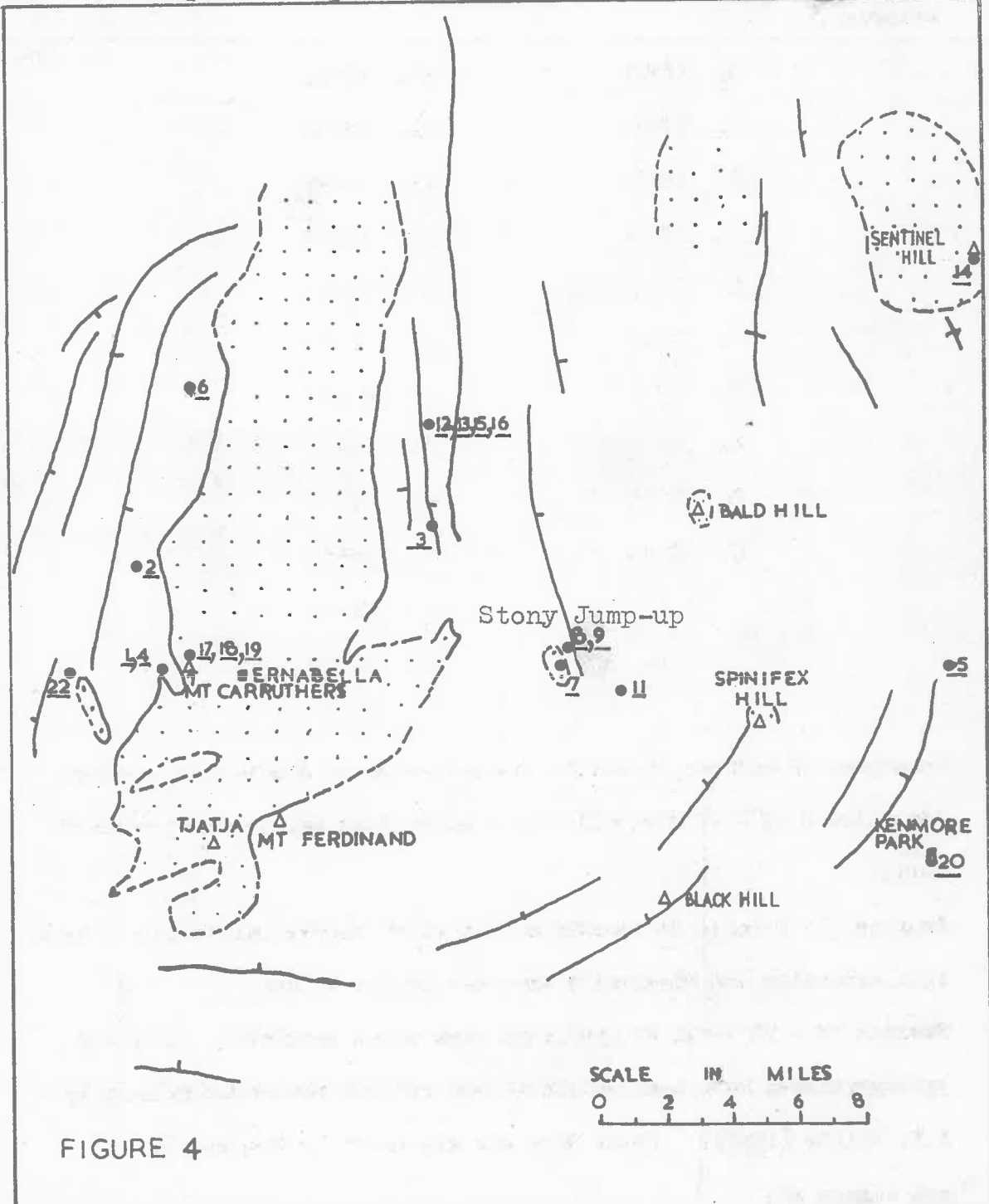


FIGURE 4

Figure 5

Map of the Barrier Ranges, N.S.W., showing distribution of the three metamorphic zones in the Archaeozoic Willyama Complex (from Binns, 1964).

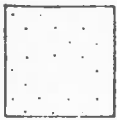
Numbers used in Figure 5 correspond to the following samples from which coexisting feldspars have been extracted and analysed.

1. 462, 465, 466
2. 18L
3. 469
4. 642
5. 447
6. 410

# WILLYAMA COMPLEX

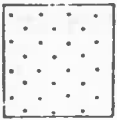
# TORROWANGEE SERIES

## ZONE A



Amphibolites with blue-green hornblende

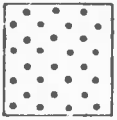
APPROXIMATE BOUNDARY



## ZONE B

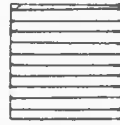
Amphibolites with brown green hornblende

ORTHOPIYROXENE ISOGRAD



## ZONE C

Hornblende - pyroxene gneisses



## SERIES

(Proterozoic)

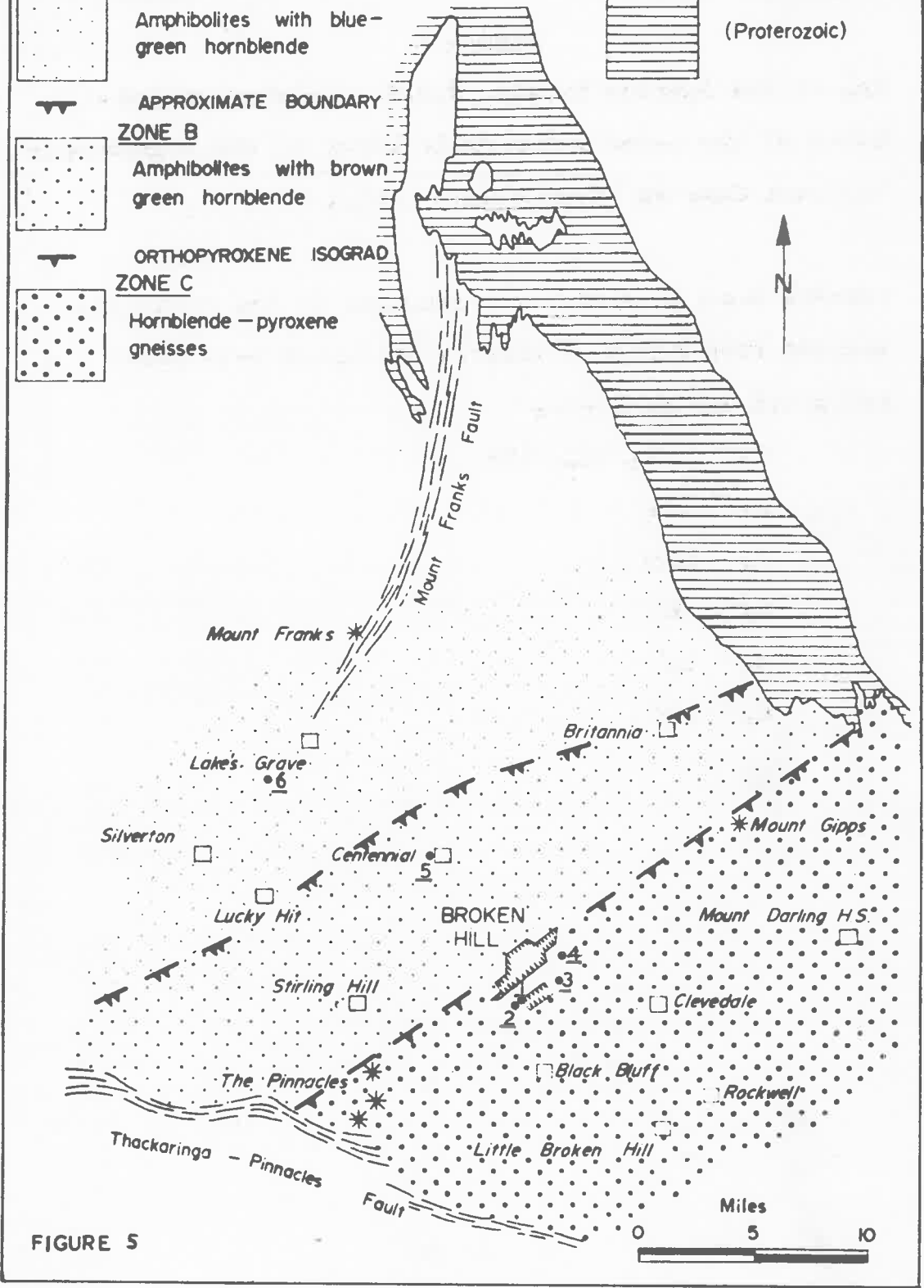


FIGURE 5

Figure 6

Preliminary tectonic map of Ceylon (Oliver, 1957) showing distribution of major Pre-Cambrian units (Cooray, 1962).

Numbers used in Figure 6 correspond to the following samples from which coexisting feldspars have been extracted and analysed.

1. OL181
2. OL164
3. OL158
4. OL166
5. O1584
6. A152/630
7. E23518A
8. A152/79
9. A152/794

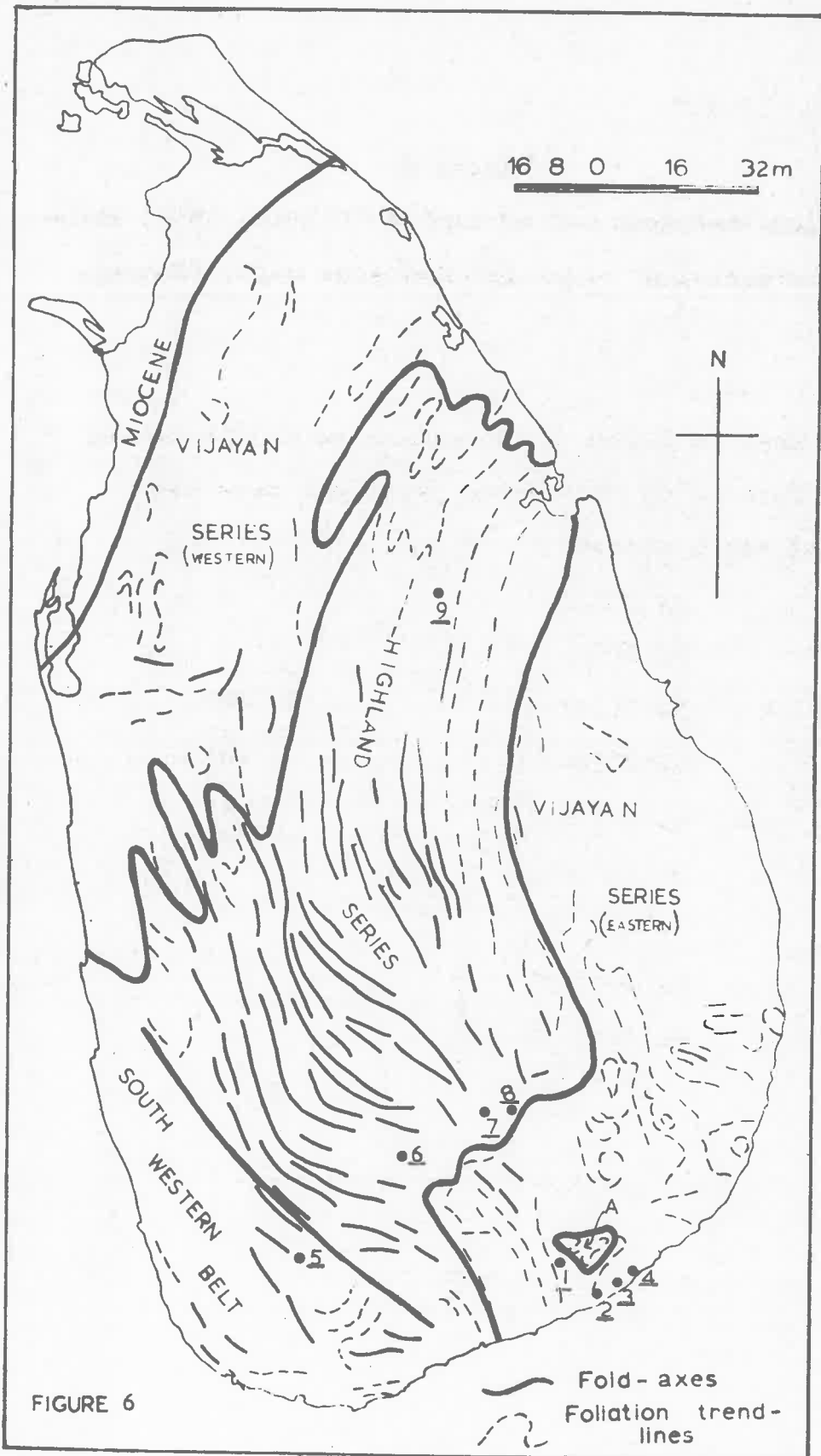


FIGURE 6

Figure 7.

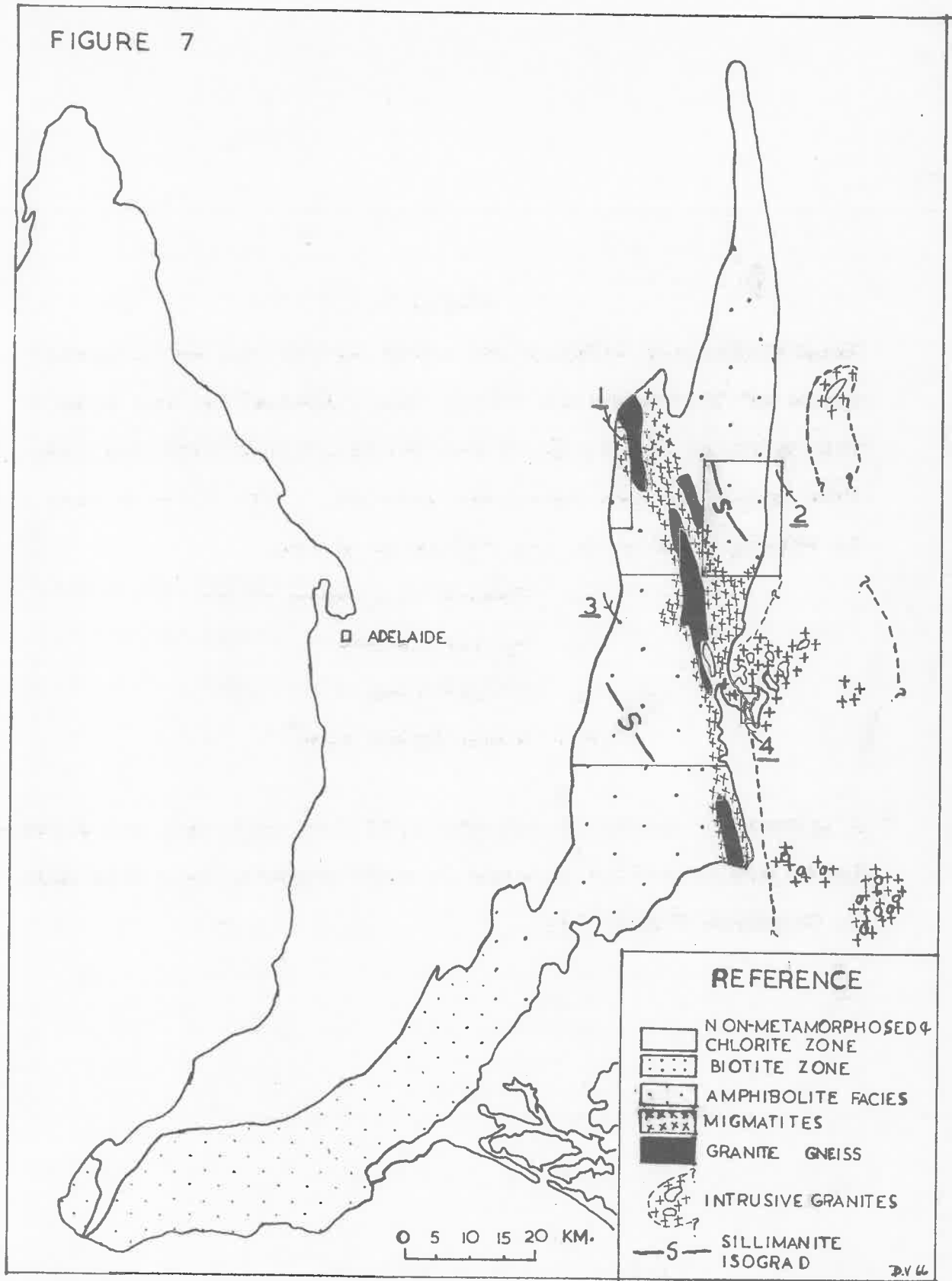
Generalized map showing the areal extent and metamorphic grade of the Kanmantoo Group, South Australia, and also the relative locations of the various areas near Adelaide from which samples have been studied. The numbers used in Figure 7 refer to the following areas:

1. Pewsey Vale area
2. Springton area
3. Palmer area
4. Reedy Creek area\*

\* A systematic study of samples from this area was not undertaken but reference is made to some samples from this area in Chapters V and VII.

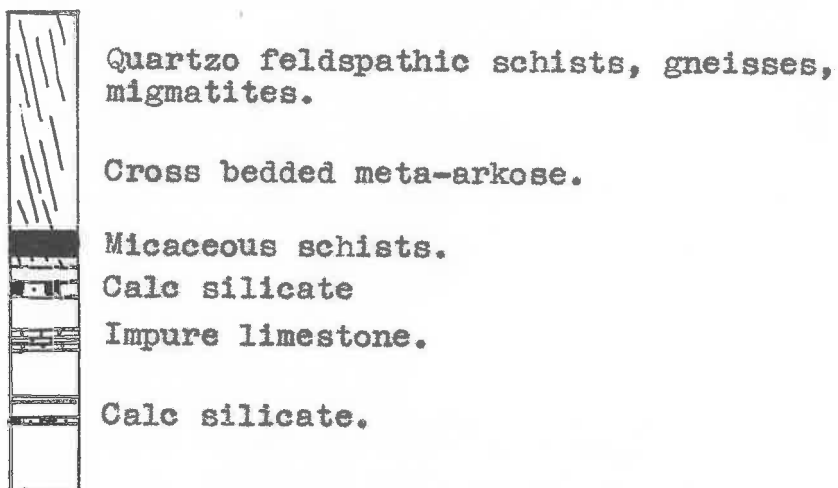


FIGURE 7



LEGEND TO ACCOMPANY FIGURE 8

KANMANTOO GROUP.



- ~ ~ Stauroilite zone
- Kyanite zone
- - Sillimanite isograd
- ~ ~ Sillimanite orthoclase isograd
- . . . . Outer migmatite boundary

Figure 8.

Generalized geological map of the Springton area, South Australia. Numbers referred to in Figure 8 correspond to the following samples from which coexisting feldspars have been extracted and analysed.

1. A185/706
2. A185/784
3. A221/54
4. A221/52
5. A221/57
6. A221/58
7. A221/48

Sample A221/57 occurs 0.4 miles W. of the plotted position in Figure 8.



FIGURE B

ONE MILE

### Figure 9

Generalized geological map of the Palmer area, South Australia. Numbers referred to in Figure 9 correspond to the following specimen numbers.

1. AJWH6
2. DVH2
3. 188
4. A221/41
5. 191
6. PR12
7. AU8308

Samples 1, 2, 4, 6 and 7 refer to the specimens from which coexisting feldspars have been extracted and chemically analysed by the writer.

Samples 3, 4, 5 and 6 refer to samples from which coexisting K-feldspar and biotite has been extracted and analysed by A.J.R. White (1966b). Reference is made to these samples in Figure 46. White has analysed two samples from the same location as 221/41 and these are referred to as 192 and 193 in Figure 46.

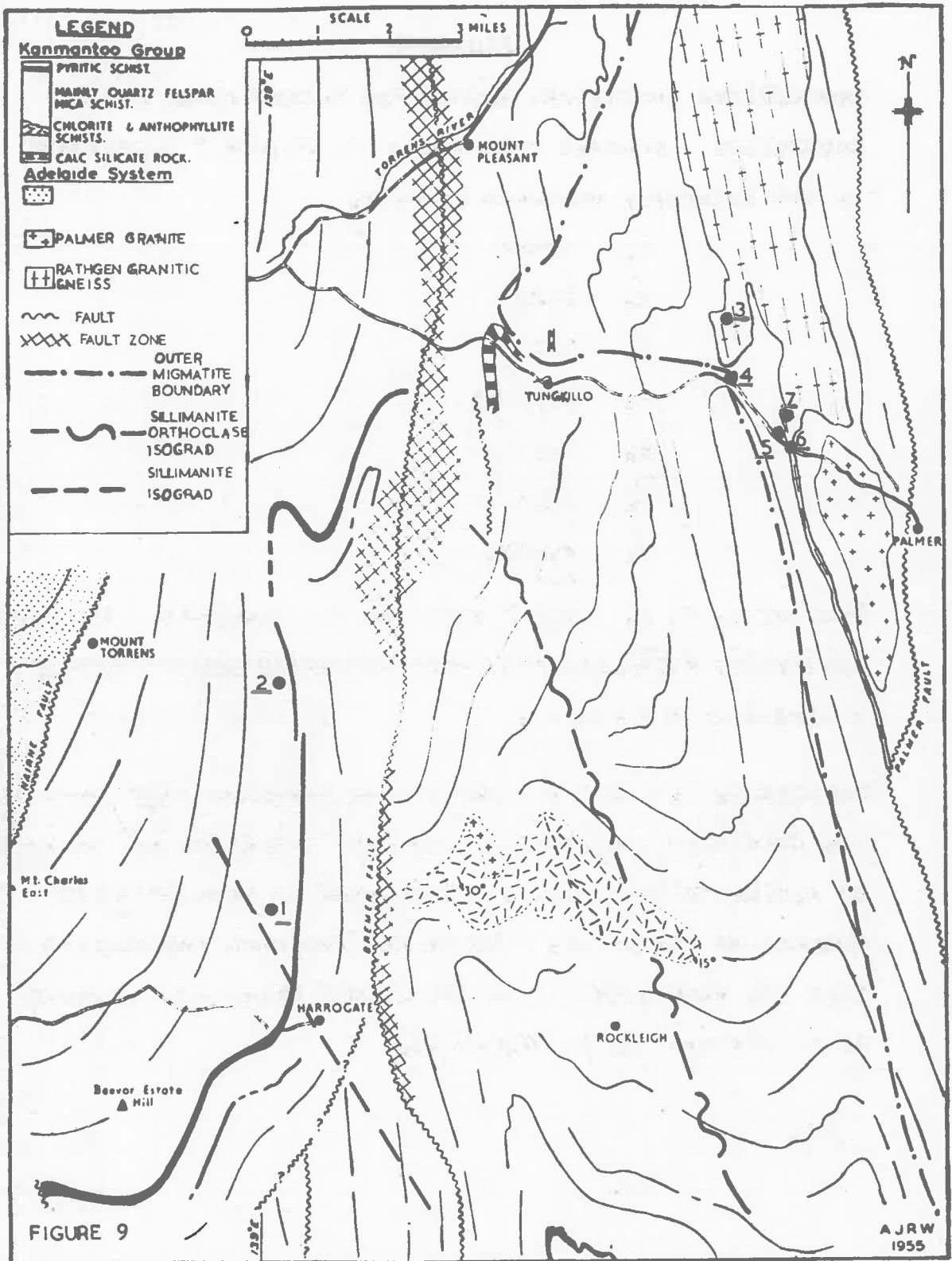


Figure 10.

Generalized geological map of the Pewsey Vale area, South Australia.


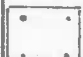

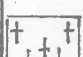

Numbers used in Figure 10 correspond to the following samples from which coexisting feldspars have been extracted and analysed.

1. A200/887
2. A200/423
3. A200/561
4. A200/124A
5. A200/670B
6. A200/27
7. A200/871A

S, KF and M refer to sillimanite, K-feldspar and muscovite respectively.

Figure 10

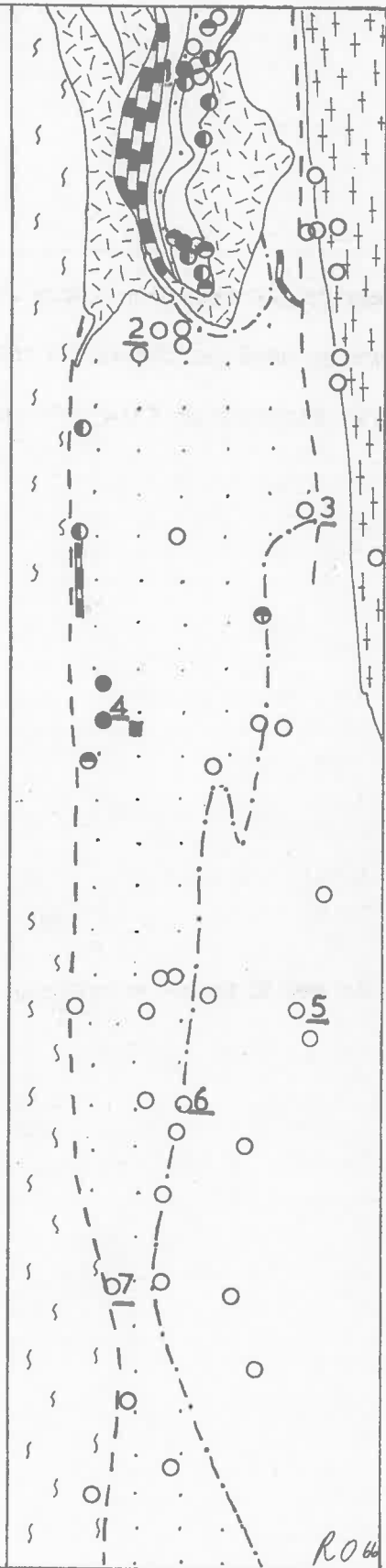
KANMANTOO GROUP

-  Calc-Silicate
-  Migmatite
-  Quartzo-Feldspathic Schists
-  Tanunda Creek Gneiss
-  Albitised Mt Kitchener Granite. Albite.

ASSEMBLAGES

- S-KF
- S-M-KF } Pelites
- S-M
- M
- S-M } Q-F Schists, Migmatites
- — — FAULT
- · - · - · MIGMATITE BOUNDARY
- Pewsey Vale Homestead

○ 1 MILES



orthopyroxene is either rare or absent. In both areas the different sub facies occur in close proximity and may be inter-layered and it would appear necessary to postulate locally contrasting environmental conditions e.g. different water vapour pressure and chemical compositions to explain the variation in facies.

In the Broken Hill area charnockites do not occur and the acidic rocks are represented by garnetiferous and non-garnetiferous granitic gneisses (the complex history of these rocks is discussed by Andrews, 1922; King and Thompson, 1953 and Binns, 1964),

The almandine-amphibolite facies rocks in different areas are different mineralogically and a discussion of these and of rocks transitional from the granulite to the almandine-amphibolite facies is given below.

1. Musgrave Range area

Mapping has not yet been carried out in sufficient detail to delineate an isograd between the two facies. The assemblages characteristic of the almandine-amphibolite facies have been taken from the "Stony Jump-Up" area (Figure 4). These rocks are different mineralogically from the granulite facies assemblages and significant differences are listed below in some detail because despite A. F. Wilson's publications (1947a,b, 1948, 1950a,b, 1952, 1953, 1954a,b, 1955, 1960a,b) these data are not available in the literature.



- (a) Abundant sphene up to 2 - 3 volume percent, as separate grains and as coronas around ilmenite is found only in almandine-amphibolite facies rocks. Titanium in the granulite facies is contained in rutile (as inclusions in quartz and feldspar) and presumably in the hornblende (Ramberg, 1952).
- (b) Biotite is much more abundant in the amphibolite facies rocks (viz. 4.0 to 7.0 volume percent in the samples examined in this study) and has the pleochroic scheme\*: X = straw yellow, Z = dark chocolate and  $\beta = 1.631 \pm .001$ . In the granulite facies biotite is < 1.0 volume percent and has a different pleochroic scheme: X = pale fawn, Z = brownish red and  $\beta = 1.629 \pm .001$ .
- (c) Orthopyroxene is absent in the almandine-amphibolite facies.
- (d) Hornblende of the amphibolite facies has the pleochroic scheme: X = pale greenish fawn, Y = khaki green, Z = greenish blue and  $\gamma = 1.690 \pm .001$ . In the granulite facies rocks, the hornblende has the pleochroic scheme X = pale fawn or greenish yellow, Y = khaki or brownish green, Z = pale fawn or greenish khaki and  $\gamma = 1.674 \pm .001$ .
- (e) The K-feldspar in the lower grade rocks is a cross
- 
- \* pleochroic schemes and R.I. data for both the biotite and hornblende phases are from Wilson (1954b).
-

hatch twinned microcline ( $\Delta = .76$  to  $.96$ ) whereas in the granulite facies rocks the K-feldspar is monoclinic (there is a single  $131/1\bar{3}1$  peak).

## 2. Broken Hill area

Specimens from this area have been selected on the basis of recent interpretations of the metamorphism by Binns (1963, 1964). Within this area the transition from the almandine-amphibolite to the granulite facies is marked by the incoming of orthopyroxene in basic rocks (Binns 1962, 1964). Samples selected from the two facies include granitic gneisses and pelites. At metamorphic grades lower than granulite facies Binns (op. cit.) has delineated two zones referred to as Zones A and B in Figure 5 on the basis of different pleochroic schemes of hornblende in the basic rocks. He has noticed also that there is relatively more muscovite in the Zone A pelites than in those of Zone B, and on this basis has tentatively correlated the boundary between these two zones with an "orthoclase isograd". However the overall lack of pelitic assemblages and the tendency for these where they do occur to reflect subsequent metamorphism makes the position of the above isograd indefinite. Samples from the almandine-amphibolite facies include specimens from both Zones A and B.

## 3. Ceylon

The distribution of the major pre-cambrian units in

Ceylon referred to as the Highland (granulite facies) and the Vijayan (almandine-amphibolite) series is shown in Figure 6. From the work of Oliver and Erb (1957) and Cooray (1961, 1962) the Vijayan can be subdivided into a "Transitional zone" and the "Vijayan Series proper". The latter consists of "microcline bearing biotite and hornblende gneisses, granitic and granodioritic in composition which have been effected by several stages of migmatization (Vitanage, 1959 p. 57; Cooray, 1961 p. 105). They are extremely variable in appearance; the granitic component is widespread, is clearly separate from the host rocks; and is later in time. Within these gneisses there are rare scattered relic bands of metasediments (mainly calcareous) and pyroxene free amphibolites" (Cooray, 1962). The eastern Transitional zone varies in width and in the Kirindi Oya basin where most of the writer's samples have been taken is 10 - 12 miles in width, (Oliver and Erb, 1957). Rocks in this zone are predominately biotite and biotite hornblende migmatitic gneisses, charnockites and charnockitic gneisses. In the field the different facies types are intermixed and cannot be mapped separately. Cooray (op. cit.) suggests that the Vijayan has resulted from widespread migmatization and granitization under almandine-amphibolite facies conditions and in the presence of water, of a pre-existing series of rocks that were regionally metamorphosed under granulite

facies conditions. Whereas the Vijayan Series proper contains few remnants of previously existing high grade rocks, the Transitional Zone has only been partially modified and still contains widespread evidence of Highland Series rocks. It is this relationship between the Vijayan and the Highland Series that has led to Cooray (1962 p. 265) suggesting that some other factor than load pressure and temperature is critical in the transitions from high to low grade minerals. There is reasonable evidence in Ceylon to suggest that water may be this important factor.

C. LOCAL AREAS NEAR ADELAIDE

An extensive belt of metasediments referred to as the Kanmantoo group occurs on the eastern side of the Mt. Lofty Ranges, South Australia (see Figure 7). The central part of this area is occupied by almandine-amphibolite facies rocks culminating as an approximately north - south, elongate zone in migmatites, granitized gneisses (Hossfeld, 1925; Johns and Kruger, 1949; Rattigan and Wegener, 1951; Hopkins, 1950; Sando, 1957; Chinner, 1955 and White 1956, and (a) in prep), and intrusive granites (White et al. in prep., and Mills, 1964).

Within this metasedimentary group, the following areas were sampled by the writer, because they show metamorphic zoning and in addition they are amongst the few areas that have been mapped in detail in the Kanmantoo group: Springton area (Mills, 1964); Palmer area (White, 1956); and the

Pewsey Vale area (Offler, 1966). A brief discussion of each area is given.

1. Springton area

Mills (1964) established the following progressive sequence of metamorphic zones in this area: biotite; andalusite-staurolite; kyanite; sillimanite-muscovite (see Figure 8). Specimens from below the sillimanite zone were found unsuitable for the writer's study owing to incomplete recrystallization in the meta-arkosic types and a lack of two feldspar bearing assemblages in other rock types. It is noted that the highest grade rocks in the sillimanite-muscovite zone are migmatites in which muscovite is in disequilibrium with sillimanite although a separate sillimanite--K-feldspar zone is not established.

2. Palmer area

Metamorphic studies in this area have been reported by White (1956; in prep. (a) and (b)). White has delineated a sillimanite muscovite and a sillimanite K-feldspar isograd (see Figure 9) although a separate sillimanite--K-feldspar zone is not found. Pelitic assemblages at the sillimanite isograd contain andalusite and sillimanite in contrast to this isograd in the Springton area where kyanite also is found. Different  $P_L - T$  conditions can therefore be inferred. Again the highest grade rocks in this area are migmatites, granitic gneisses and in suitable rock types

muscovite is in disequilibrium with sillimanite (cf Springton area).

### 3. Pewsey Vale area

In this area Offler (1966) has grouped rocks according to sillimanite-muscovite and sillimanite--K-feldspar sub facies. Rocks of the latter group occur as lenses of variable size within the sillimanite-muscovite grade country rocks and in such rocks muscovite does not occur and is presumed to have decomposed according to the reaction:



where  $P_{\text{H}_2\text{O}} < P_L$  (Offler 1966 and pers. comm.).

The sillimanite--muscovite zone rocks examined include both migmatized and non migmatized varieties (see location map, Figure 10). Their relative relationship to the sillimanite isograd (cf Springton and Palmer areas) is not known and a uniform grade of metamorphism is presumed to exist in these rocks (Offler op. cit.).

#### D. SAMPLE SELECTION and SUITABILITY OF SPECIMENS

Some important criteria in sample selection are:

- (a) samples fully representing a particular metamorphic grade were collected.
- (b) the final specimens used were selected on the basis of equilibrium textures and the absence of obvious poly-metamorphic effects.
- (c) the presence of other minerals likely to accept the

trace elements Ba, Sr, and Rb could not be avoided in most cases. The significance of their presence is examined in the relevant chapters.

Fortunately the minor element abundances is sufficiently varied to permit examination of their distribution over a satisfactory range of concentrations. That is to say the values do not cluster about points on the Distribution diagrams, e.g. strontium distributions show at least a three-fold variation in concentration for most isofacial groups of rocks.

#### E. SAMPLING and MINERAL SELECTION

Comparatively small hand specimen sized samples (approximately 4 - 5 cms. in diameter) were used in this study. Kretz (1961) stressed the importance of small specimens to ensure that local equilibrium conditions exist throughout.

The rock samples were crushed to 12 - mesh in a fly-press and further crushed to 90 - mesh using a hardened steel plate and pestle: a cardboard guard around the plate prevented loss of material. The 90 - mesh fraction was split: half being set aside for whole rock analysis and the other half for mineral separation. A sieved fraction of the latter such that the K-feldspar grains were many times larger than the scale of the perthitic intergrowths and both feldspar grains were free of composite grains, was finally

used for mineral separation: generally the 90 - 120 mesh fraction was suitable.

Initial separation was by means of a Magnetic Separator. Final separations were carried out by centrifuging in tetrabromo-ethane liquid diluted with dimethyl-sulphoxide. The necessary liquid SG was adjusted with the aid of crystals of K-feldspar, albite and quartz. During the separation, the purity of all concentrates was checked with an optical microscope.

It was a comparatively simple procedure with repeated centrifuging to obtain a K-feldspar concentrate to a purity > 99 volume per cent. It was more difficult to remove quartz from the plagioclase. Final plagioclase concentrates contained < 1 volume per cent of K-feldspar and impure quartz and plagioclase grains, and variable quantities of quartz. The quantity of feldspar material separated was usually between .5 and 1.0 grams and this was ground as discussed in Chapter IV (p. 34 ) before analysis.



ANALYTICAL TECHNIQUES.

Analytical techniques for determinations of Na, K, Ca, Ba, Sr and Rb in feldspars are here discussed. Alkali determinations have been carried out using standard photometric methods. For trace element analyses two methods have been used, the least successful of which, optical spectrography, is discussed in Appendix II. More successful have been X-ray spectrographic techniques by means of which Ba, Sr, Rb and Ca in both alkali feldspars and plagioclases have been analysed. Chemical analyses of the coexisting feldspars used in this study are given in Appendix VI.

#### A. WET CHEMICAL METHODS

##### 1. Alkali analyses

Sodium and potassium have been determined using an Eel flame photometer. A Na interference filter, K gelatin filter and an air-propane flame were used.

##### (1) Sample preparation

Approximately 25 mgms. of undried powdered feldspar\* were digested with 2 ml. hydrofluoric acid and  $\frac{1}{2}$  ml. 50% sulphuric acid in a platinum crucible for approximately 12 hours on a sand bath at about 120°C. The contents of the crucible were evaporated on a hot plate until all the hydrofluoric acid was removed. The crucible was half filled with water, one drop of 50% sulphuric acid added, and heated on the sand bath for

---

\* The feldspar was ground as discussed on p. 34

---

several hours. The digested sample was made up with distilled water to 250 ml. Appropriate dilutions of this solution were made for the flame photometric analyses.

(ii) Standards used and flame photometric technique

Potassium and sodium standards in the range 0 - 10 p.p.m.  $K_2O$  and 0 - 5 p.p.m.  $Na_2O$  respectively were prepared from  $KNO_3$  and  $NaCOOH$  respectively. Concentrations of standards and unknowns were adjusted so that the unknown was "sandwiched" between two standards differing in concentration by 1 p.p.m.  $K_2O$  or  $Na_2O$ ; a minimum of six readings were made on all solutions. A blank correction (approximately one per cent of the maximum galvanometer reading) was necessary for sodium determinations.

(iii) Precision and Accuracy

Initially the method was calibrated against several feldspar standards and these were rechecked at various times during the course of the writer's work. Average determinations of these standards by the writer are compared with recommended values in Table 3. Unknown samples were initially prepared in duplicate but subsequent determinations were made only once. Some results are given in Table 4; estimated relative deviation of  $K_2O$  and  $Na_2O$  determinations at the

Table 3. Accuracy of Alkali Analyses using Flame Photometer.

Sample	Flame Photometer*		Recommended Values	
	Na <sub>2</sub> O	K <sub>2</sub> O	Na <sub>2</sub> O	K <sub>2</sub> O
N.B.S. Feldspar 70	2.38	12.40	2.38	12.58
N.B.S. Feldspar 99	10.60	.40	10.73	.41
Plagioclase A.U. 16949	10.83	1.15	10.70	1.17
K-feldspar A.U. 17263	3.59	11.51	3.65	11.52

\* D. Virgo, analyst.

Table 4. Precision of Alkali Analyses in unknown feldspar samples using Flame Photometer.

Sample	K-feldspar		Plagioclase	
	K <sub>2</sub> O	Na <sub>2</sub> O	K <sub>2</sub> O	Na <sub>2</sub> O
A221/104	14.28*	1.795*	.800*	8.32*
	14.35*	1.796	.761	8.26
	14.33			
	14.30			
30829	13.49*	2.10*	.286*	6.02*
	13.32	2.07	.290	5.85
	13.33	2.14	.283	
34611	13.15*	2.14*	.144*	1.458*
	13.15	2.14	.135	1.476
		2.17		
A221/1	14.20*	1.42*	.511*	7.40*
	14.37	1.46	.492	7.47
	14.28		.450	7.52
OL181	14.70*	1.48*	.770*	8.07*
	14.53	1.41*	.850*	8.10
	14.48	1.46	.766	
		1.43	.820	
A152/79	12.96*	2.17*	.292*	4.63*
	13.04	2.12	.250*	4.65*
		2.14	.219	4.67
		.195		
A200/423	14.35*	1.23*	.22	7.63
	14.50*	1.13	.20	7.56
	14.44	1.13	.23	
	14.65			

\* implies analysis of a second portion of the sample.

concentration levels found in the writer's feldspar samples are indicated in Table 5.

## 2. Calcium analyses

Calcium analyses were carried out titrimetrically on a selection of plagioclase - quartz concentrates of varying CaO content. The same samples were used to establish a calibration curve for calcium determinations using an X-ray fluorescent technique (see p. 48 ).

### (i) Sample preparation

Approximately 25 mgms. of undried powdered feldspar\* were digested with 4 ml. hydrofluoric acid, 0.5 ml. perchloric acid in a platinum crucible for approximately 12 hours on a sand bath at about 120°C. The contents of the crucible were evaporated on a hot plate until all the hydrofluoric acid was removed. Finally the crucible was half filled with water, .5 ml. perchloric acid added and again heated on a sand bath for several hours. The digested sample was made up to 50 ml. with water and aliquots of this solution were then titrated.

### (ii) Titration technique and standards used

To an aliquot of the unknown in a glass titrating vessel were added: 3 ml. of 15% NaOH and 5 ml. of 50% triethylamine (to suppress aluminium) and the volume made up to 20 ml. with water. Ten drops of .05% acid

---

\* The feldspar was ground as discussed on p. 34

---

Table 5. Estimates of relative deviation\* for  $K_2O$  and  $Na_2O$  at the concentration levels found in the writer's feldspar samples.

Feldspar type	$Na_2O$	$K_2O$
K-feldspar	2	1
Plagioclase	1	5

\* Relative deviation referred to in this table and elsewhere in the text is the standard deviation expressed as a percentage of the mean value.

alizarin black were added as an indicator. The titration was made using E.D.T.A. as titrant (.5 mg./ml.) and the end point determined graphically from a plot of "ml. of E.D.T.A. added" against "galvonometer reading". Filter no. 608 gave reasonable end points. Calibration of the E.D.T.A. was made against several synthetic standards viz. 1.0 mg. and 0.50 mg. CaO/ml. Three careful titrations of all solutions were made.

(iii) Precision and accuracy

The precision and accuracy of the method was checked against a laboratory standard plagioclase containing 14.30 per cent CaO. Repeat determinations of this standard indicate that a relative deviation of .4 per cent can be expected in the analysed plagioclase samples (Table 12 ).

B. X-RAY FLUORESCENT ANALYSIS

1. Theoretical considerations

The theory of quantitative analysis by X-ray spectrography is well known, (Birks, 1959; Liebhafsky et al., 1960) and will not be discussed in detail in this text. However some facts concerning X-ray spectrography, pertinent to this study, will be mentioned.

Quantitative analyses by X-ray spectrography involve a correlation between the intensity of the analytical line and the weight per cent of the element. For accurate analyses



a linear relationship between fluorescent intensities and elemental concentrations cannot be assumed. The causes of deviation from linearity are many (Liebhafsky, op. cit. p. 172). The principal cause is the "matrix effect" which is a function of the bulk composition of the sample. These matrix effects are the result of absorption by the sample and include the following:

- (a) absorption of the incoming polychromatic primary beam.
- (b) absorption of the outgoing monochromatic characteristic radiation of the element concerned.
- (c) enhancement of the characteristic radiation of the element concerned by the characteristic radiation of other elements in the sample.

Corrections for these effects are necessary before quantitative results can be obtained.

(i) Enhancement effects

Matrix effect (c) above, occurs when an element in the sample is radiating at a wavelength shorter than the absorption edge of the element to be determined. Mutual enhancement is an inefficient process but is important when the element causing the enhancement is present in high concentrations. For trace elements with atomic numbers greater than the highest atomic numbered major constituent in the sample (in most common rocks and minerals this will be iron) these

effects can be ignored: this will apply to Rb and Sr analyses in the writer's samples. Enhancement effects can also be neglected in the writer's techniques for Ba analysis using the  $BaLa_1$  line\* and Ca analysis using the  $CaK\alpha_1$  line.

(ii) Absorption effects

With regard to matrix effects (a) and (b) above, Liebhafsky (op. cit.), Hower (1961) and Norrish† (pers. comm.) have developed equations of the following type to relate fluorescent intensity of the analytical line and elemental concentrations in an infinitely thick

$$\text{sample: } C = \frac{K X}{A_1 \sec\theta + A_2 \sec\psi} \quad \dots \dots (1)$$

where C is the counts / sec. of the analytical line; X is the weight fraction of the element of interest;  $A_1$  and  $A_2$  are the mass absorption coefficients of the sample for the incident and fluorescent radiations respectively;  $\theta$  and  $\psi$  are the angles that the incident and emergent beams make with the normal to the surface of the sample assuming a fixed geometrical relationship between the X-ray tube, the sample and the analysing crystal as in commercially made spectrographs; K is

---

\* Enhancement of the  $BaLa_1$  line does occur but this is due to overlapping of the tail of the  $TiK\alpha$  peak on the  $BaLa_1$  position (see p. 45 for further discussion).

† C.S.I.R.O. Soils Division, Adelaide.

---

the quotient of several factors including a measure of the absorption and conversion of incident to characteristic radiant energy.

Equation (1) becomes useful practically by making the following assumption (Norrish, op. cit.):  $A_1$  is related to  $A_2$  in a constant way for all samples and for any element provided the absorption edge of another major element does not occur between  $\lambda_1$  (the effective incident wavelength) and  $\lambda_2$  (the fluorescent radiation of the analytical line). If such does occur the relationship of the mass absorption coefficient of the sample with  $\lambda_1$  and  $\lambda_2$  will be different on each side of the absorption edge. This cannot be for elements where the wavelength of the analytical line is less than the wavelength of the K absorption edge of iron, the most common heavy matrix element in silicate bearing rocks and minerals.

It can be shown then that under most sample conditions equation (1) is modified to:

$$X = \frac{kA_2C}{K - C} \quad \dots \dots (2)$$

which for low concentrations reduces to

$$X = k^1 A_2 C \quad \dots \dots (3)$$

The symbols  $X$ ,  $A_2$  and  $C$  refer to the same above mentioned variables:  $k$ ,  $k^1$  and  $K$  are constants which are

determined empirically using standards of known concentrations. By introducing an equation similar to (3) for a standard sample, the following equation can be written which is the basis of the writer's trace and major element techniques.

$$X^u(\text{Percent element in the unknown sample}) = \frac{C^u A_2^u}{C^s A_2^s} X^s \dots (4)$$

where the subscripts U and S refer to the unknown and standard respectively.

It follows then that quantitative analyses can be carried out provided a correction for the mass absorption coefficient  $A_2$  is made for both unknown and standard samples. The way in which this has been accomplished is discussed later with reference to Sr and Rb, Ba and Ca analyses.

## 2. Equipment and operating conditions

The X-ray analyses were carried out with a Philips All-Vacuum Spectrograph. A list of the components comprising this equipment is given in Appendix III and the instrumental settings are given in Appendix IV. All intensity measurements were corrected using the dead times also given in Appendix IV.

## 3. Sample preparation

### (1) Grain size effects

Experimentation indicated that for a suite of

samples made up of single feldspars, mixtures of feldspar and quartz and common rock types, the following technique yielded a powder of sufficiently small and uniform grain size so that the fluorescent radiation (CaK $\alpha$  and SrK $\alpha$ ) did not change with further grinding. Approximately 700 mgms. of sample were ground under acetone for one hour using a motor driven Fisher Mill made up of a mullite mortar and pestle. Measurements of the ground powder indicated that 90 per cent of the grains were < 20 microns and the rest not coarser than 40 microns.

(ii) Pelletizing procedure

One of the main problems concerned with applying X-ray spectrography to the writer's unknown feldspar samples was to develop a sample preparation technique whereby  $\frac{1}{2}$  gm. or less of feldspar powder could be used. This was necessary because of the limited quantities of material (in particular, plagioclase) available. Experimentation led to a modification of a sample preparation method proposed by Baird (1961). In Baird's method, the sample powder is compressed to a flat cake which is encased by borax powder. Approximately  $1\frac{1}{2}$  gms. of sample is necessary to exceed the critical thickness (Liebhafsky, op. cit. p. 153) for Rb and Sr analyses and in addition  $\frac{1}{4}$  gms. of borax are used. By

modifying Baird's specimen die so that the "loading cylinder" has an internal diameter of only  $15\frac{1}{2}$  mms., it was found that on compression 500 mgms. of feldspar or rock powder more than satisfied the requirements of critical thickness at the SrK $\alpha$  wavelength. This resulted however in the edge of the sample, set within the borax backing being ill-defined and also small parts of the sample tended to be scattered in the borax. It was thus necessary to focus the X-ray beam onto the surface of the sample so that fluorescent radiation is not generated from the ragged margin of the sample. This is discussed further in the following section. These borax buttons were used in the Philips holders PW 1527/20 with some modifications.

During the early stages of the writer's work, using the method of standard additions (discussed on p. 49 ) the sample was directly compressed into the holders, type PW 1527/60, with the aid of the pressing plate and plunger, type PW 1527. For this, approximately  $1\frac{1}{2}$  gms. of sample were required.

The samples in each of the above methods were compressed in an hydraulic press at pressures of about 2300 p.s.i. Experimentation has indicated that over a range of pressures, changes in the fluorescent intensity were insignificant.

(iii) Focusing of X-ray beam

Two different methods were tried:

- (a) the X-ray tube window was reduced to a hole (3 mm. in diameter) and the thickness of the lead window increased so that the incident beam was confined to the central part of the powder in the borax button and therefore a minimum amount of divergent x-rays impinged on the borax backing. Fluorescent radiations were drastically reduced, however.
- (b) a more satisfactory method involved replacing the central ring of the Philips holder PW 1527/20 with a mask of internal diameter,  $13\frac{1}{2}$  mms. This removed the ragged margin of the sample in the borax button from contact with the X-rays. Two pairs of masks were made from electrolytic pure zinc and copper as these prevent Mo and Cr radiation reaching the unexposed part of the sample. Each mask was an exact copy of the circular mask which they replaced in the Philips holder PW 1527/20 except for the smaller internal diameter. The Cu masks were used for Ca, Sr and Rb determinations and the Zn masks for Ba determinations. Towards the end of the writer's work, Al masks with a tungsten backing and internal diameters 2, 5, 10, or 20 mms. were made available by Philips. Two of these

masks (10 mm. in diameter) were used for some Ba determinations.

#### 4. Technique for strontium and rubidium analysis

##### (i) Mass absorption corrections

As indicated previously corrections of  $A_2$  for both unknown and standard samples are necessary. Two methods of correction have been tried. The least successful (Compton scattering technique), introduced by Reynolds (1963) is discussed in Appendix V. A method involving the absolute measurement of the mass absorption coefficient ( $A_2$ ), suggested to the writer by Norrish (op. cit.) proved reliable, and is discussed here.

(a) Theoretical considerations -- consider a parallel narrow beam of monochromatic X-rays (wavelength  $\lambda$ ) with intensity  $I_0$  passing through a planar layer of sample, thickness  $l$  cms., with surfaces normal to the beam direction and more than covering the total beam cross section. Then the emergent intensity  $I$  is given by

$$I = I_0 e^{-ul} \quad . . . . (5)$$

where  $u$  is the linear absorption coefficient of the sample at wavelength  $\lambda$ . Equation (5) is modified in the following way by introducing the density of the sample.



$$\frac{\mu}{\rho} = \frac{\ln_e \frac{I_0}{I}}{\rho l} \dots (6)$$

where  $\mu$  is the mass absorption coefficient at the wavelength  $\lambda$  and  $\rho l$  is the mass / sq. cms. of the sample.

It is possible by making a slight modification to commercially available spectrographic equipment, to make a measurement of  $\frac{I_0}{I}$  and  $\rho l$  for any powdered sample, and therefore  $\frac{\mu}{\rho}$  or what is by analogy  $A_2$ , can be determined at the wavelength of the analytical line (with some restrictions).

- (b) Practical considerations -- an outline of the way in which  $A_2$  is measured at the SrK $\alpha$  wavelength is given as an example. The goniometer is set to receive SrK $\alpha$  radiation, which is achieved by exciting the fluorescent radiation from a sample of SrCO<sub>3</sub> in the normal sample position of the spectrograph. A measurement of the intensity [ $I_0$  in equation (6)] is made. A known weight of sample (in which strontium is to be determined) is compressed into a hole of known area in a plastic slide and this is inserted into the path of the SrK $\alpha$  radiation at position S in Figure II. The attenuated intensity [ $I$  in equation (6)] is measured:  $A_2$  can then be calculated for the sample

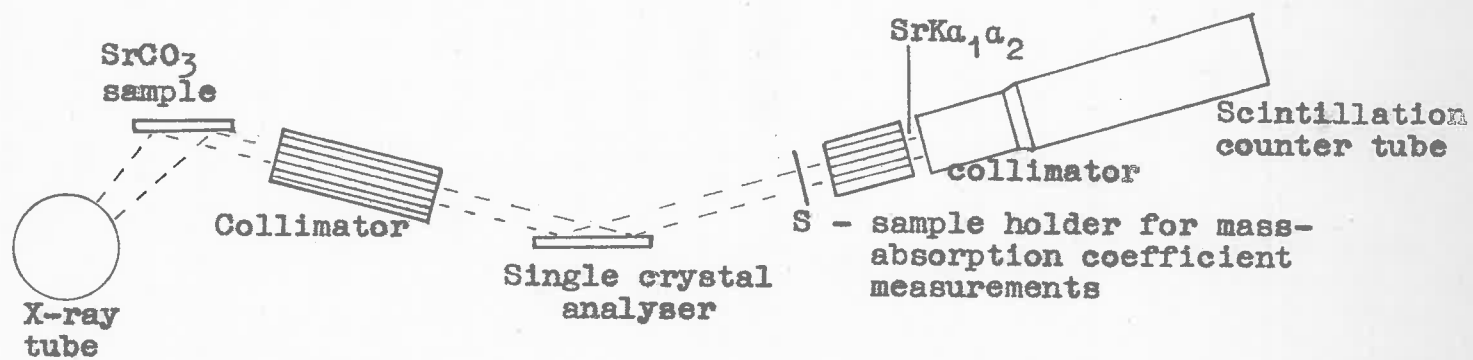


Fig. 11. Basic geometry of an X-ray spectrograph showing the relative position where the mass absorption coefficient is measured.

using equation (6).

An additional piece of apparatus is required so that the plastic slide can be held in the incident X-ray beam.\* This equipment is attached to the goniometer arm of the spectrograph and is placed in front of the exit collimator associated with the scintillation counter. The slightly ragged margin of the sample in the plastic slide is eliminated from the incident X-ray beam by a stainless steel mask.

- (c) Preparation of the sample for measurement of  $A_2$  -- measurement of  $A_2$  is made on a powdered sample ground as discussed on p. 34. The only limitation of the grain size is that if the powder is too coarse a self supporting sample will not form. The sample is compressed into a 1 cm. hole (during the course of the writer's work 12 identical slides, area 1.2521 sq. cms., were used) under a pressure of about 100 p.s.i. A special jig\* is used to press the sample into the slide and this ensures that the sample surfaces are parallel and also perpendicular to the incident beam when inserted into the sample holder. Approximately  $\frac{1}{2}$  gm.

---

\* Details of this apparatus can be obtained from the Geology Department, University of Adelaide.

---

of sample is used\*, the actual weight being measured to four significant places.

Hence knowing the weight of the sample and the area of the hole, the mass / sq. ins. ( $\rho l$  in equation (6)) can be calculated.

- (d) Measurement of  $I_0$  and  $I$  -- strontium carbonate and rubidium chloride were used to generate the incident intensities of SrK $\alpha$  and RbK $\alpha$  respectively. The instrumental conditions are the same as those in Appendix IV for the elemental determinations of Sr and RbK $\alpha$  intensities: the counting strategy is shown in Table 6. The unattenuated counting rate is adjusted to about 60,000 c.p.s., although higher values were used when measuring  $A_2$  of the K-feldspars because of the larger attenuation factors as compared with those of plagioclases.
- (e) Reproducibility of  $A_2$  -- the reproducibility of the  $A_2$  values was checked initially using different  $I_0$  values: in this way the accuracy of the Dead time correction was tested. These results are given in

---

\* After the  $A_2$  measurement has been carried out, the same sample (0.50 gms.) is made into a borax button using the technique discussed on page 34. This sample is then used to measure the Rb, Sr, Ba and Ca fluorescent intensities.

---

Table 6.  $I^*$  and  $I_0^*$  intensity measurements in mass absorption determinations for K-feldspars and Plagioclases.

Feldspar type	Total counts accumulated	
	$I_0$	$I$
K-feldspar	$2 \times 10^5$	$2 \times 10^4$
Plagioclase	$2 \times 10^5$	$2 \times 10^5$

\*  $I$  and  $I_0$  correspond to the same symbols given in equation (6), p. 38 of the text.

Table 7 and it is concluded that the  $A_2$  values at different  $I_0$  values are within the experimental error. Also  $A_2$  measurements were repeated on varying weights of powder and by changing slides. Replicate determinations are given in Table 8. On the basis of this data a relative deviation of .5 - 1.0 per cent can be expected in the  $A_2$  values of all feldspars used in this study.

- (f) Measurement of  $A_2$  at  $\lambda = \text{SrK}\alpha$  and  $\lambda = \text{RbK}\alpha$  --- measurements of  $A_2$  at different wavelengths corresponding to  $\lambda = \text{SrK}\alpha$  and  $\lambda = \text{RbK}\alpha$  (Table 9) indicate a relative deviation of .23 per cent for the ratio  $\frac{A_2(\lambda = \text{RbK}\alpha)}{A_2(\lambda = \text{SrK}\alpha)}$ . Thus measurement of  $A_2$  at either wavelength could be used in Rb and Sr analyses: the writer chose to measure  $A_2$  at the SrK $\alpha$  wavelength, for all unknown samples (Appendix VII).
- (ii) Measurement of analytical line intensities for Rb and Sr analyses.

Each unknown sample was compared against a sample of the standard granite G1 and the intensity measurements on the standard and unknown were made alternatively at the goniometer positions given in Table 10: the total counts accumulated at each position are also given in Table 10. The background intensities on both sides of the peak were averaged and subtracted from the

Table 7. Mass absorption coefficient measurements ( $A_2$ ) at different  $I_0$  values ( $\lambda = \text{SrK}\alpha$ ).

Sample	$I_0$ counts/sec.	$A_2$	$I_0'$ counts/sec.	$A_2'$
221/35 P*	73,665	7.67	36,062	7.64
152/79 P	73,992	7.26	36,483	7.25
OL181 P	74,613	7.26	36,303	7.23
30829 P	72,674	7.53	36,046	7.54
200/561 P	61,256	6.94	37,144	6.92
34611 P	73,597	6.97	35,807	6.93
30829 KF*	73,381	9.27	44,563	9.24
34611 KF	73,733	9.45	44,838	9.46

\* P and KF refer to Plagioclase and K-feldspar, respectively.

Table 8. Replicate determinations of the mass absorption coefficient ( $A_2$ ) using different weight's of powder and different slides ( $\lambda = \text{SrK}\alpha$ ).

Sample	Mass Absorption Coefficient		
221/35 P*	7.66	7.64	7.67
152/79 P	7.24	7.25	
OL181 P	7.24	7.28	
30829 P	7.69	7.67	7.67
34611 P	6.96	6.92	6.95
S 28 P	8.91	8.88	8.90
G1	8.64	8.67	8.65
30829 KF*	9.27	9.24	
34611 KF	9.48	9.46	
30575 KF	9.39	9.25	
152/79 KF	9.46	9.45	
200/561 KF	9.83	9.80	

\* P and KF refer to Plagioclase and K-feldspar respectively.



Table 9. Measurement of mass absorption coefficients at two wavelengths:  $\lambda = \text{SrK}\alpha$  and  $\lambda = \text{RbK}\alpha$ .

Sample	Mass Absorption Coefficient		Ratio $\frac{A_2^{\lambda=\text{RbK}\alpha}}{A_2^{\lambda=\text{SrK}\alpha}}$
	$\lambda = \text{SrK}\alpha$	$\lambda = \text{RbK}\alpha$	
30829 KF*	9.25	10.90	1.1784
34611 KF	9.46	11.128	1.1763
152/79 KF	9.45	11.115	1.1762
221/35 KF	10.27	12.076	1.1759
221/104 KF	9.48	11.180	1.1793
200/423 KF	9.54	11.200	1.1740
221/1 KF	9.65	11.333	1.1744
0L181 KF	9.39	11.085	1.1805
34611 P*	6.94	8.17	1.1772
152/79 P	7.26	8.57	1.1804
221/104 P	7.23	8.53	1.1798
200/423 P	6.92	8.19	1.1835
221/1 P	7.24	8.55	1.1809
S 28 KF	8.90	10.486	1.1781
G1	8.63	10.184	1.1800

$$\text{Mean } \frac{A_2^{\lambda=\text{RbK}\alpha}}{A_2^{\lambda=\text{SrK}\alpha}} = 1.1783$$

$$\text{Standard Deviation} = 26.627 \times 10^{-4}$$

$$\text{Relative Deviation} = .226 \text{ per cent}$$

\* P and KF refer to Plagioclase and K-feldspar respectively.

Table 10. Counting strategy for Rb and Sr, Ba and Ca intensity measurements for both K-feldspars and Plagioclases.

Analysis element	Goniometer position	Intensity measurement	Total counts accumulated	
			K-feldspars	Plagioclases
Rb, Sr	24.24	Background	$2 \times 10^4$	$2 \times 10^4$
	24.97	SrKa	$4 \times 10^4$	$4 \times 10^4$
	25.67	Background	$2 \times 10^4$	$2 \times 10^4$
	26.46	RbKa	$4 \times 10^4$	$4 \times 10^4$
	27.17	Background	$2 \times 10^4$	$2 \times 10^4$
Ba	86.10	TiKa	$4 \times 10^3$	$4 \times 10^3$
	87.15	BaLa1	$4 \times 10^4$	$4 \times 10^3$
	89.5	Background	$2 \times 10^3$	$2 \times 10^3$
Ca	111.5	Background	$2 \times 10^2$	$2 \times 10^3$
	113.09	CaKa	$4 \times 10^3$	$4 \times 10^5, 4 \times 10^4*$
	114.50	Background	$2 \times 10^2$	$2 \times 10^3$

\* For CaO concentrations in plagioclase feldspars in the range 0 - 2 per cent,  $4 \times 10^4$  counts were accumulated at the CaKa peak position. For higher CaO concentrations  $4 \times 10^5$  counts were accumulated.

total peak intensity to obtain the net counting rate for Rb and SrK $\alpha$ .

(iii) Recommended values of Rb and Sr in G1 and W1.

Three samples previously analysed for Rb and Sr by Dr. W. Compston\* using isotope dilution techniques were used to analyse the standard rocks G1 and W1 using the method previously discussed. The recommended values of these standards and the resultant average values for G1 and W1 are given in Table 11. Rubidium and strontium concentrations in the writer's feldspar samples (Appendix VI) are relative to these determined values for G1.

(iv) Precision of Rb and Sr analyses.

Relative deviation of Rb and Sr analyses for the feldspars used in this study (with the exception of Rb analyses in plagioclase feldspars), is 2 per cent. Precision of Rb analyses in plagioclases is closer to 10 per cent. These levels of precision have been calculated from repeated determinations of unknown samples.

5. Technique for barium analysis

(1) Mass absorption corrections

The mass absorption coefficient at the BaLa $\alpha$  wavelength was not measured with the technique outlined

---

\* Department of Geophysics, Australian National University.

Table 11. Recommended values of Rb and Sr for standards used to analyse G1 and W1, and the resultant values on G1 and W1 using the writer's technique discussed in the text.

Sample	Sr p.p.m.	Rb p.p.m.
229 *	356	202
352 *	103	245
S28 *	37.5	522.7
G1 †	257	195
W1 †	216	23

\* Rb and Sr values on these standards were determined using isotope dilution methods (Dr. W. Compston, Australian National University; analyst).

† D. Virgo, analyst.

previously for Rb and Sr wavelengths because of the high degree of absorption. An alternative method of calculating the  $A_2$  values at the BaLa1 wavelength using elemental mass absorption data and the bulk composition of the sample was used.

Calculation of  $A_2$  was made using the following equation:

$$A_2 = W^A A_2^A + W^B A_2^B + \dots + W^m A_2^m$$

where  $W^A$  is the weight fraction of the element;  $A_2^A$  is the mass absorption coefficient of the element A; etc.

These calculations were made at  $\lambda = 2.75\text{\AA}$  (wavelength of the BaLa1 line equals  $2.775\text{\AA}$ ) using the elemental mass absorption data given in the "International Tables for X-ray Crystallography Vol. III". To calculate the  $A_2$  values in this way it is necessary to correct for all major elements but in the case of the writer's feldspar samples, complete chemical analyses were not available. The most important elements absent from the writer's analyses were Si and Al: the elements Ti, Mn, P and Mg can be considered as minor elements in feldspar analyses and can be ignored for the purpose of calculation of  $A_2$ . The Si and Al components were allowed for in the following way for each feldspar type.

(a) K-feldspars -- an average value of the Si and Al contents of microclines and orthoclases was

calculated from feldspar analyses given by Deer et al. (1963 Volume IV Tables 4 and 5). These were Si=29.894 and Al=10.097. The  $A_2$  values of unknown feldspars were calculated using these determined Si and Al values and the K, Na, Ca and derived O values. A better approximation of the  $A_2$  values is obtained by allowing for the presence of Ba: the final Ba values were calculated using these adjusted mass absorption coefficients.

(b) Plagioclases -- the presence of variable quantities of quartz and variable quantities of Si and Al in plagioclases of different anorthite content makes the correction of  $A_2$  for plagioclases more involved. From analyses of albite, oligoclase and andesine feldspars given by Deer et al. (op. cit. Tables 12, 14 and 15) graphs were constructed to indicate the Si and Al contents of plagioclases of different composition. The  $A_2$  values of the plagioclases used in this study were calculated using these determined Si and Al values and the K, Na, Ca and derived O values. A second approximation of the  $A_2$  values using the determined Ba concentration was not carried out.

The calculated  $A_2$  values for both feldspar types are given in Appendix VII. Precision of the

$A_2$  values for K-feldspars and plagioclases respectively is 2 and 3 per cent.

(ii) Measurement of analytical line intensities for Ba analyses

Measurement of the net  $BaLa_1$  intensity involves a correction in addition to subtracting the background intensity. This correction is due to an enhancement effect caused by the overlapping of the  $BaLa_1$  line by the tail of the  $TiKa$  peak. A correction factor is determined to allow for this overlap using a sample containing 100 per cent Ti. This factor is determined for each batch of samples analysed and the percentage overlap at the  $BaLa$  position was 1.7. For unknown and standard samples the intensity of the  $TiKa$  was measured and 1.7 per cent of this intensity subtracted from the  $BaLa_1$  line intensity.

Intensity measurements were made alternatively at the goniometer positions shown in Table 10, on the same sample used to measure Rb and  $SrKa$  intensities: each unknown sample was compared against a sample of the standard granite G1. A fixed count method was employed and the total counts accumulated at each angular position are given in Table 10.

(iii) Recommended value of Ba for G1.

Barium concentrations in the writer's feldspar

samples (Appendix VI) are relative to 1250 p.p.m. Ba in G1 (Taylor and Kolbe, 1964). This absolute value was checked against a laboratory standard phlogopite containing 1.05 per cent BaO. The writer's determinations were within 3 per cent of the recommended value for G1.

(iv) Precision of Ba analyses

Calculated relative deviation of Ba analyses, determined from replicate analyses of unknown samples is 3 and 5 per cent for K-feldspars and plagioclases respectively, at the concentration levels in the feldspars used in this study.

6. Technique for calcium analysis

(1) Theoretical considerations

In the analysis of powdered samples by X-ray spectrography, it is possible to regard the matrix of the sample as constant except for the variable being determined which may be an element, a compound or a mineral. In these cases calibration curves can be used which are unaffected by unknown "matrix effects"; in other words the  $A_2$  value in equation (4) for the unknown can be considered constant in a suite of samples. Provided standards of similar bulk composition to the unknowns are used the  $A_2$  values of the standards can also be regarded as the same as the unknowns. The writer has found that calcium analyses in K-feldspars



and plagioclases can be treated in this way and linear calibration curves have been constructed using feldspars as standards and CaO as the variable quantity.

(ii) Absorption effects

An important absorption effect in calcium analyses using the CaK $\alpha$  line, is absorption of CaK $\alpha$  intensity by the K absorption edge of potassium. The effect of potassium is to reduce the CaK $\alpha$  intensity by an amount dependent on the potassium concentration. In view of this effect calcium analyses cannot be reliably made in materials containing significant quantities of both potassium and calcium. It is possible to quantitatively determine calcium in both feldspar types because:

- (a) in plagioclases where the K content is low, the above absorption effect can be ignored.
- (b) in K-feldspars, although the K content is high, the absorption effect on the CaK $\alpha$  intensity can be ignored due to the low Ca content in the K-feldspars.

Both (a) and (b) above have been verified in practice.

(iii) Measurement of analytical line intensities for Ca analyses

Intensity measurements were made at the goniometer positions given in Table 10 on the same sample used to measure Rb and SrK $\alpha$  intensities. A fixed

count method was employed and the total counts accumulated at each goniometer position are also given in Table 10. For each sample, the intensities at both background positions were averaged and subtracted from the total CaK $\alpha$  intensity, to obtain the net CaK $\alpha$  counting rate.

The calcium concentrations of the unknown feldspar samples were read directly from respective calibration curves for K-feldspars and plagioclases: each unknown sample was measured against a standard of similar CaO concentration. Before the unknown CaO concentration was determined a correction of the net CaK $\alpha$  intensity was usually made depending on the change in counting rate of the reference standard, from that used initially to construct the curve.

(a) Calibration curve for plagioclase feldspars -- for plagioclase feldspars the calibration curve was constructed using plagioclase samples previously analysed by the titrimetric method discussed on p. 28. The data used to construct the curve is given in Table 12: the CaK $\alpha$  intensities are averages carried out during the course of the writer's work. A linear relationship between "per cent CaO" and "counts / sec" is obtained although the graph does not pass through the origin

Table 12. Data used to construct the calibration curve for plagioclase feldspars.

Sample	Net CaK $\alpha$ intensity counts/sec.	CaO content (per cent)		Deviation
		Chemical*	X-ray estimate	
OL181	3410	3.56	3.50	- .06
221/104	3547	3.71	3.68	- .03
30829	5273	5.43	5.43	0
34611	1098	1.12	1.08	- .04
221/35	5694	5.78	5.90	+ .12
152/79	3036	3.23	3.10	- .13
200/423	2368	2.47	2.41	- .06
185/706	4559	4.69	4.70	+ .01
185/784	3038	3.28	3.11	- .17
Frit 1†	6160	6.30	6.38	+ .05

Standard deviation = .008 per cent CaO.

\* D. Virgo, analyst.

† Synthetic plagioclase.

due to a small blank correction. The expression relating the above two variables is

$$\text{per cent CaO} = \frac{\text{counts / sec} - 96.45}{992.84}$$

To provide a measure of the accuracy of the calibration curve, the positive and negative deviations between the chemical and X-ray estimates of the analysed feldspar samples were treated statistically assuming the titrimetric values to be correct. Relative deviation of these X-ray results from the wet chemical values were calculated assuming  $\bar{x} = 1.0\%$  CaO,  $\bar{x} = 3.0\%$  CaO and  $\bar{x} = 6.0\%$  CaO, to cover the range of CaO in most feldspars used in this investigation. The relative deviations are:

$$C_{1.0\%} = .8$$

$$C_{3.0\%} = .26$$

$$C_{6.0\%} = .13$$

Similar relative deviations of the CaO concentrations of the unknown plagioclase sample in Appendix VI are expected.

(b) Calibration curve for K-feldspars — initially it was necessary to obtain several feldspar standards containing reliable, low CaO contents (i.e. <.5% CaO). The CaO content of two feldspar samples was determined using the method of

additions. Four additions of spec-pure  $\text{CaCO}_3$  were made to both a potassium rich (A.U. 17263\*) and a sodium rich feldspar (A.U. 16949\*) and the mixing was carried out under acetone in an alundum mortar. The results of this work are given in Table 13. The CaO concentration of each addition has been calculated using the following equation:

$$\text{p.p.m. CaO} = C \times \frac{I_1}{I_2}$$

where C is the increase in CaO concentration of each addition;  $I_1$  is the CaK $\alpha$  intensity of the feldspar 16949 or 17263 and  $I_2$  is the increase in intensity of the net CaK $\alpha$  line of each addition due to addition of CaO.

The relative deviation of the mean CaO value for the feldspars 17263 and 16949 is 4.2 and 3.2 per cent respectively. These two feldspars and in addition N.B.S. 99 soda feldspar, and N.B.S. 70 K-feldspar were used to construct a calibration curve. The data used to construct the curve is given in Table 14: a linear curve is obtained between "per cent CaO" and "counts / sec" although the graph does not pass through the origin.

---

\* Feldspar standards established in the Geology Department, University of Adelaide.

---

Table 13. Results of method of additions\*, applied to Feldspars 17263 and 16949

K-feldspar 17263 Sample	Increase in percent CaO	$\frac{\text{wt. CaO added}}{\text{wt. of K-feldspar 17263 + wt. of CaCO}_3 \text{ added}}$	Net CaK $\alpha$ intensity counts/sec.	P.p.m. CaO in K-feldspar 17263
Feldspar 17263		0	97.5	
Addition 1		.156	268.1	890
Addition 2		.384	492.5	950
Addition 3		.778	839.5	970
Addition 4		1.071	1171.4	980

Mean = 947 p.p.m.

Standard deviation = 20 p.p.m.

Relative deviation = 4.2 per cent

Na-feldspar 16949 Sample	Increase in percent CaO	$\frac{\text{wt. CaO added}}{\text{wt. of Na-feldspar 16949 + wt. of CaCO}_3 \text{ added}}$	Net CaK $\alpha$ intensity counts/sec.	P.p.m. CaO in Na-feldspar 16949
Feldspar 16949		0	410.7	
Addition 1		.361	931.0	2851
Addition 2		.879	1709.0	2781
Addition 3		1.235	2177.0	2872
Addition 4		1.794	2984.8	2862

Mean = 2845 p.p.m.

Standard deviation = 45 p.p.m.

Relative deviation = 3.2 per cent

\* This method was carried out using  $1\frac{1}{2}$  grams of powdered sample compressed directly into the Philips holder PW 1527/60. However, in constructing the calibration curve for K-feldspars (p. 13 in the text), using feldspars 17263, 16949, NBS 70 and NBS 99, the normal method of sample preparation using 500 mgms. of sample was used.

Table 14. Data used to construct the calibration curve for K-feldspars.

Sample	CaK $\alpha$ intensity counts/sec.	CaO content p.p.m.		Deviation
		Recommended value	X-ray estimate	
NBS 99	403	3,630	3,550	- 80
NBS 70	153	700	800	+ 100
Feldspar 16949	350	2,845	2,990	+ 145
Feldspar 17263	171	947	1,000	+ 53
Plagioclase 34611	1098	11,200	11,200	0
Filter paper pulp	62.2			
Pure Qtz	78.7			
Synthetic albite	87			

Standard deviation = 90 p.p.m. CaO.

Measurement of the CaK $\alpha$  intensity on several materials (Table 14) chosen to contain no calcium, indicate that the deviation of the calibration curve from the origin is due to a slight impurity of calcium fluorescent radiation in the incident beam. In this case the equation relating the variables "per cent CaO" and "counts / sec" is

$$\text{per cent CaO} = \frac{\text{counts / sec} - 80.8}{909}$$

The deviations between the CaO values of these standards read from the calibration curve (X-ray estimate in Table 14) and the recommended values assuming the latter to be correct were treated statistically. Relative deviations of these X-ray values from the recommended values assuming  $\bar{x} = 1000$  p.p.m. CaO and  $\bar{x} = 3000$  p.p.m. CaO are:

$$C_{1000 \text{ p.p.m.}} = 9.0$$

$$C_{3000 \text{ p.p.m.}} = 3.0$$

Similar relative deviations of the CaO concentrations of the unknown K-feldspar samples in Appendix VI are expected.



DISTRIBUTION OF SODIUM

### A. INTRODUCTION

As previously stated (this text p. 5) Barth suggested that the distribution of sodium between coexisting feldspars approximates to the Nernst distribution law and that different average  $Kd_{Ab}^*$  values could be correlated with temperature differences.

To test this hypothesis the distribution of sodium between coexisting feldspars from different grades of metamorphism in several areas has been measured and the results and discussion are included in this chapter.

Application of the "Barth geothermometer" by Heier (1960) and Engel and Engel (1960) to granulite-amphibolite facies rocks is re-examined in the light of the writer's findings.

### B. RELATIONSHIP BETWEEN SODIUM PARTITION COEFFICIENTS AND METAMORPHIC GRADE.

Compositions of coexisting feldspars from the rocks studied by the writer are given in Tables 21 - 23 and 26 - 29 (Appendix VIII). The K-feldspar compositions have been recalculated to 100 per cent in terms of Or and Ab and the plagioclase compositions in terms of Ab and An end-members. In this way the sodium partition coefficients are analogous to those computed by Barth (1956), Heier (1960) and Engel and Engel (1960). Data given by Heier and Engel and Engel

---

\* See page 12.

---

relating to coexisting feldspars from Langöy, Northern Norway and Adirondack lowlands, New York respectively are also presented (Tables 24 and 25, Appendix VIII). The deduced temperatures of equilibration using the "Barth geothermometer" are given with the determined partition coefficients in all Tables.

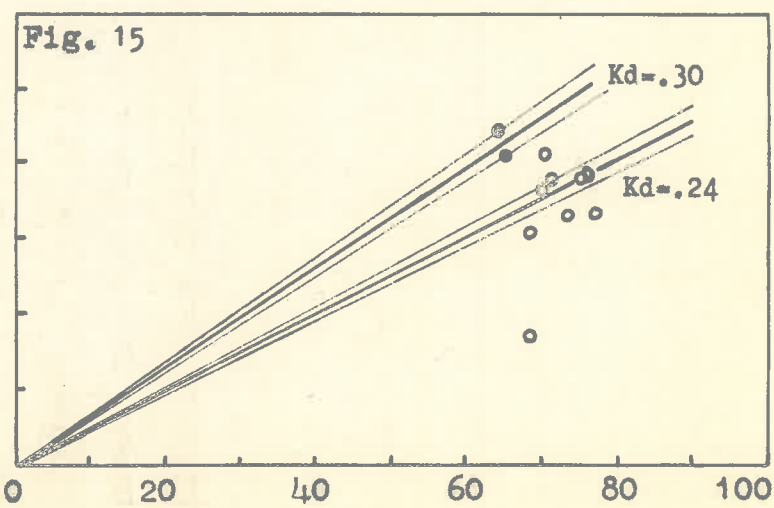
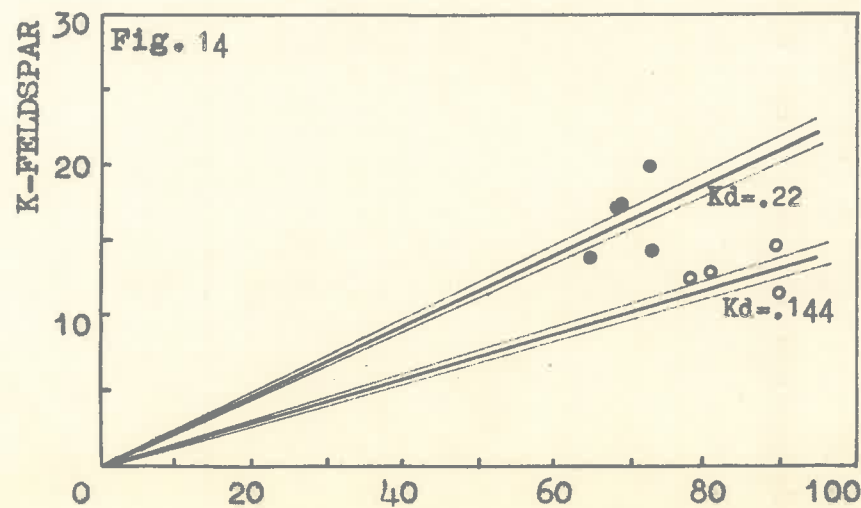
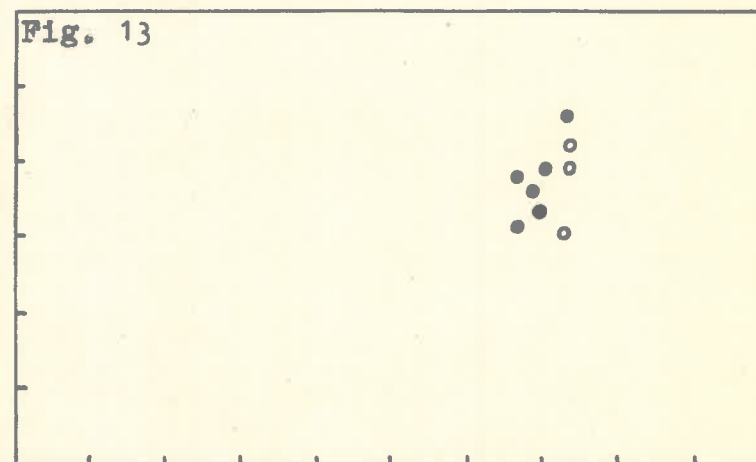
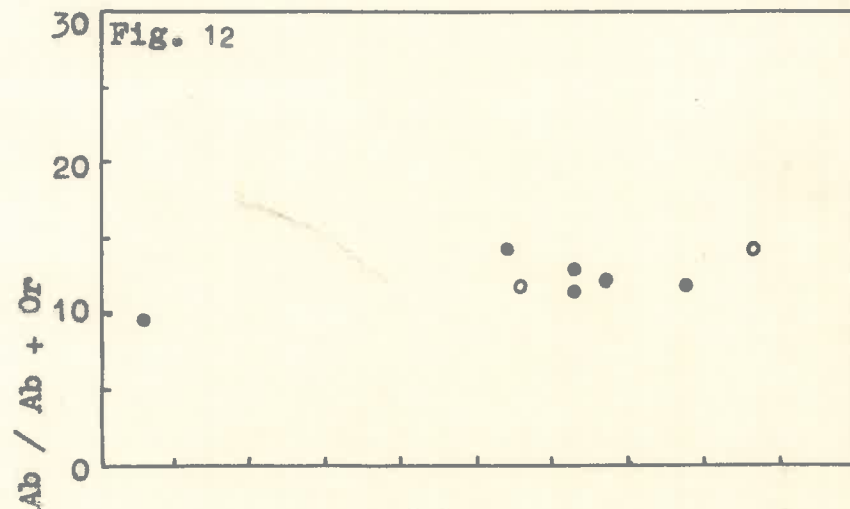
1. Granulite - amphibolite facies areas

Data from the Broken Hill, Musgrave Range, Ceylon, Adirondack lowlands and Langöy, Northern Norway areas are given in Tables 21 - 25 and summarized in the distribution diagrams, Figures 12 - 16 respectively. In each of these areas samples were analysed from the granulite and amphibolite facies. From the Broken Hill and Musgrave Range areas (Figures 12 and 13) it is evident that there is considerable scatter of sodium distribution coefficients in isofacial rocks. Furthermore there is no significant difference even in average  $Kd_{Ab}$  values between the metamorphic zones of each area. Data from the Ceylon, Adirondack lowlands and Langöy areas plotted in Figures 14, 15 and 16 indicate that for isofacial rocks an equilibrium partition is also not achieved although there are different average  $Kd_{Ab}$  values between the metamorphic zones in each area. This is shown in these figures by lines drawn as representing the distribution law, assuming that it is applicable, through the cluster of points representative of each metamorphic zone. Scatter of

Figures 12 - 15 refer respectively to the following areas:  
Broken Hill, Musgrave Range, Ceylon and Adirondack lowlands.  
In these figures, the symbols used refer to

- Granulite facies
- Almandine-amphibolite facies

Data used to plot these Figures is given in Appendix VIII.



PLAGIOCLASE Ab / Ab + An

Distribution of Albite between K-feldspar and Plagioclase

distribution points outside the estimated experimental error is shown by a  $\pm 4$  per cent range in  $Kd_{Ab}$  in Figures 14, 15 and 16. In the Langöy area lines are drawn representing only the rocks from the almandine - amphibolite facies and both groups of granulite facies (Groups VIII, IX and V, III respectively, Table 25).

## 2. Almandine - amphibolite facies areas

Coexisting feldspars from schists, gneisses and migmatites from the sillimanite - almandine - muscovite and sillimanite - almandine orthoclase sub facies of the Kanmantoo group, Mt. Lofty Ranges, South Australia are given in Tables 26 - 29 and summarized in the distribution diagrams in Figures 17, 18 and 19. In these Figures the scatter is smaller than in Figures 12 - 16, although still considerable and generally not indicative of an equilibrium distribution according to the Nernst distribution law.

In comparison with the rocks from the upper amphibolite facies of the amphibolite - granulite facies areas discussed above, it is evident that the distribution coefficients for rocks from the Kanmantoo group are lower [though compare data from the Reedy Creek area\* (Table 29, Figure 19)]. No

---

\* A systematic collection of material in this area was not undertaken. Samples 221/104 and 221/35 can be regarded respectively as typical of the migmatites and granite gneisses in this area, and the grade of metamorphism is upper almandine - amphibolite facies (Sando, 1957).

---

Figures 16 - 19 refer respectively to the following areas:  
Langöy, Pewsey Vale, Springton and Palmer (P) and Reedy  
Creek(RC).

The symbols used in the respective figures refer to:

Figure 16  $\Delta$  Granulite facies (Group III Table 25).

● Granulite facies (Group V Table 25).

+ Retrograde samples (Group IV Table 25).

x Transitional rocks (Group VII Table 25).

○ Upper Almandine-amphibolite facies (Group  
VIII Table 25)

◊ Lower Almandine-amphibolite facies (Group  
IX Table 25).

Figure 17 ● Sillimanite-almandine-K-feldspar sub facies.

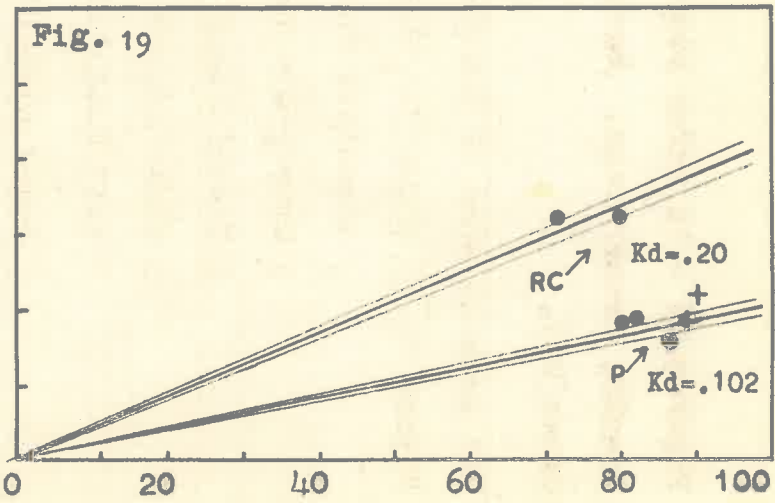
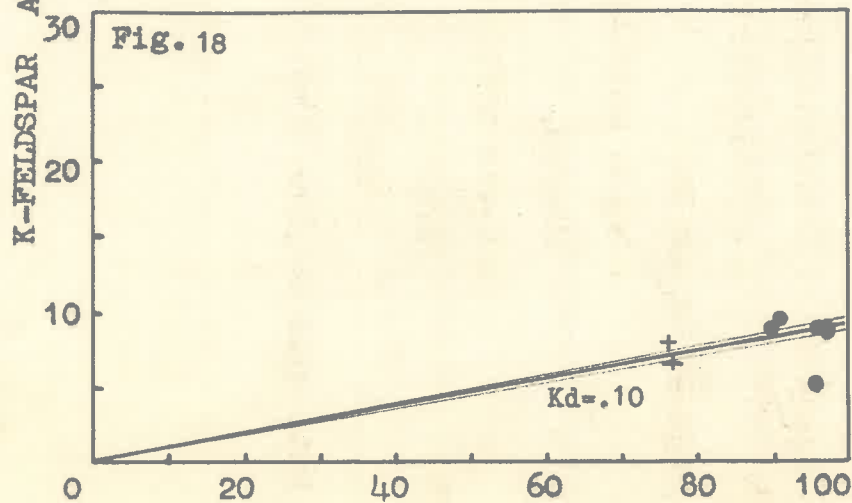
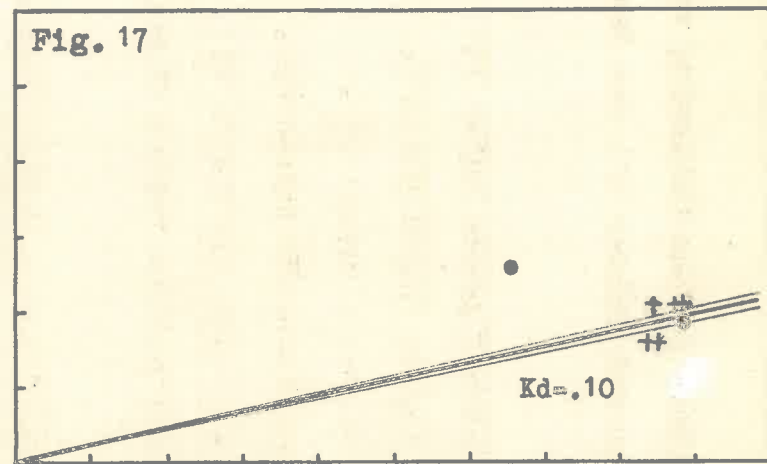
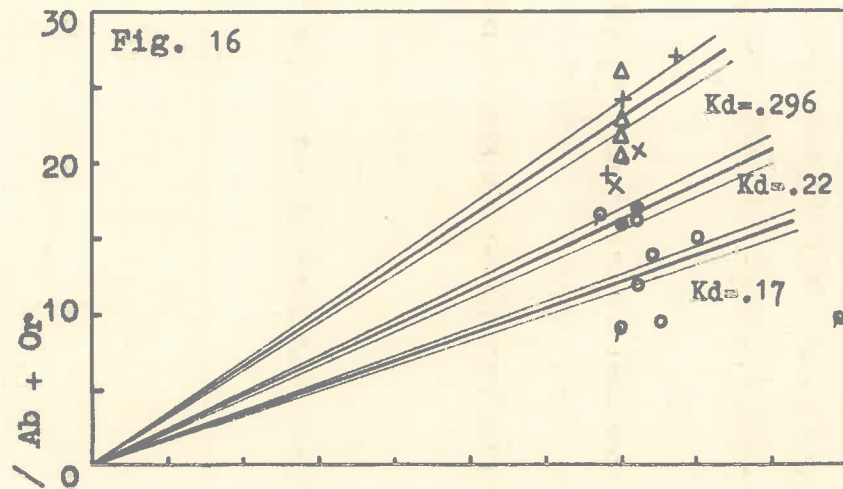
+ Sillimanite-almandine-muscovite sub facies.

Figures 18 and 19

● Upper sillimanite-almandine-muscovite sub  
facies.

+ Lower sillimanite-almandine-muscovite sub  
facies.

Data used to plot these figures is given in Appendix VIII.



Distribution of Albite between K-feldspar and Plagioclase



systematic differences occur in the sodium distribution coefficients of samples from different metamorphic grades within each of the Palmer and Springton areas (see discussion of Sr partitioning from these two areas, Chapter VII).

### 3. Discussion

Barth (1956) indicated that although sodium distribution between feldspars is not ideal there is an approach to the Nernst distribution law such that different  $Kd_{Ab}$  values can be correlated with temperature differences.

But the writer's data is not in accordance with this hypothesis. In most cases the scatter of sodium partition coefficients for isofacial rocks is well outside that predicted for equilibrium partitioning and also in some instances average  $Kd_{Ab}$  values are insensitive to changes in metamorphic grade. Furthermore significantly different average  $Kd_{Ab}$  values for feldspars from rocks of the amphibolite and granulite facies in Ceylon are not in agreement with the field relationships between the two facies rocks (see Chapter III p. 19), and also the inferred temperature differences from the Barth geothermometer are inconsistent with the results of strontium partitioning between these same feldspars (see Chapter VII p. 83). Hence it is thought that the sodium partitioning in the Ceylon feldspars may not follow the Nernst distribution law.

In the Langöy area several discrepancies occur between

the average  $Kd_{Ab}$  values and metamorphic grade. The charnockitic granulites (Group V Table 25) have significantly lower  $Kd_{Ab}$  values than the lower grade rocks of Group VII. Also rocks of Group IV have been affected by retrogressive metamorphism and have mineral assemblages characteristic of all facies between granulite and epidote - amphibolite facies: yet  $Kd_{Ab}$  values for two samples of this Group viz. 318/55 and 238/55 which exhibit almandine amphibolite facies mineral paragenesis are higher than for the unaffected charnockitic granulites (Group V Table 25). Also, Heier (1960 p. 149) on the basis of the "Barth geothermometer" has attempted to account for the large temperature range within the granulite facies (given by the feldspars from the rocks of Groups III and V, Table 25) by the preferential loss of sodium by exsolution from the fine grained K-feldspars in the rocks of Group V in contrast with less loss from the porphyroblastic K-feldspars in the rocks of Group III. He prefers this explanation of the large temperature differences within the granulite facies to one invoking steep temperature gradients in the deep zones of high grade metamorphism. It is evident that many anomalies occur in this area when the average  $Kd_{Ab}$  values are compared with the known metamorphic grade.

Also the relatively high average  $Kd_{Ab}$  value in the Reedy Creek area compared with other rocks from the Kanmantoo group does not conform to the known metamorphic history of

the area. This anomaly would seem to indicate, contrary to recommendations by Dietrich (1961 p. 16), the unreliability of the Barth geothermometer even within small areas of regional metamorphism.

In view of the assumptions by Barth (1956) and subsequent application of the feldspar geothermometer by Heier (op. cit.) and Engel and Engel (op. cit.) some explanation of sodium partitioning is necessary because of the degree of variability of the  $Kd_{Ab}$  values in most instances.

The non-conformity of sodium distribution with the Nernst distribution law may be a function of one or more of the following more important possibilities\*.

- (1) Variations in the temperature of equilibration or quenching within a group of feldspar pairs.

On the basis of the hypothesis it is necessary to postulate steep localized temperature gradients. However, the variability of albite distribution coefficients due to different physical conditions (pressure and temperature) is not consistent with the regular trace element partitioning between the same coexisting feldspars (Chapter VII) nor with major element partitioning between coexisting pyroxenes in associated basic rocks from the Musgrave Range and Broken Hill areas (see Chapter VII p. 90).

---

\* See also Dietrich (1961 p. 15).

---

- (ii) Chemical equilibrium was not established between all feldspar pairs from a given area or it was not retained.

Evidence for lack of equilibrium is seen in samples from the Adirondack lowlands area (Engel and Engel, 1960 p. 12). However large scale disequilibrium factors are guarded against by using small volumes of rock (see also p. 24).

- (iii) Non infinite dilution.

Infinite dilution is generally a condition for the Nernst distribution law but Barth (1956) suggests that although the distribution of sodium between feldspars would not be ideal within the range  $Ab_{5-35}$  in the plagioclase and  $Ab_{10-30}$  in the K-feldspar, an approach to the Nernst distribution law can be expected.

- (iv) Influence of bulk composition.

Winkler (1961), amongst others, indicates from some experimental work (briefly discussed in Chapter I p. 6) that the bulk rock composition (including all the major components of common metamorphic rocks) is important in controlling feldspar compositions. The writer concurs with these conclusions of Winkler.

Before the influence of compositional factors on the writer's data is discussed however, it is worthwhile to consider the results of some detailed experiments designed

to test the Barth geothermometer, and carried out by Mr. P. Slade in the writer's laboratory. The results from these experiments have an important bearing on the writer's data since the effects of both temperature and bulk composition have been investigated.

C. EXPERIMENTAL DETERMINATION OF CATION EXCHANGE  
BETWEEN COEXISTING FELDSPARS.

Experiments carried out by Mr. P. Slade have been concerned with the partitioning of the major elements Ca, K and Na and the trace element Sr between coexisting feldspars within a closed system. Synthetically made feldspars (compositions given in Table 15) are contained separately at each end of a sealed platinum phial in a "cold-seal bomb": physical admixture of these materials is prevented but elemental exchange between the feldspars is possible by way of a liquid phase (composition also given in Table 15). In these experiments a pressure of 17,000 p.s.i. has been used and the feldspar compositions have been determined at various temperatures. Some results are given in Table 15.

It is clear that in a system of fixed bulk composition,  $Kd_{Ab}$  increases with increasing temperature linearly, but that in systems of certain different bulk composition at the same temperature,  $Kd_{Ab}$  is different.

Changes in resultant feldspar compositions in these synthetic experiments with changes in temperature and bulk

Table 15.

- \* Experiments 26 and 23 were duplicated, and the  $Kd_{Ab}$  values were found to be identical. An approximate  $\pm 2$  per cent range in  $Kd$  can be expected on the basis of analytical errors, alone.

Data from Experiment 30 is not plotted in Figure 20, as these results were obtained after this Figure was drafted.

Table 15. Results of some cation exchange experiments designed to test the Barth geothermometer.

Experiment number	Composition of the vapour phase	Temperature °C	Starting Materials		Distribution coefficient $K_{dAb}$
			K-feldspar	Plagioclase	
10	.5% SrCl <sub>2</sub> in water	520	Or80 Ab20	An30 Ab70	.068
8	" "	660	Or80 Ab20	An30 Ab70	.262
7	" "	777	Or80 Ab20	An30 Ab70	.363
11	" "	880	Or80 Ab20	An30 Ab70	.448
24	" "	515	Or80 Ab20	An15 Ab85	.115
25	" "	650	Or80 Ab20	An15 Ab85	.242
26	" "	765	Or80 Ab20	An15 Ab85	.358
28	" "	840	Or80 Ab20	An15 Ab85	.446
21	.5% SrCl <sub>2</sub> in an alkali soln. such that $\frac{K}{K+Na} = 30\%$	515	Or100	An30 Ab70	.115
23	" "	650	Or100	An30 Ab70	.186
20	" "	515	Or93 Ab7	An30 Ab70	.100
30	.5% SrCl <sub>2</sub> in water	520	Or80 Ab20	An75 Ab25	.260

composition are diagrammatically represented in Figure 20 and are to be compared later with similar changes in natural systems. In this Figure the distribution coefficient  $Kd_{Ab}$ , calculated as stated on p. 52 is plotted against the resultant feldspar compositions in terms of the An and Or contents of the plagioclase and K-feldspar respectively. It can be seen that for a given bulk composition and in the range of temperatures studied the An/Ab ratio of the plagioclase remains approximately constant whereas the Ab/Or ratio of the K-feldspar increases with increasing temperature: thus the  $Kd_{Ab}$  value changes. The effect of different bulk compositions at a given temperature is to shift the plagioclase feldspar compositions across the Figure, irregularly in those instances where  $Kd_{Ab}$  has changed: the change in K-feldspar composition in systems of different bulk composition is comparatively small. In these experiments it is inferred that in systems of different bulk composition, the concentrations of sodium, potassium, and calcium are the important factors in limiting the  $Kd_{Ab}$  values at a given temperature.

On the basis of these experiments Mr. Slade has concluded that  $Kd_{Ab}$  values for natural coexisting feldspars are unreliable as temperature indicators because of sensitivity to bulk composition. The writer's data are now further examined in the light of conclusions deduced from



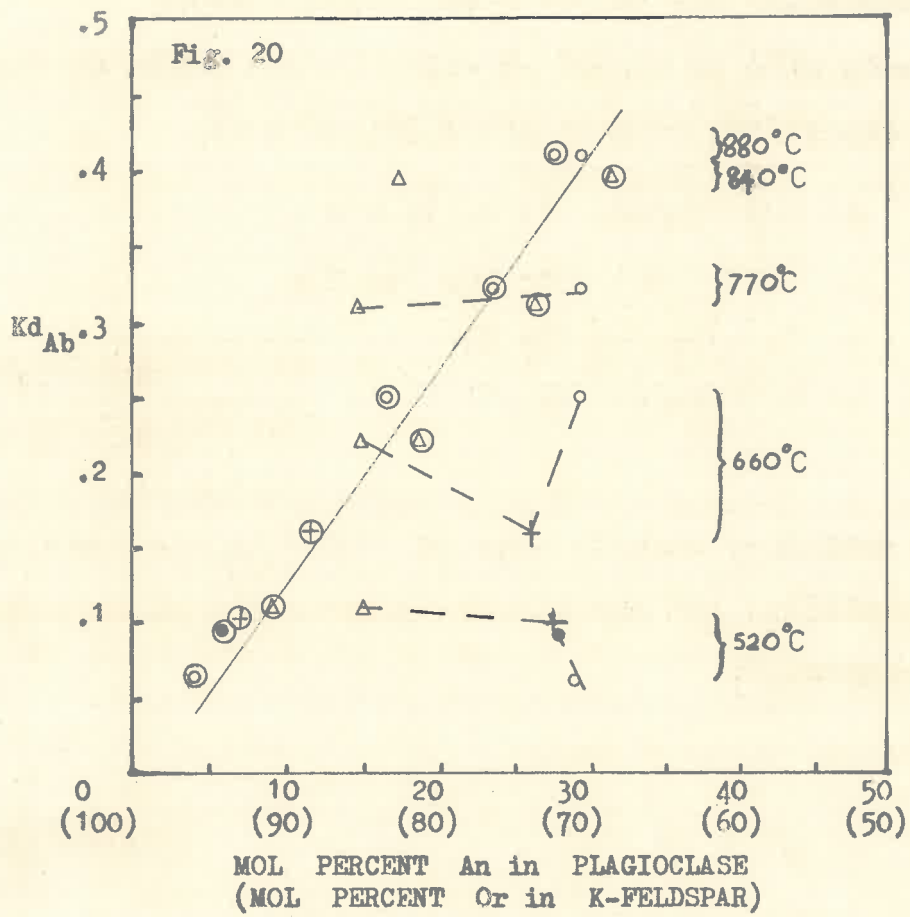
Figure 20

Plot of the Distribution coefficient ( $Kd_{Ab}$ ) versus the resultant K-feldspar and Plagioclase compositions, determined experimentally in systems of different bulk compositions and at different temperatures.

Symbols used in Figure 20 refer to the following respective experiment numbers given in Table 15.

- Experiments 10, 8, 7, 11.
- △ Experiments 24, 25, 26, 28.
- + Experiments 21, 23.
- Experiment 20.

The encircled symbols e.g. ⊕ refer to the K-feldspar compositions and the others refer to the plagioclase compositions.



these synthetic experiments in relationship to the effects of temperature and bulk composition.

D. THE EFFECT OF ENVIRONMENTAL FACTORS ON THE SODIUM DISTRIBUTION COEFFICIENT.

1. Relationship of  $Kd_{Ab}$  and feldspar composition.

If sodium obeys the Nernst distribution law its distribution coefficient should be independent of the composition of the plagioclase and K-feldspar.

In Figures 21 - 25  $Kd_{Ab}$  values for the feldspar pairs from the Broken Hill, Pewsey Vale, Musgrave Range, Springton, Palmer and Reedy Creek areas are plotted against the Or and An contents of the coexisting K-feldspar and plagioclase respectively. Within a single diagram an average line has been drawn through the points to indicate the relationship between  $Kd_{Ab}$  and feldspar compositions: although the scatter is considerable the overall trends are rather similar. Some generalizations can be drawn:

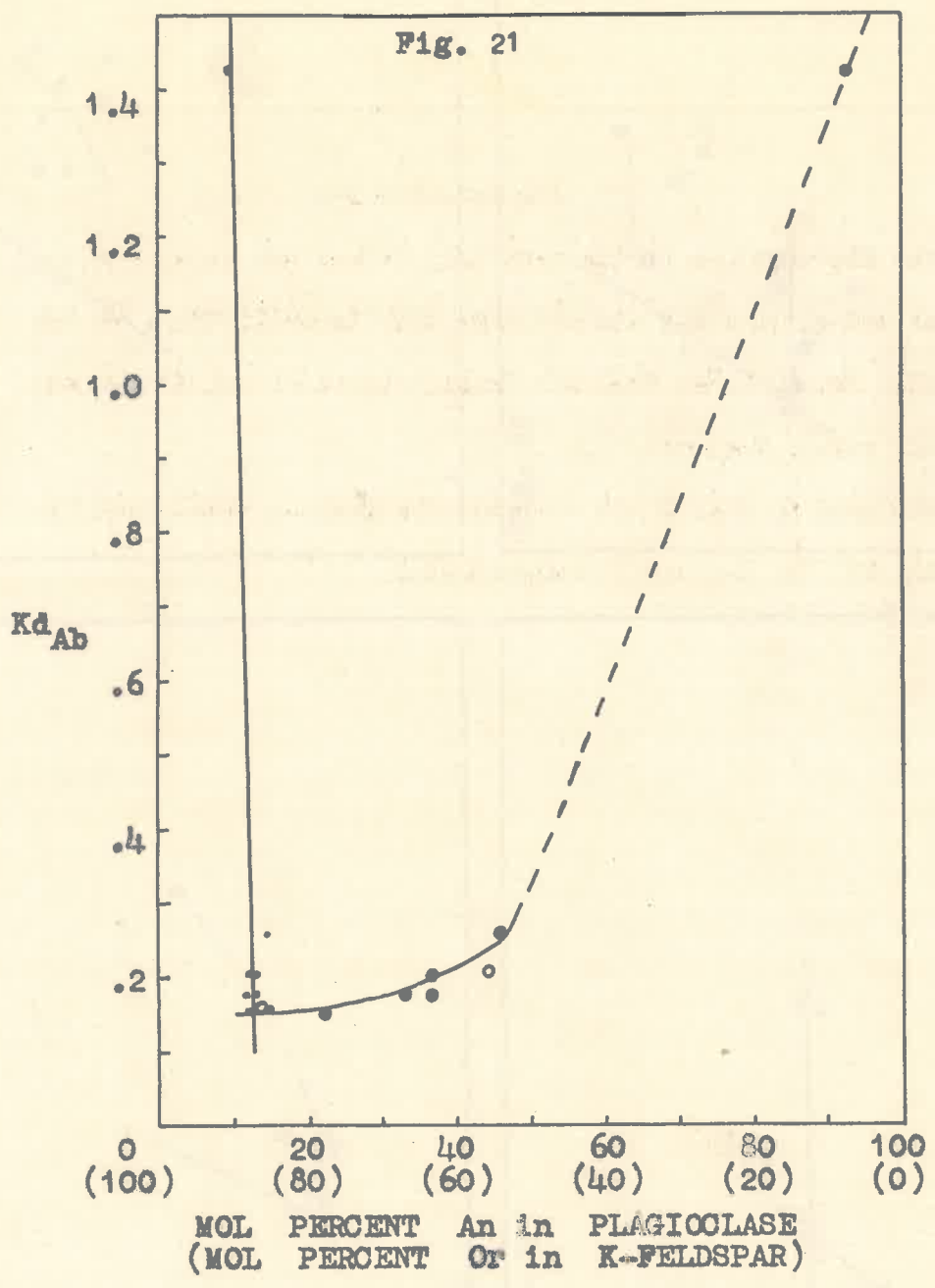
- (a) For plagioclase compositions less calcic than about  $An_{24}$  the distribution coefficient for any single area tends to be constant but even in these cases the scatter of  $Kd_{Ab}$  values is generally outside the experimental error, i.e.  $\pm 4$  per cent range in the  $Kd_{Ab}$  value.
- (b) For plagioclase compositions more calcic than  $An_{24}$  the distribution coefficient varies with anorthite content in fairly regular manner, although curves from

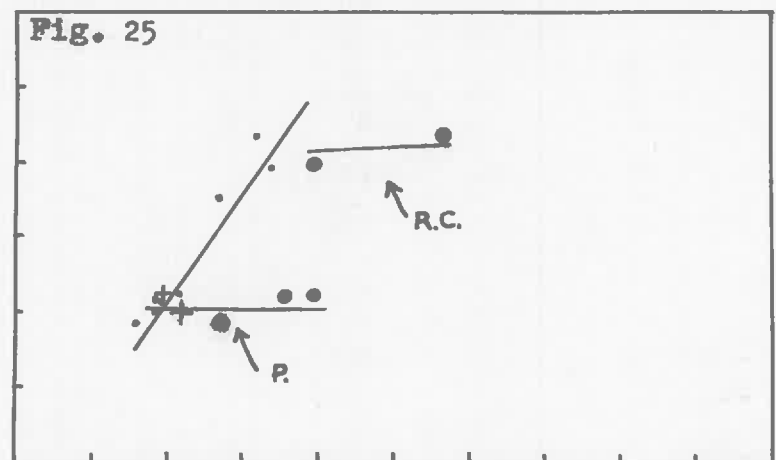
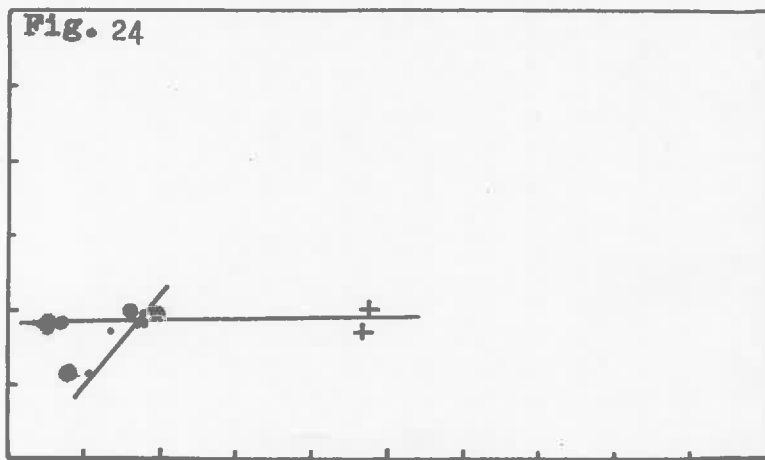
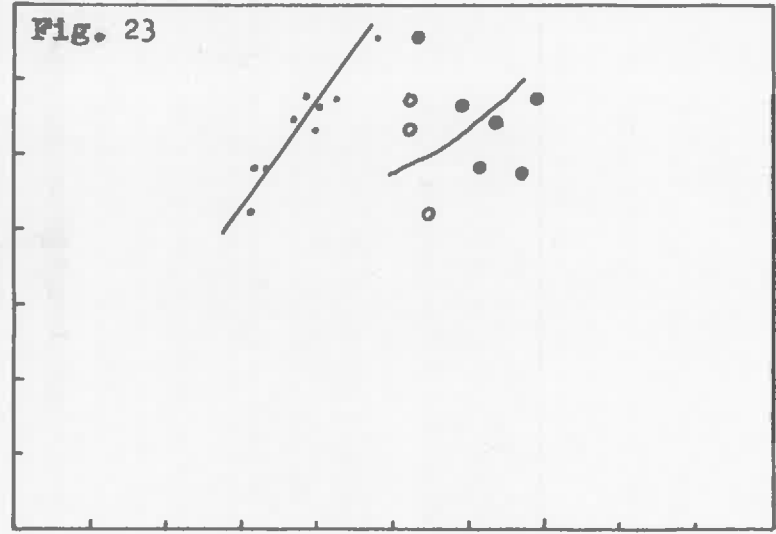
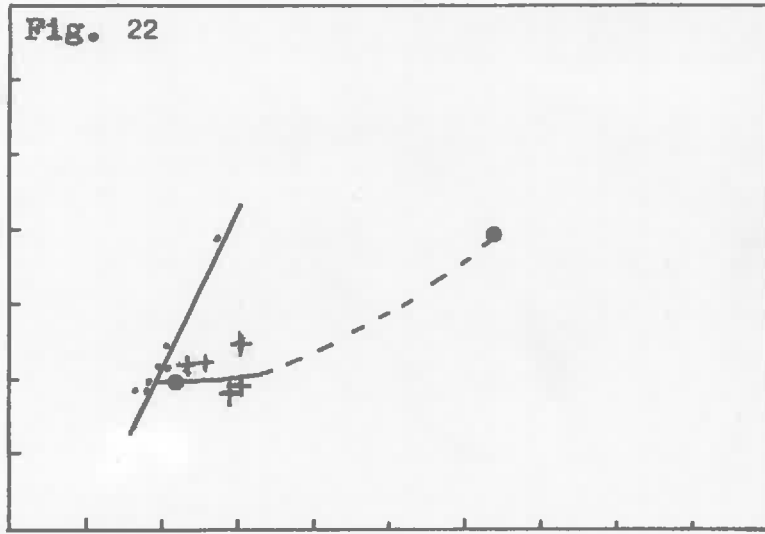
Figures 21 - 25.

Plot of the distribution coefficient ( $K_d$ ) versus the determined K-feldspar and plagioclase compositions from Appendix VIII, for the Broken Hill, Pewsey Vale, Musgrave Range, Springton and Palmer and Reedy Creek areas, respectively.

The symbols used in Figures 21 - 25 are the same as those used in Figures 12, 17, 13, 18, and 19 respectively for the plagioclase compositions; the small dots in all figures refer to the K-feldspar compositions.

Fig. 21





0 (100) 10 (90) 20 (80) 30 (70) 40 (60) 50 (50) 0 (100) 10 (90) 20 (80) 30 (70) 40 (60) 50 (50)

MOL PERCENT An in PLAGIOCLASE  
(MOL PERCENT Or in K-FELDSPAR)

different areas are displaced along the ordinate direction.

- (c) It is evident that the  $Kd_{Ab}$  values show a linear relationship with the Or content of the K-feldspar at least within the compositional range available. The variation in  $Kd_{Ab}$  is similar and comparable in the different graphs e.g. at  $Or_{85}$   $Kd_{Ab}$  is approximately 0.2.

## 2. Discussion

Coexisting feldspars in rocks from the same grade of metamorphism should show constant distribution coefficients which are also independent of the feldspar compositions, but examination of the graphs (e.g. Figures 21 - 23) indicates that this is not the case.

The relationship between  $Kd_{Ab}$  and the K-feldspar composition in natural isofacial systems is directly comparable to the same relationship observed in previously discussed synthetic experiments in systems of uniform temperature and different bulk compositions (e.g. see Figure 20 with reference to experiments at  $520^{\circ}C$ ). An interpretation of  $Kd_{Ab}$  - K-feldspar composition relationships in natural systems in terms of bulk composition effects is therefore inferred. Experimentally this same trend is observed with changes in temperature, but the different  $Kd_{Ab}$  values in natural systems cannot obviously be correlated with temperature changes since the rocks have come from the one grade of

metamorphism.

With regard to plagioclase -  $Kd_{Ab}$  relationships, data from natural and synthetic systems are partly comparable: a scatter of points in systems of different bulk compositions and at the same temperature in Slade's synthetic experiments (see Figure 20) has been previously noted and can be compared with the variability of  $Kd_{Ab}$  values for isofacial rocks, in natural systems. It is the writer's hypothesis that the cause of this scatter is the same in both systems viz. bulk composition effects. The average trend of increasing  $Kd_{Ab}$  with increasing An content of the plagioclase, observed in some natural systems (viz. Figures 21, 22 and 23) is not noted from the synthetic experiments carried out to date. In terms of the writer's hypothesis the significantly different  $Kd_{Ab}$  values in these natural systems are due to large changes in the bulk composition, resulting in a less albite rich plagioclase and for this reason a higher  $Kd_{Ab}$  value. Similar results may occur experimentally when systems, significantly different in bulk composition are considered (e.g. calcium rich bulk compositions), though it is likely that bulk composition effects on natural feldspar compositions may not be strictly comparable with the synthetic experiments in view of the more complex nature of natural systems (viz. greater number of components and phases). As previously inferred, it is the writer's conclusion then,



that the feldspar compositions in natural systems are due primarily to bulk rock compositions.

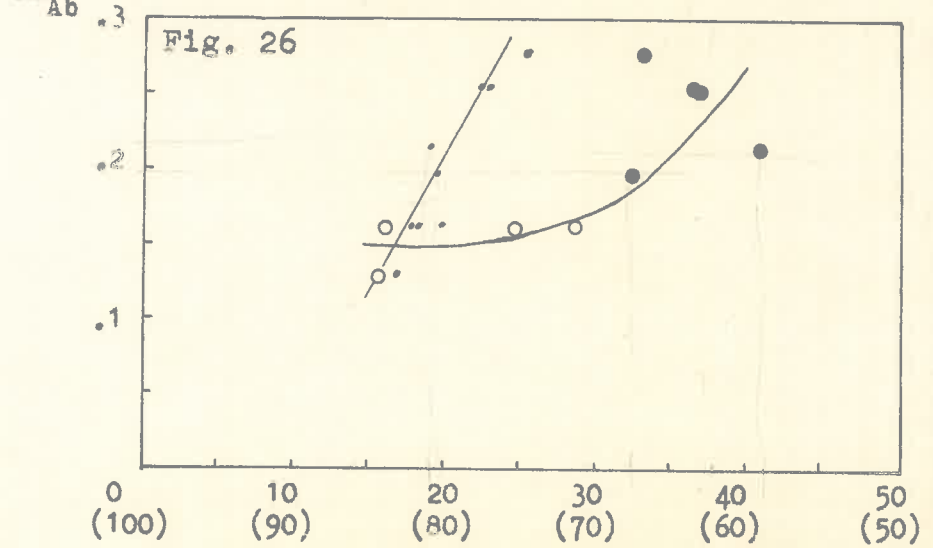
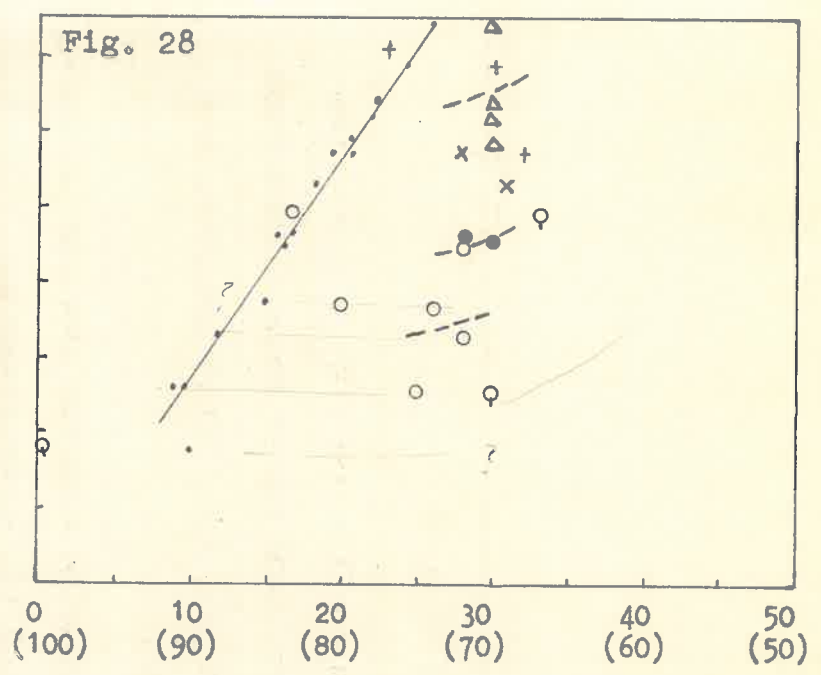
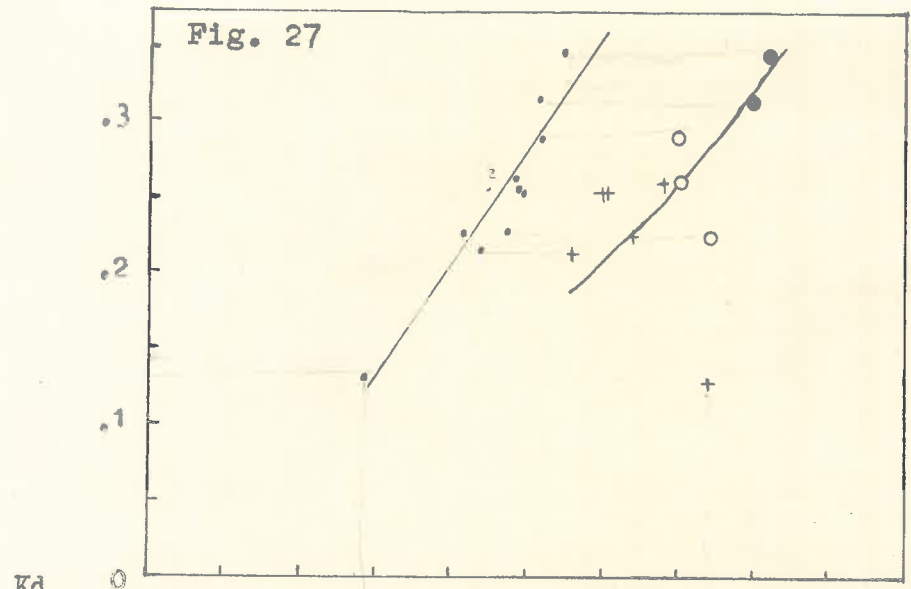
It has been noted on p. 53 that in the Ceylon, Adirondack and Langby areas different average  $Kd_{Ab}$  values from rocks of different metamorphic zones are perhaps indicative of gross temperature changes (temperatures read from the "Barth temperature scale"). The distribution coefficients from these areas are plotted against the coexisting feldspar compositions in Figures 26, 27 and 28 respectively. The trends in these figures (except Figure 28) are comparable to those observed in Figures 21, 22 and 23 and it is likely that the former trends could also be explained in terms of bulk rock composition differences. Some data in support of this hypothesis is given with regard to the Ceylon and Adirondack lowlands areas.

In Table 16 available chemical and modal analyses of acidic rocks typical of the Highland and Vijayan Series are given. Coexisting feldspars from samples K689, K827B and OL92 have not been analysed, but these rocks can be considered mineralogically similar to those Ceylon rocks of the same metamorphic facies, from which feldspars have been extracted and analysed. It is considered that the higher CaO and Na<sub>2</sub>O values for samples K689 and K827B (CaO equals 3.85 and 2.26 per cent and Na<sub>2</sub>O equals 2.33 and 3.12 per cent respectively) compared with A152/630 (CaO equals

### Figures 26 - 28

Plot of the distribution coefficient ( $Kd_{Ab}$ ) versus the determined K-feldspar and plagioclase compositions from Appendix VIII for the Ceylon, Adirondack lowlands, and Langöy areas respectively.

The symbols used in Figures 26 - 28 are the same as those used in Figures 14, 15 and 16, respectively, for the plagioclase compositions: The small dots in all figures refer to the K-feldspar compositions.



MOL PERCENT An in PLAGIOCLASE  
(MOL PERCENT Or in K-FELDSPAR)

Table 16. Chemical and modal analyses of samples of granulites and gneisses from Ceylon.

	Almandine-Amphibolite facies		Granulite facies		
	OL181	OL92	A152/630	K689	K827B
SiO <sub>2</sub>	72.41	75.50	63.92	69.93	73.11
TiO <sub>2</sub>	.42	.18	.98	.86	.97
Al <sub>2</sub> O <sub>3</sub>	13.66	13.34	14.95	13.65	14.19
Fe <sub>2</sub> O <sub>3</sub>	.32	.03	.61	1.55	.82
FeO	1.96	1.13	7.81	4.20	1.03
MnO	.09	.04	.24	.26	.05
MgO	.45	.22	4.14	tr	.50
CaO	<u>1.72</u>	<u>1.65</u>	<u>1.82</u>	<u>3.85</u>	<u>2.26</u>
Na <sub>2</sub> O	<u>3.00</u>	<u>2.91</u>	<u>1.91</u>	<u>2.33</u>	<u>3.12</u>
K <sub>2</sub> O	<u>5.31</u>	<u>4.56</u>	<u>3.60</u>	2.61	3.32
H <sub>2</sub> O	nd	nd	nd	H <sub>2</sub> O <sup>+</sup> =.41	H <sub>2</sub> O <sup>+</sup> =.31
P <sub>2</sub> O <sub>5</sub>	nd	nd	nd	H <sub>2</sub> O <sup>-</sup> =.05	H <sub>2</sub> O <sup>-</sup> =.13
				.09	tr
Total	99.34	99.56	99.86	99.79	100.08
		Modes			
Quartz	34	37	30		
Plagioclase	25	26	19		
K-feldspar	32	31	28		
Biotite and chlorite	5	5	1		
Garnet	3	.1	21		
Accessories	1	.5	.5		

K689 is an acid charnockite containing quartz, plagioclase, alkali feldspar, garnet, uralitized hypersthene, clinopyroxene, and Fe ore.

K827B is an acid charnockite containing quartz, plagioclase, alkali feldspar, hypersthene, apatite and Fe ore.

Analyses of A152/630, OL181 and OL92 by Dr. R.L. Oliver (Geology Dept., University of Adelaide). Analyses of K689, and K827B by J.P.R. Fonseka (Dept. of Mineralogy, Ceylon).

1.82 and  $\text{Na}_2\text{O}$  equals 1.91 per cent) are related to larger amounts of plagioclase of similar composition in the former two rocks. Actual modal analyses to confirm this were not available. Significant differences in some chemical components between the two facies rocks are compared with plagioclase and K-feldspar compositions in Table 17. It is fairly certain that the higher  $\frac{\text{Na}_2\text{O}}{\text{CaO}}$  and higher  $\text{K}_2\text{O}$  content of the almandine - amphibolite facies rocks can be correlated with the more sodic plagioclase feldspars and the more Or rich K-feldspars respectively as compared with the feldspars from the granulite facies rocks.

It follows that for these reasons the  $\text{Kd}_{\text{Ab}}$  values for the Highland Series rocks must be higher than the Vijayan Series rocks (see Table 23 Figure 14) regardless of different grades of metamorphism. These conclusions are consistent with the earlier stated doubtful significance of a temperature difference gradient (derived from the different  $\text{Kd}_{\text{Ab}}$  values and the Barth temperature scale) between the two facies rocks, (see also Chapter VII p. 93).

From the Adirondack lowlands area, modal and chemical analyses of four samples of "least altered gneiss" are given in Table 18 and in Table 19 the plagioclase and K-feldspar compositions are compared with the  $\frac{\text{Na}_2\text{O}}{\text{CaO}}$  ratio and  $\text{K}_2\text{O}$  content of these rocks. In Table 19 the lower grade samples from the Emeryville area (sillimanite-almandine-muscovite

Table 17. Correlation of rock and feldspar compositions from the Ceylon area.

Sample number	<i>Holland</i> Almandine-Amphibolite Facies		<i>Vijayan</i> Granulite Facies		
	OL181	0192	A152/630K689K827B		
$\frac{\text{Na}_2\text{O}}{\text{CaO}}$ (rock)	1.74	1.76	1.05	.605	1.38
$\text{K}_2\text{O}$ (rock)	5.31	4.56	3.60	2.61	3.32
An content of Plagioclase	19.63	22-23*	27.41	†	†
Or content of K-feldspar	87.12	-	85.84	-	-
Distribution coefficient $\text{Kd}_{\text{Ab}}$	.160	-	.195	-	-

\* Determined from extinction angles to (010) in sections perpendicular to  $\alpha$  or  $\gamma$  (Oliver, in press).

† Composition similar to A152/630 (see also text p. 64).

Table 18. Chemical and modal analyses of samples of least altered gneiss from the Adirondack lowlands, New York.

	Sillimanite-Almandine Muscovite sub facies.		Granulite facies	
	Bgn27	Qb228	Bgn18	Bgn21
SiO <sub>2</sub>	67.92	68.12	61.27	68.63
TiO <sub>2</sub>	.70	.87	.78	.52
Al <sub>2</sub> O <sub>3</sub>	15.53	14.44	17.94	16.06
Fe <sub>2</sub> O <sub>3</sub>	.77	.33	.67	1.02
FeO	3.51	4.89	6.81	.86
MnO	.05	.04	.05	.05
MgO	2.04	2.17	3.01	1.71
CaO	<u>2.22</u>	<u>2.32</u>	<u>3.29</u>	<u>3.61</u>
Na <sub>2</sub> O	<u>3.90</u>	<u>3.30</u>	<u>3.51</u>	<u>3.34</u>
K <sub>2</sub> O	<u>2.67</u>	<u>2.46</u>	<u>1.93</u>	<u>1.02</u>
H <sub>2</sub> O <sup>+</sup>	.72	.87	.56	.36
P <sub>2</sub> O <sub>5</sub>	.11	.09	nd	nd
F	.07	.08	.04	.03
Total	100.21	99.98	99.86	100.21
		Modes		
Quartz	34.33	32.35	22.58	36.27
Plagioclase	44.37	46.35	46.83	48.90
K-feldspar	1.71	.67	3.08	.73
Biotite	19.97	19.85	15.66	7.07
Garnet	-	.10	9.70	5.87
Muscovite	.80	.01	.76	.17
Chlorite	.47	.17	-	-
Accessories	.35	.50	1.39	.99

Analyses from Engel and Engel (1958).

Table 19. Correlation of rock and feldspar compositions from the Adirondack lowlands area.

Sample number	Sillimanite-almandine Muscovite sub facies		Granulite Facies	
	Bgn27	Qb228	Bgn18	Bgn21
$\frac{\text{Na}_2\text{O}}{\text{CaO}}$ (rock)	1.76	1.42	1.07	.92
$\text{K}_2\text{O}$ (rock)	2.67	2.46	1.93	1.02
An content of Plagioclase	25	29	36	35
Or content of K-feldspar	80.7	81.0	77.7	79.5
Distribution coefficient $K_{d_{\text{Ab}}}$	.257	.267	.348	.315



sub facies samples in Table 24) have a lower CaO content and hence a more acidic plagioclase (Ab75, Ab71) than the Colton samples (Ab64, Ab65 - granulite facies samples in Table 24). Also the slightly more Or rich K-feldspars in the rocks from the Emeryville area can be correlated with the higher  $K_2O$  content of these lower grade rocks in comparison with those from the Colton area. With these relatively smaller changes in the K-feldspar compositions, consequently the  $Kd_{Ab}$  values in the Colton rocks must be higher regardless of the change in grade of metamorphism. Furthermore within the Emeryville area itself those rocks which are lower in metamorphic grade (Engel and Engel 1958 Plate I) have higher  $Kd_{Ab}$  values. This inverse relationship of  $Kd_{Ab}$  and metamorphic grade is furthermore suggestive that sodium partitioning does not follow a temperature dependent distribution law.

The different average  $Kd_{Ab}$  values for rocks from different metamorphic zones in the Langöy area have been interpreted by Heier (1960) as temperature dependent. In comparison to Figures 21 - 27, Figure 28 relating to the Langöy area is different in that the plagioclase composition remains approximately constant in rocks from all metamorphic zones. In rocks from a single zone it would seem that the  $Kd_{Ab}$  values are related to the K-feldspar composition although admittedly the change in average  $Kd_{Ab}$  values with increasing metamorphic grade could be interpreted in terms of temperature changes

(cf. Figure 20).

Rock compositions of samples from which the feldspars in Table 25 were separated are available in only a few samples (Heier, 1960). The present writer has found however that in some of the available cases there was no correlation between the feldspar compositions and the rock analyses. This may be partly due to experimental errors, but also perhaps to the complicated manner in which chemical factors govern the feldspar compositions (Winkler, 1961 p. 11). There are no field relationships which are inconsistent with the existence of a temperature gradient between the two major facies rocks (cf. Ceylon area) and also the distribution of strontium between a few of the same feldspars is in agreement with a correlation between temperature and the different average  $Kd_{Ab}$  values for the almandine - amphibolite facies and granulite facies (see Chapter VII p. 82). A strict correlation of  $Kd_{Ab}$  with metamorphic grade leads to many anomalies however (see discussion on p. 56).

Hence the general pattern of sodium partitioning between coexisting feldspars, when all data is considered is an inconsistent one: attempted correlation of average  $Kd_{Ab}$  values with metamorphic grades in different areas leads to many anomalies; for example the metamorphic transition almandine - amphibolite facies to granulite facies corresponds to different  $Kd_{Ab}$  values in different areas (cf. the  $Kd_{Ab}$

values of the highest grade almandine - amphibolite facies rocks in all areas). This inconsistent picture of correlation of  $Kd_{Ab}$  with similar metamorphic grades contrasts with the general pattern of Sr partitioning between the same feldspars, which is believed to be consistent with the Nernst distribution law. In this case systematic changes in Sr distribution occur with changes in metamorphic grade e.g. the transition almandine - amphibolite facies to granulite facies coincides with  $Kd_{SrF}$  equal to unity. Because of the inconsistencies concerned with sodium partitioning between feldspars, the relationship between  $Kd_{Ab}$  and metamorphic grade is obviously more complicated than it would be if an approach to the distribution law is achieved: in terms of the writer's hypothesis these inconsistencies are the result of different bulk rock compositions.

It is fairly clear that from data discussed in this chapter, feldspar compositions as far as the major feldspar components are concerned are primarily controlled by the rock compositions in a more or less regular manner. The nature of this control is unknown but can be discussed. The writer suggests that, in order to explain why different  $Kd_{Ab}$  values in uniformly metamorphosed rocks are approximately related to both feldspar compositions (viz. Figures 21 - 28), certain elemental ratios of a rock may control the feldspar compositions (see discussion of different  $Kd_{Ab}$  values in

different facies rocks from the Ceylon and Adirondack lowland areas). A strict relationship may not always be observable because of the many different rock components which can be involved, in addition to the main components of both feldspars (see also Winkler, 1961).

E. SUMMARY.

It has been shown in this chapter, that an attempt to account for sodium distribution between coexisting feldspars according to the Nernst distribution law reveals many inconsistencies which cannot be satisfactorily explained. It has been suggested on the basis of chemical and mineralogical evidence that the feldspar compositions are determined by the rock composition. In this way the variability of  $Kd_{Ab}$  values in rocks from the same metamorphic grade as well as different  $Kd_{Ab}$  values and in other instances the similarity of  $Kd_{Ab}$  values in rocks from different metamorphic grades within the one area can be best explained.

It is concluded that the distribution of sodium is not related to metamorphic grade.

DISTRIBUTION OF BARIUM, RUBIDIUM AND CALCIUM.

### A. INTRODUCTION

As previously stated (this text p. 10) Barth suggested that the distribution of Ba, Sr and Ca between coexisting feldspars is consistent with the Nernst distribution law and that the distribution coefficient for these elements increases regularly, with changes in temperature (see Figure 2): also that the distribution of Rb, Cu, Li and Pb between the same feldspars is completely random (see further discussion p. 10). In the light of Barth's hypotheses the writer has investigated the distribution of Ca, Ba, Rb, and Sr between the same feldspars as were discussed in Chapter V; the results relating to Ca, Ba and Rb are considered in this chapter, and the distribution of Sr is dealt with in the following chapter.

### B. RELATIONSHIP BETWEEN THE ELEMENTAL PARTITION COEFFICIENTS AND METAMORPHIC GRADE.

The Rb, Ca and Ba concentrations as weight percents and the corresponding theoretical feldspar components (Rb-feldspar, Ba-feldspar, etc.) as weight and molecular percents in both feldspar types are given in Appendix VI. Elemental distributions pertaining to the areas examined are plotted in Figures 29 - 34a and b and similar data from Heier (1960) and Howie (1955) are plotted in Figures 35a and b. The diagrams show mol per cent feldspar component in the K-feldspar against mol per cent feldspar component in the plagioclase plotted on a log-log scale. In this way lines of

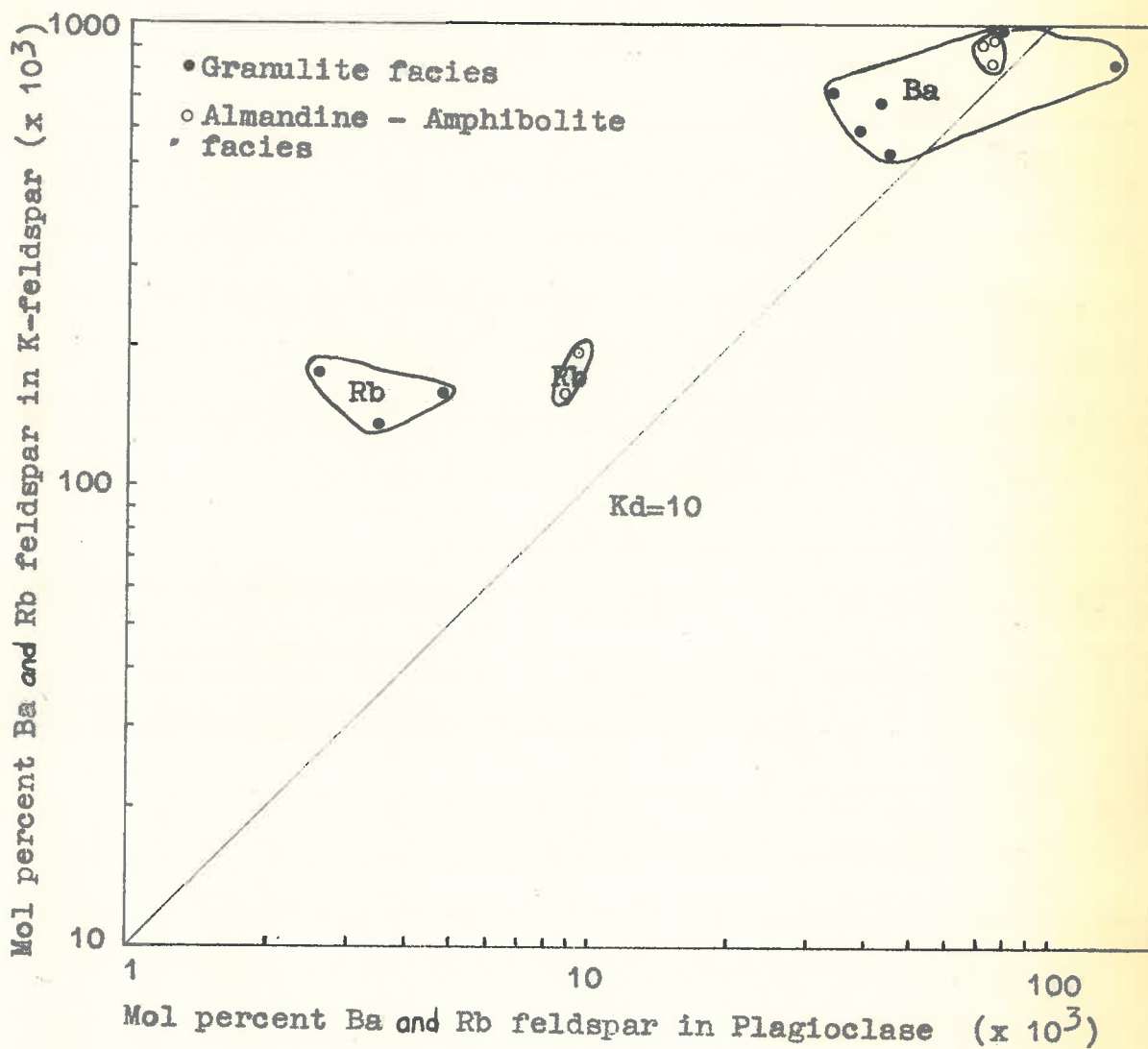


Fig. 29a. Distribution of Ba & Rb-feldspar between coexisting feldspars. Musgrave Range Area.

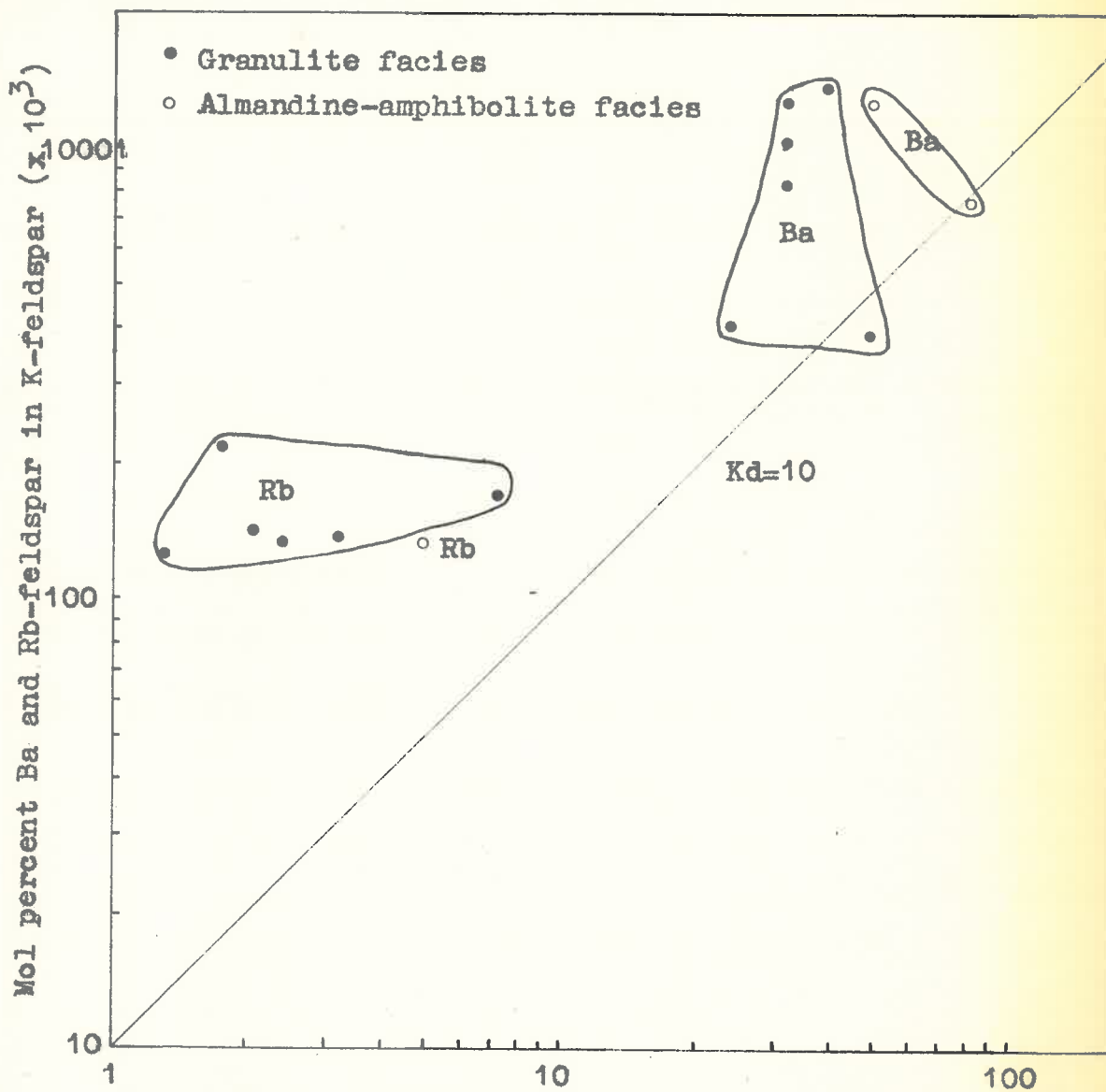


Fig. 30a. Distribution of Ba and Rb-feldspar between coexisting feldspars.

Broken Hill area.



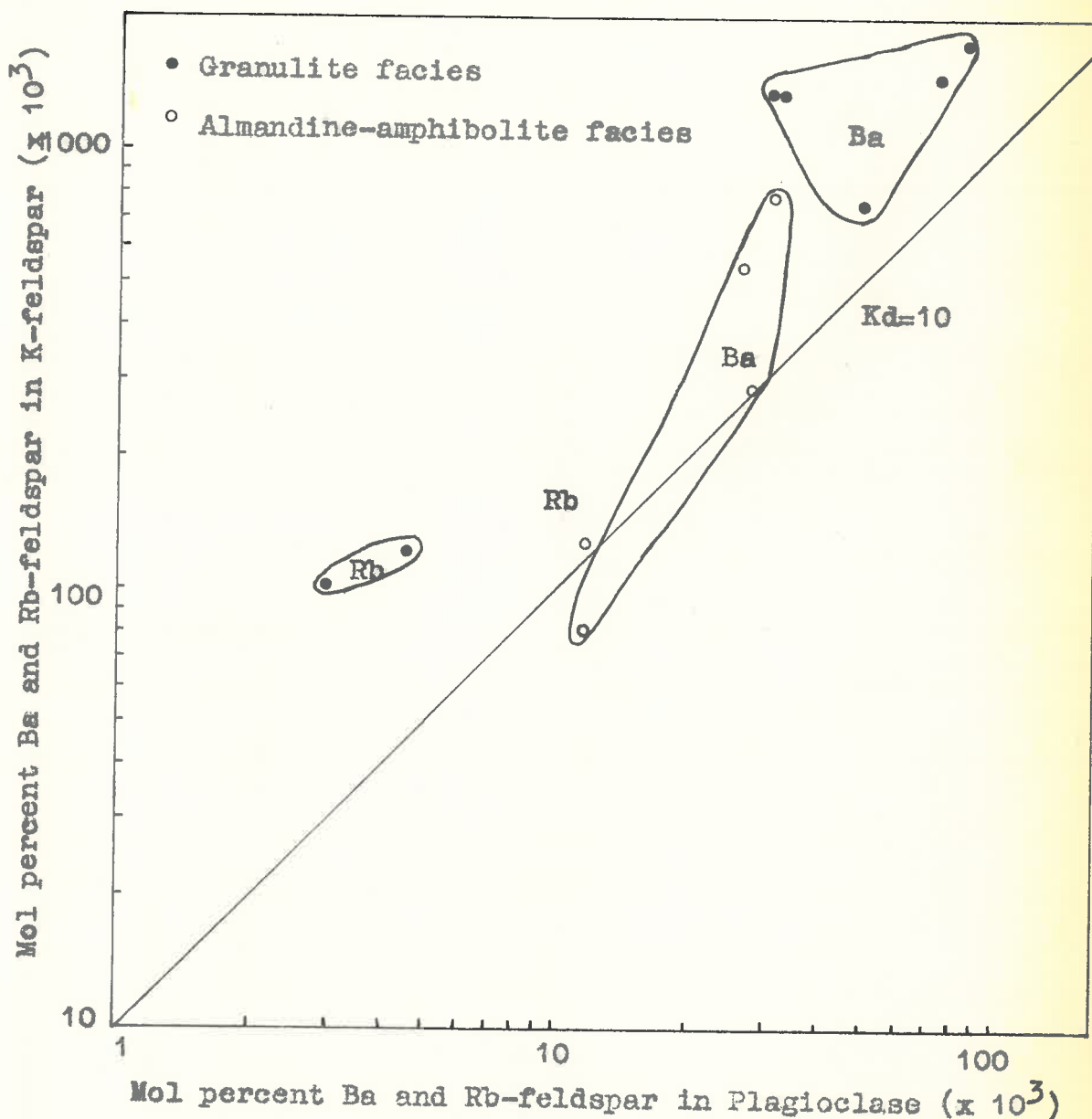


Fig. 31a. Distribution of Ba and Rb-feldspar  
 between coexisting feldspars.  
 Ceylon area.

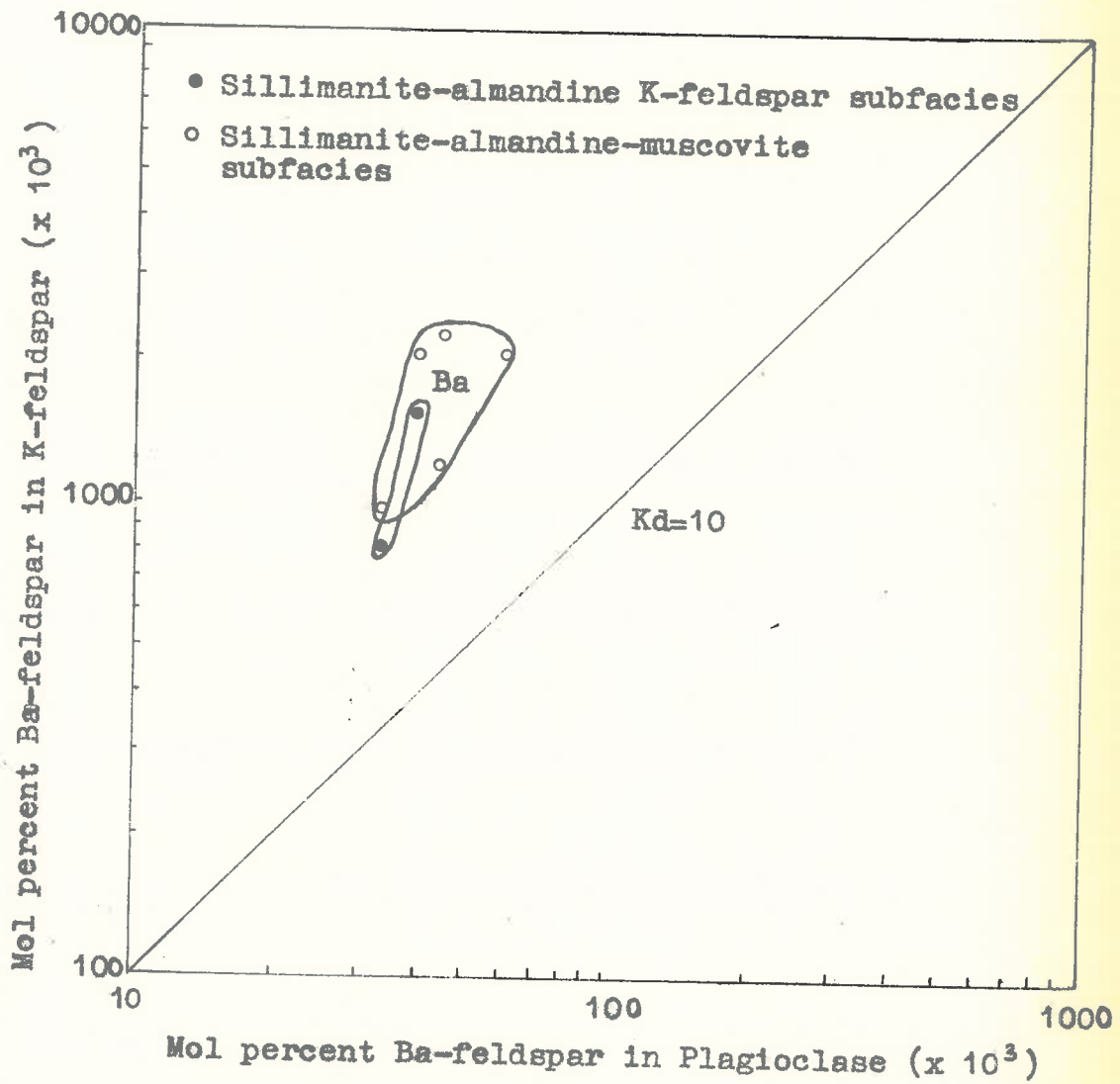
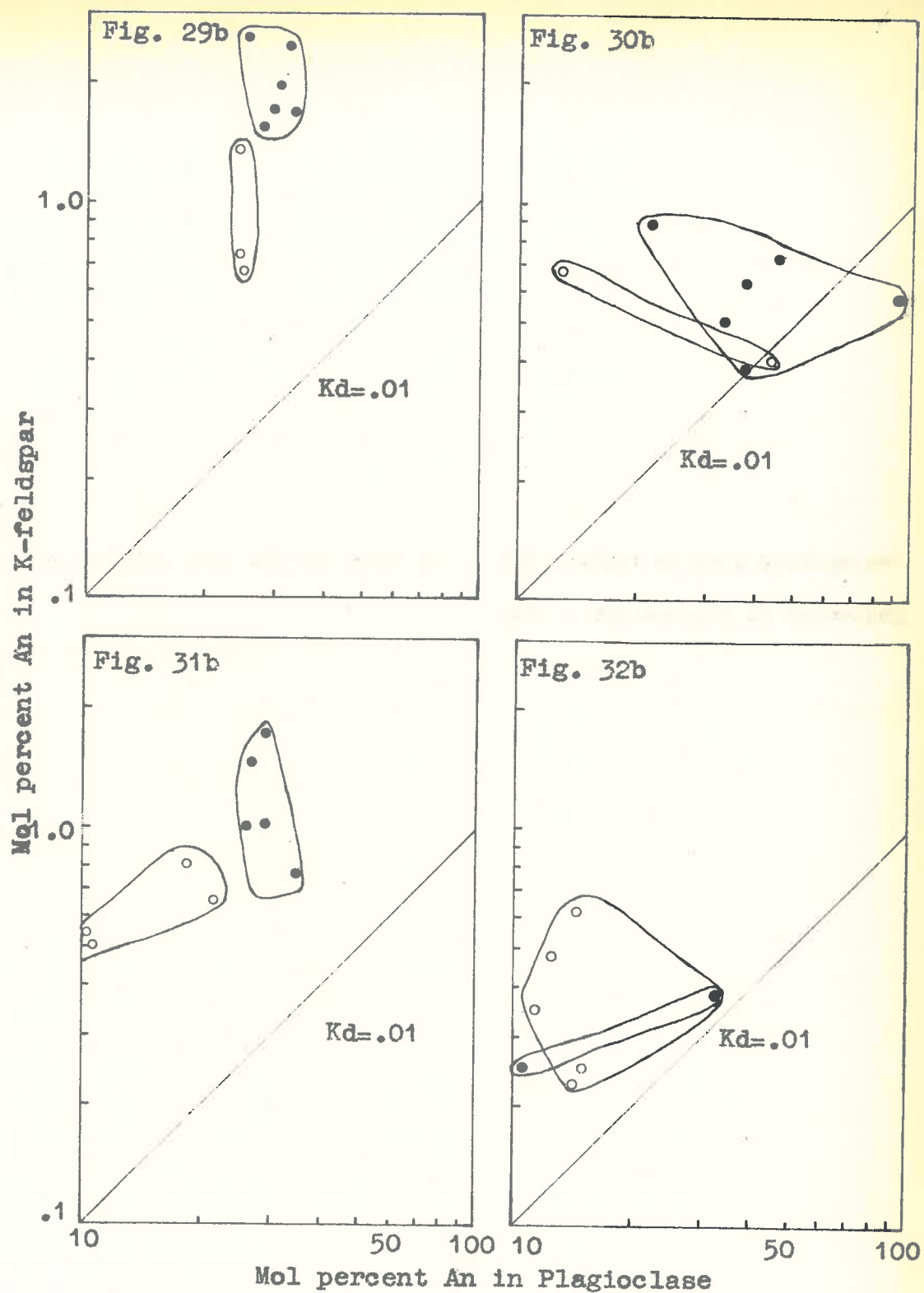


Fig. 32a. Distribution of Ba-feldspar between coexisting feldspars. Pewsey Vale area.

The symbols used in Figures 29b - 34b refer to the same samples as indicated in Figures 29a - 32a.



Figs. 29b-32b. Distribution of Anorthite between coexisting feldspars.

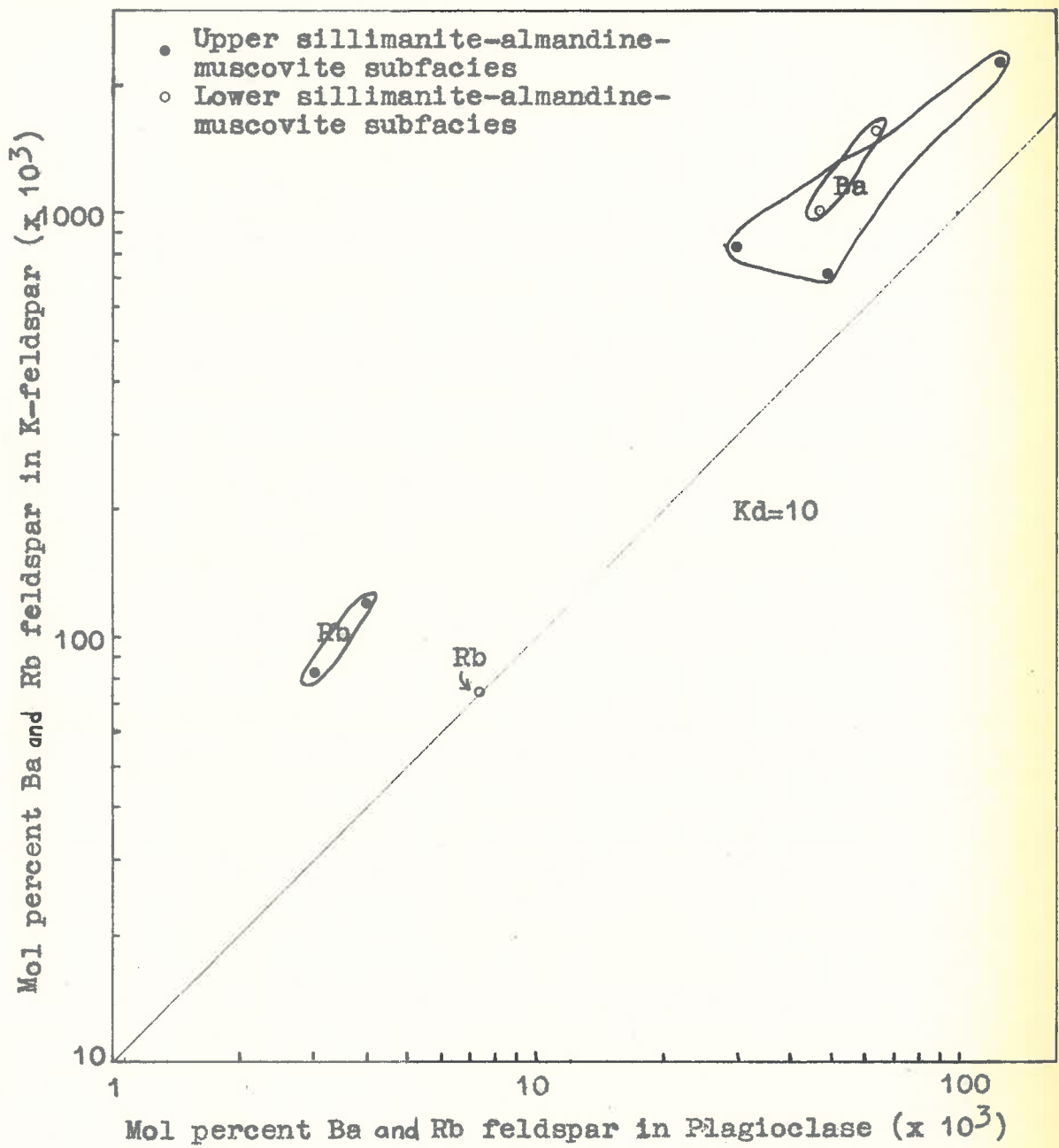


Fig. 33a. Distribution of Ba & Rb-feldspar between coexisting feldspars. Palmer Area.

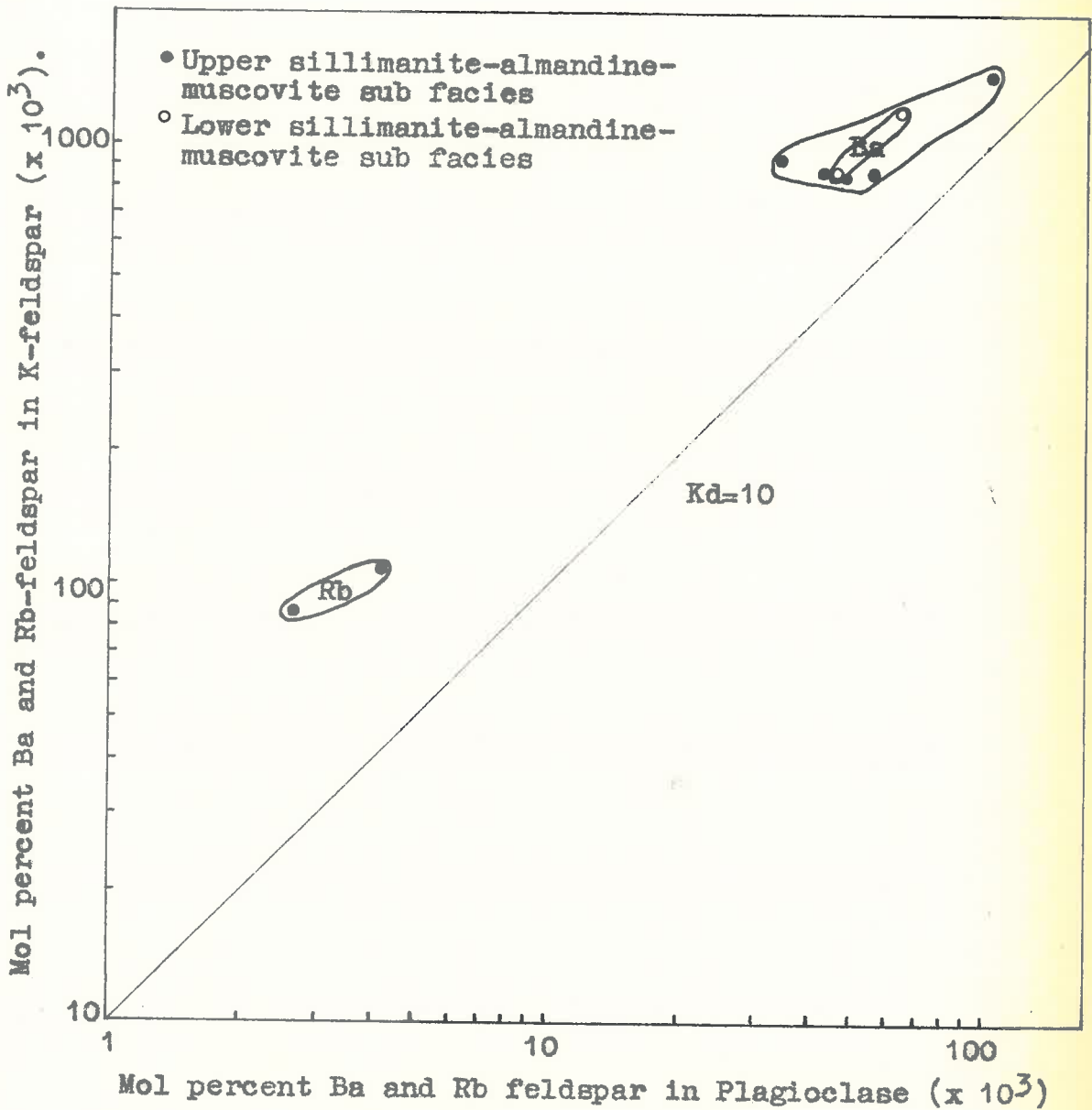
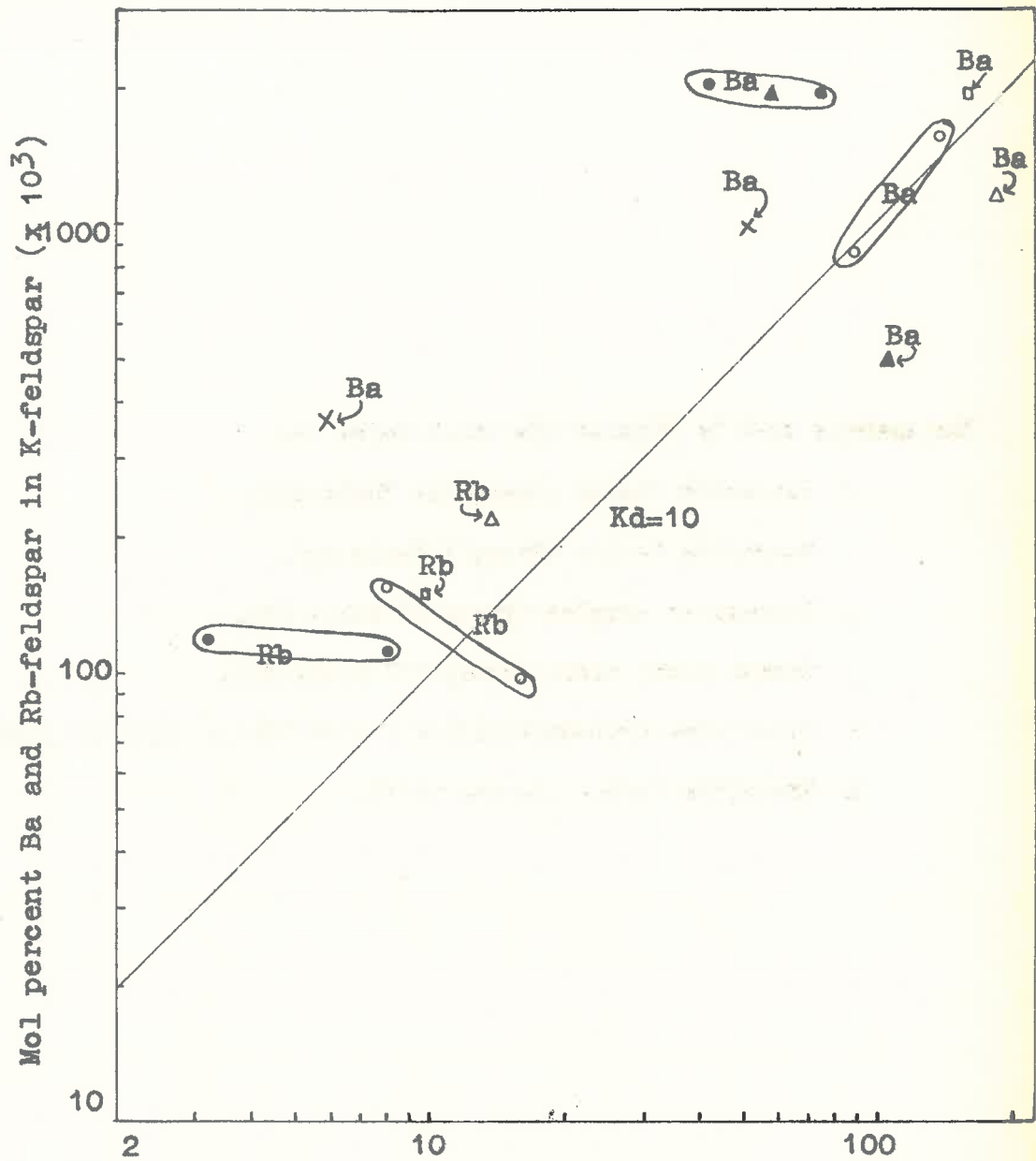


Fig. 34a. Distribution of Ba and Rb-feldspar between coexisting feldspars. Springton area.

The symbols used in Figures 35a and b refer to:

- Granulite facies (Group III Table 25).
- Granulite facies (Group V Table 25).
- ▲ Retrograde samples (Group IV Table 25).
- △ Transitional rocks (Group VII Table 25).
- Upper almandine-amphibolite facies (Group VIII Table 25).
- x Granulite facies (Howie, 1955).

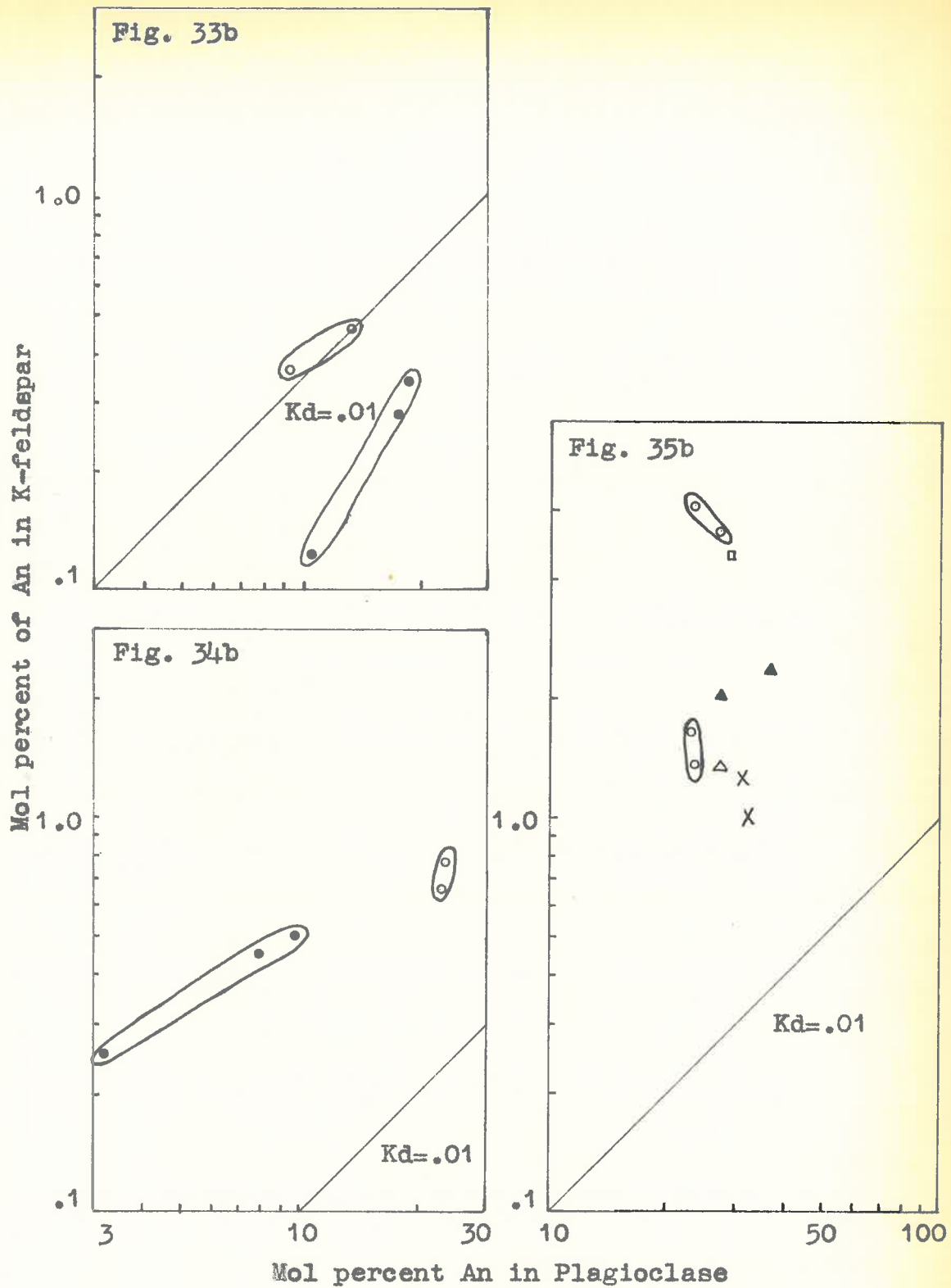


Mol percent Ba and Rb-feldspar in Plagioclase ( $\times 10^3$ )

Fig. 35a. Distribution of Ba and Rb-feldspar between coexisting feldspars.

Langöy and Madras areas.





Figs. 33b-35b. Distribution of Anorthite between coexisting feldspars.

equal  $K_d$  have a  $45^\circ$  slope. The distribution coefficients<sup>\*</sup> of individual points are read from the intersection with the ordinate axis of a  $45^\circ$  line passing through a particular point. Thus  $K_{d_{BaF}}$ ,  $K_{d_{RbF}}$  and  $K_{d_{CaF}}$  in Figure 31 for the granulite facies samples are 14.0 - 42.0; 26.0 - 34.0; and .021 - .056, respectively.

These log-log plots are equivalent to the diagrams used previously in Chapter V and to those used also in Chapter VII but permit convenient plotting of more than one element on the same diagram and also indicate the degree of conformity to the distribution law in the following manner: if the elemental distributions follow the Nernst distribution law and are unaffected by compositional effects, then points representing feldspar pairs from isofacial rocks (i.e. equal pressure - temperature conditions) will cluster along one of the  $45^\circ$  lines and non equilibrium distributions will be reflected in scatter normal to the  $45^\circ$  lines. Some generalizations common to Ba, Rb and Ca distributions can be made from the Figures thus:

- (a) Barium and particularly rubidium are strongly preferred by the alkali feldspar phase whereas calcium is strongly preferred by the plagioclase lattice.
- (b) For feldspar pairs from isofacial metamorphic rocks

---

\* The distribution coefficient e.g.  $K_{d_{BaF}}$  equals

$$\frac{\text{Mol per cent Ba-feldspar in K-feldspar}}{\text{Mol per cent Ba-feldspar in Plagioclase}}$$


---

there is considerable scatter of points outside the experimental error of  $K_d$  values (a range of approximately 10 per cent can be taken as experimental error for the Ba, Rb and Ca-feldspar distribution coefficients).

- (c) There is no distinction between the distribution coefficients for feldspar pairs taken from different metamorphic grades.

It can be concluded that the observed distributions of Ba, Ca and Rb are not indicative of equilibrium partitioning.

The above results with respect to Ba and Ca are contrary to that expected from Barth's hypothesis. Some data used by Barth are shown in Figures 35a and b. It can be seen that the correlation between the distribution coefficients and metamorphic grade is not systematic: it is true that the two points for Ba from almandine - amphibolite samples lie on a  $45^\circ$  line and have distribution coefficients lower than some granulite facies samples but another granulite facies sample overlaps the values typical of the amphibolite facies samples. Also a sample transitional in metamorphic grade between granulite and almandine - amphibolite facies has a  $K_{d_{BaF}}$  value lower than the amphibolite facies samples. Howie's data for Ba also shows considerable scatter for isofacial rocks. Several inconsistencies again occur in the correlation between  $K_{d_{CaF}}$  and metamorphic grade.

The writer's data affords an appraisal more thorough than Barth's, of the nature of Ba and Ca partitioning between coexisting feldspars, and these data are inconsistent with Barth's conclusions. An explanation of the equilibrium partitioning of Ba, Rb and Ca is therefore necessary.

### C. BARIUM PARTITIONING

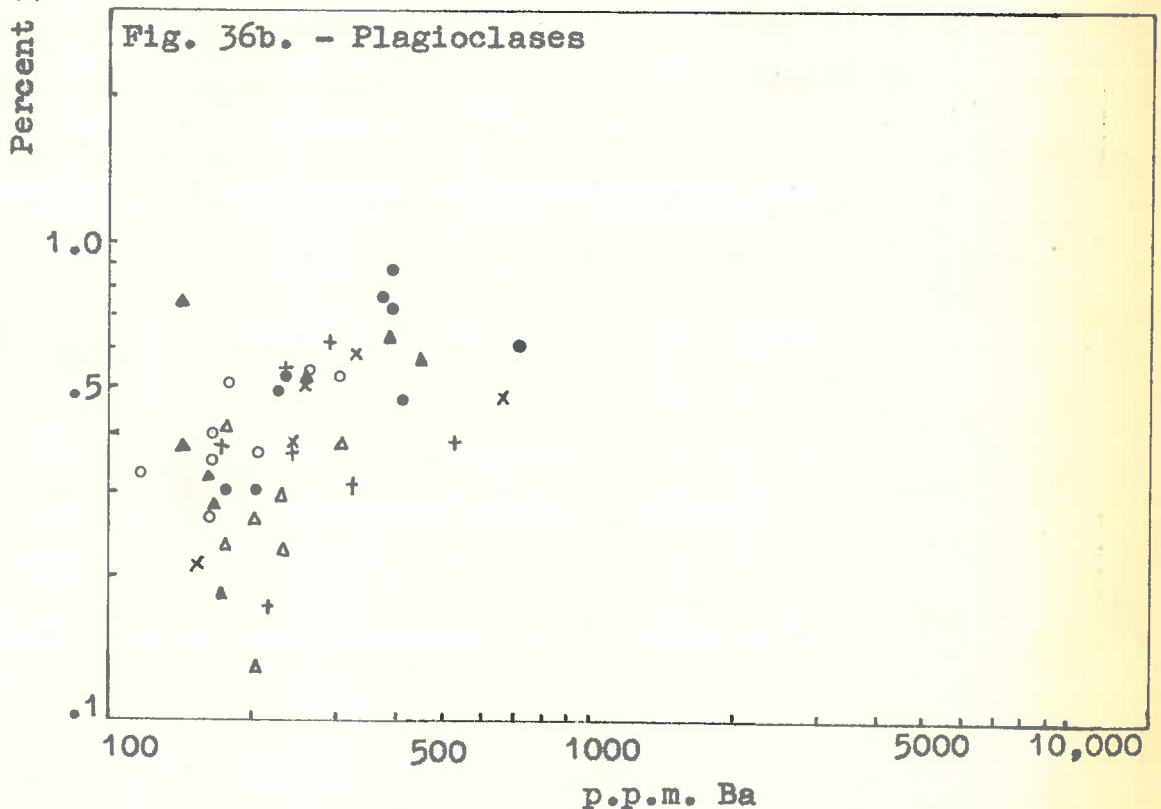
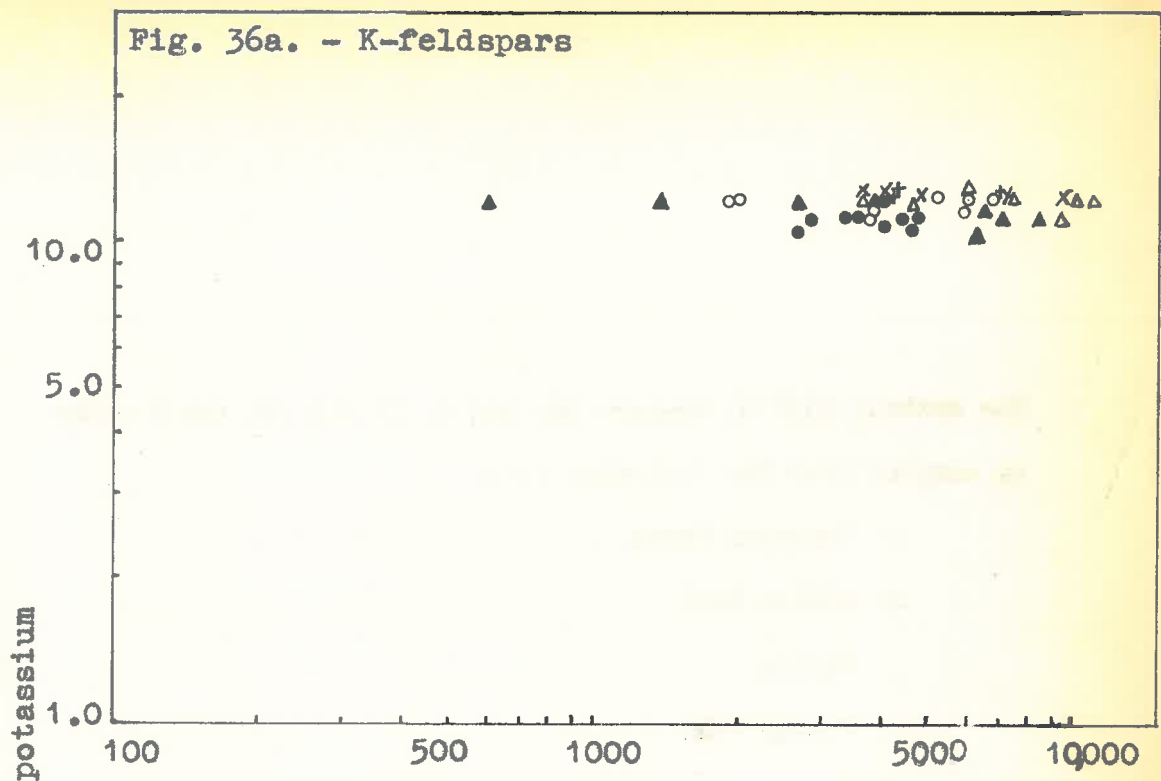
Some characteristics of the K-Ba relationship in K-feldspars and plagioclases which are considered important in explaining the observed Ba distribution are discussed below. Barium ( $\text{Ba}^{2+} = 1.34\text{\AA}^{\circ}$ ) with a similar ionic radius\* to that of potassium ( $\text{K}^{+} = 1.33\text{\AA}^{\circ}$ ) will fit suitably into K positions in the K-feldspars [this is also borne out by the similar positions of Ba in celsian and K in potassium feldspar as shown in structure determinations, Taylor 1965(b)]. The K-Ba relationship for the K-feldspars examined by the writer is plotted in Figure 36a on a log-log scale. It can be seen that whereas K remains approximately constant ( $\sim 11-13$  percent K), the Ba content varies from 3000 - 10,000 p.p.m. for most samples. The absolute amounts of Ba in the K-feldspars is presumable primarily dependent on the amount available in a given environment although this may be modified by the presence of other phases which also readily accept Ba (e.g. muscovite and biotite - see Appendix I). In isofacial rocks and from Figure 36a it can be seen that there is a large range of the K/Ba ratio for the K-feldspars and it is

---

\*Radii from Ahrens (1953).

The symbols used in Figures 36a and b, 37 and 38a and b refer to samples from the following area.

- Masgrave Range
- Broken Hill
- ▲ Ceylon
- △ Powsey Vale
- + Springton
- x Palmer



Figs. 36a & b. Plots of K vs. Ba in K-feldspars and Plagioclase.

not possible to separate the effects of environmental factors from the effect of coexistence of micas: the data show no significant differences between the K/Ba ratio of K-feldspars from biotite bearing almandine - amphibolite facies rocks and that from biotite deficient granulite facies rocks. Analyses of the Ba content of coexisting K-feldspar and biotite phases [Nockolds and Mitchell, 1948; White (b) in prep] indicate that Ba is preferentially taken into the K-feldspar lattice and Taylor (1965a) suggests that this is because of the greater difficulty in overcoming charge balance requirements in the biotite lattice.

The Ba content of the plagioclase feldspars is not only dependent on the amounts available in different environments. Because of size differences ( $Ba^{2+} = 1.34A^{\circ}$ ,  $Ca^{2+} = .99A^{\circ}$  and  $Na^{+} = .97A^{\circ}$ ) it is unlikely that Ba will substitute for Ca or Na in the plagioclase lattice. Heier (1962) suggested that the Ba content of the plagioclase feldspar was dependent on its K content and this is supported by Figure 36b where there appears to be a correlation between the Ba and K contents of the plagioclases examined in this study. This dependence of Ba on K content is reflected also by the variation of the barium-feldspar distribution coefficient as shown in Figure 37: the  $Kd_{BaF}$  values tend to be higher for those plagioclases with lower K content. This effect will certainly explain in part the random pattern of Ba

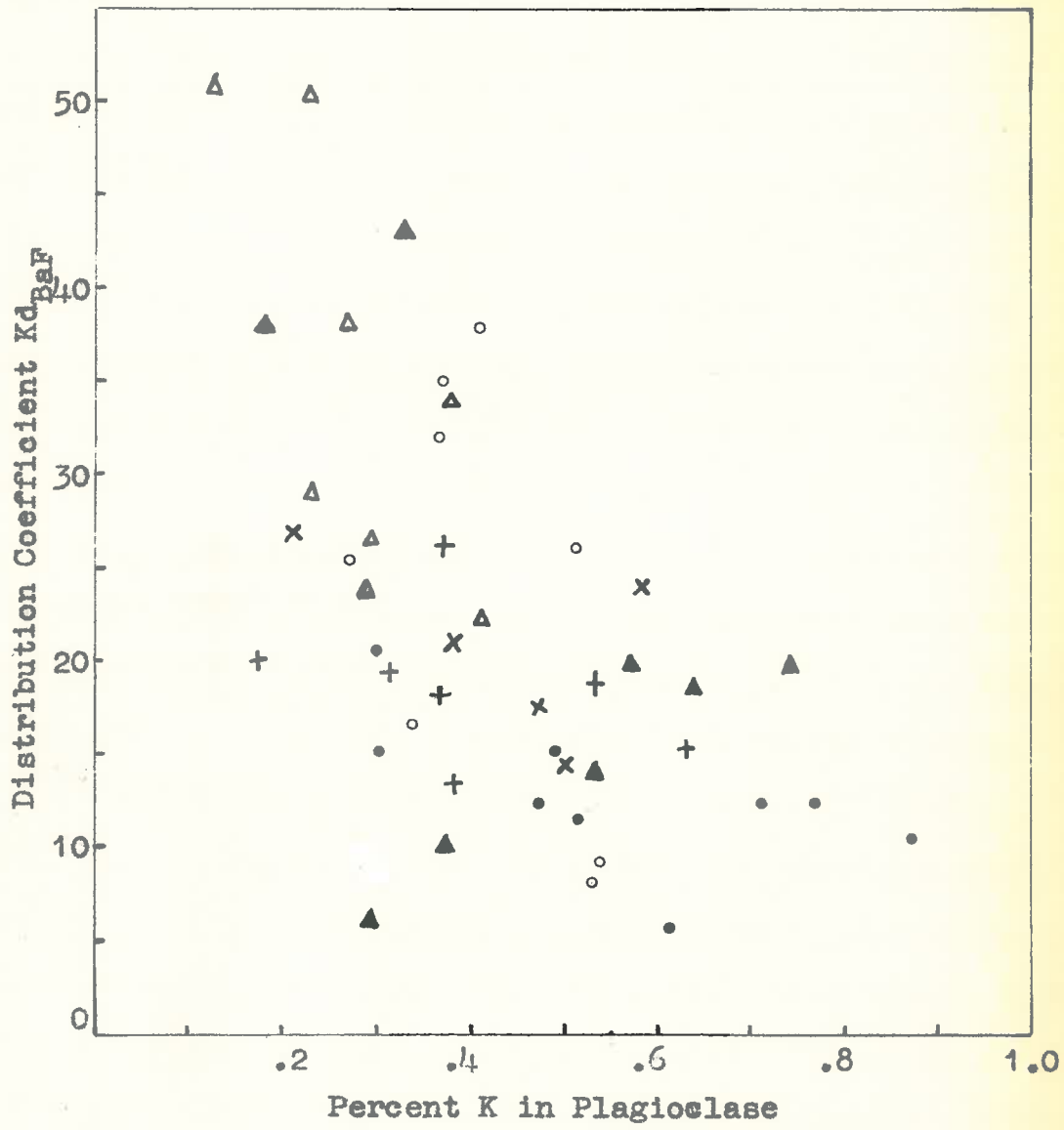


Fig. 37. Plot of barium-feldspar distribution coefficient vs percent potassium in plagioclase.

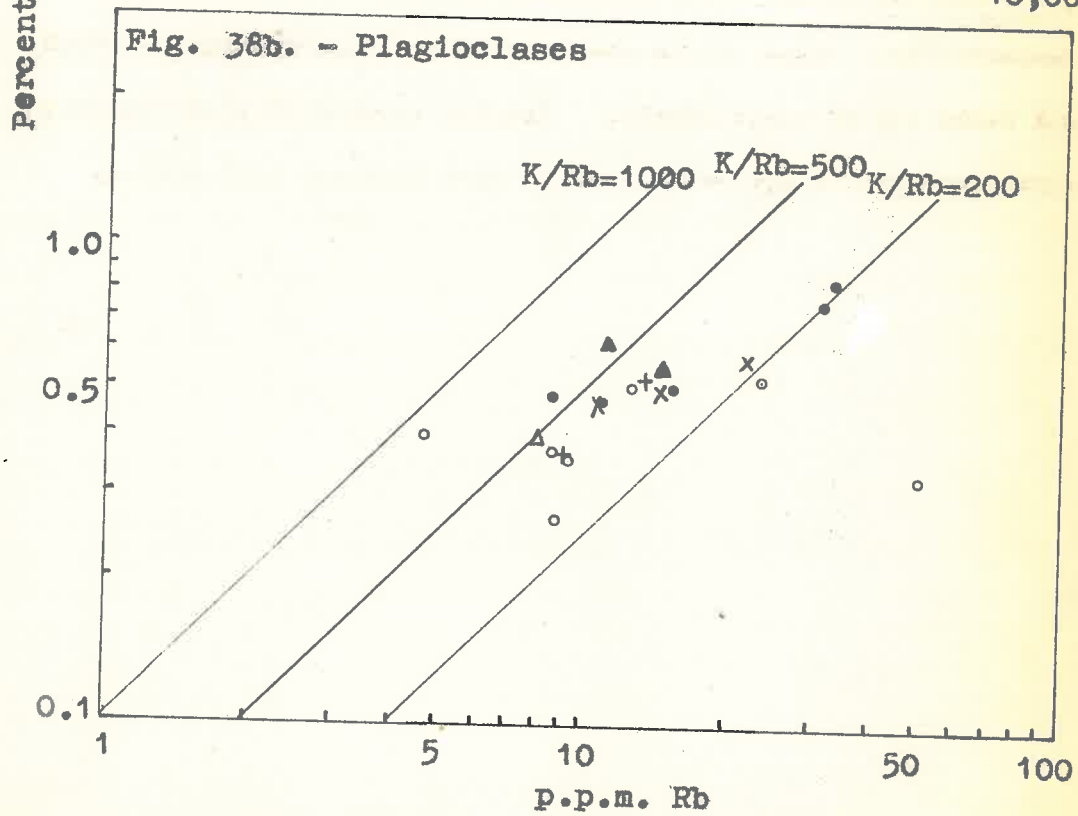
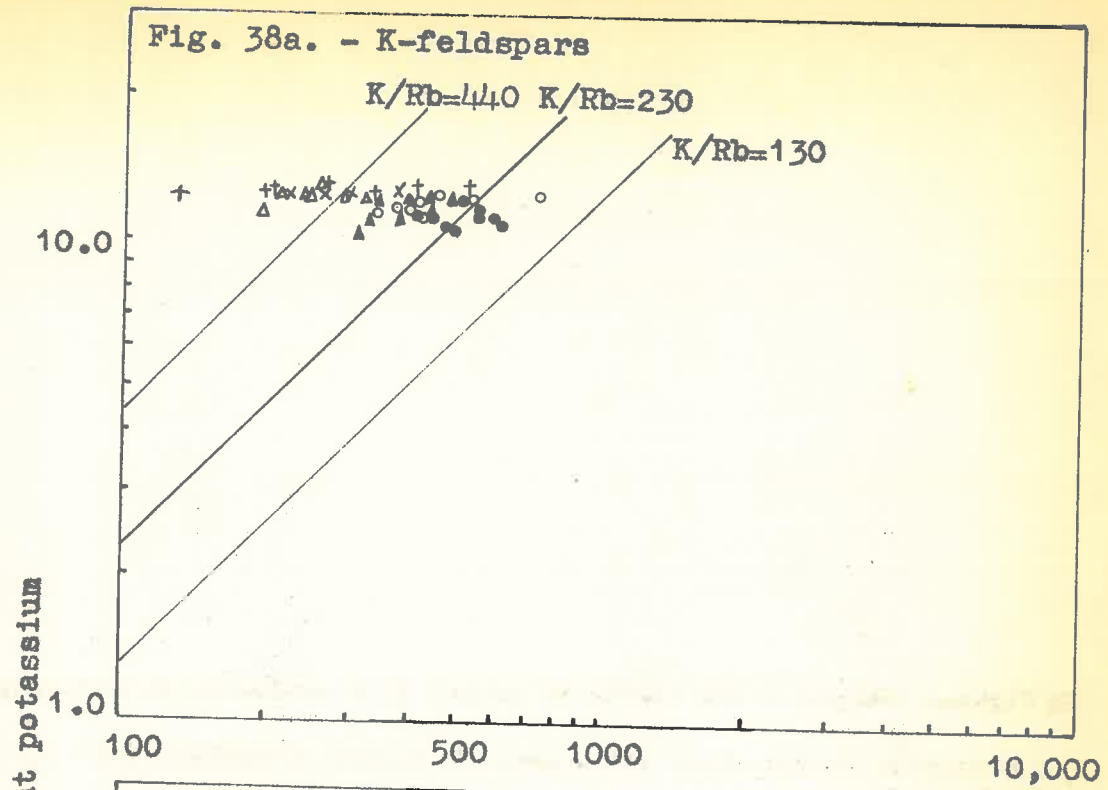


distribution but alone does not account for the apparent insensitivity of Ba partitioning to changes in metamorphic grade. This contrasts with the significant changes of Sr partitioning between the same feldspars, with changes in metamorphic grade. In view of this it is concluded that, in addition to the above effect, the relative abundances of Ba in different environments coupled with the strong affinity for Ba by the K-feldspar phase (the  $K_d$ 's are generally  $> 10$ ) are the most important factors in Ba partitioning and tend to override any temperature dependent, chemical equilibrium effects.

#### D. RUBIDIUM PARTITIONING

The observed Rb distribution between the coexisting feldspars also appears to be controlled primarily by structural factors. In view of size considerations ( $K^+ = 1.33\text{\AA}$ ,  $Rb^+ = 1.47\text{\AA}$ ) it is likely that Rb will also be located in K-sites of both feldspars. The K-Rb relationship in the writer's feldspar samples is shown in Figures 38a and b. The average K/Rb ratio of the K-feldspars is generally higher than previously accepted values (Heier and Taylor, 1959) and certain samples are outside the normal limits of scatter, indicating a depletion of Rb with respect to K. This can be explained by the preferential acceptance of Rb in mica lattices (Taylor, 1965a) which are primarily present only in almandine - amphibolite facies samples. It is evident then

In Figures 38a and b the limits of normal K/Rb ratios in K-feldspars and plagioclases are shown about average values of 230 and 500 respectively: these limits are taken from Heier and Taylor (1959) and Heier (1962) respectively. Samples whose K/Rb plot lies outside these limits are considered to have abnormal K/Rb ratios.



Figs. 38a & b. Plots of K vs. Rb in K-feldspars & Plagioclases.

that the Rb content of K-feldspars is dependent on the presence or absence of micas.

Although there are comparatively few plagioclase feldspars in which Rb was measurable, there appears to be a correlation between potassium and rubidium for this feldspar type (see Figure 38b). It is concluded that these structural controls, noted above, are the most important factors governing Rb partitioning between feldspars.

#### E. CALCIUM PARTITIONING

The K-feldspars examined by the writer contain less than .5 per cent CaO and most samples contain more Ba than Ca. Higher temperatures of crystallization of granulite facies rocks in comparison to the almandine - amphibolite facies rocks is generally supported by the higher anorthite content of the granulite facies K-feldspars (compare data from the different facies in Figures 29b<sup>-31b</sup> and 35b and also data from Figures 32b - 34b with the granulite facies samples of Figures 29b - 31b and 35b). Superimposed on this effect is the much more important one of the bulk composition of the rock controlling the feldspar compositions. It has been reasonably suggested in Chapter V that the major element chemistry of feldspars depends primarily on the rock composition and therefore the distribution coefficient  $Kd_{CaF}$  will change irrespective of temperature changes: in this way the bulk composition variation produces a scatter of points

(Figures 29b - 35b) far greater than that due to temperature variation.

F. CONCLUSIONS

The distribution of Ca, Ba and Rb between coexisting feldspars is inconsistent with the Nernst distribution equation and in the cases of Ca and Ba is inconsistent with the temperature dependent hypothesis postulated by Barth (1961). It has been shown that some characteristics of the feldspar structures and bulk composition factors, are the important factors in explaining the observed Ca, Ba and Rb distributions.

DISTRIBUTION OF STRONTIUM.

A. RELATIONSHIP BETWEEN THE STRONTIUM DISTRIBUTION AND METAMORPHIC GRADE.

Strontium concentrations as weight percents and calculated Sr-feldspar components as weight and molecular percents of the coexisting feldspars examined from different areas are given in Appendix VI. The data are plotted in Figures 39 - 44 and equivalent data from Heier (1960) are plotted in Figure 45. The graphs plot mol percent Sr-feldspar in the K-feldspar against mol per cent Sr-feldspar in the plagioclase on a natural scale.

The overall pattern of strontium distribution is such that there is little discrimination between K-feldspar and plagioclase, the distribution coefficient  $Kd_{SrF}^*$  being close to unity (cf.  $Kd_{BaF}$  and  $Kd_{RbF}$ ). Sufficient discrimination exists, however, that in the granulite facies rocks strontium is preferentially taken into the K-feldspar lattice  $Kd_{SrF} > 1$  whilst at lower grades (middle - upper almandine amphibolite facies the reverse is true. A more detailed discussion of the Sr distribution with respect to individual areas follows.

1. Granulite - almandine amphibolite facies areas.

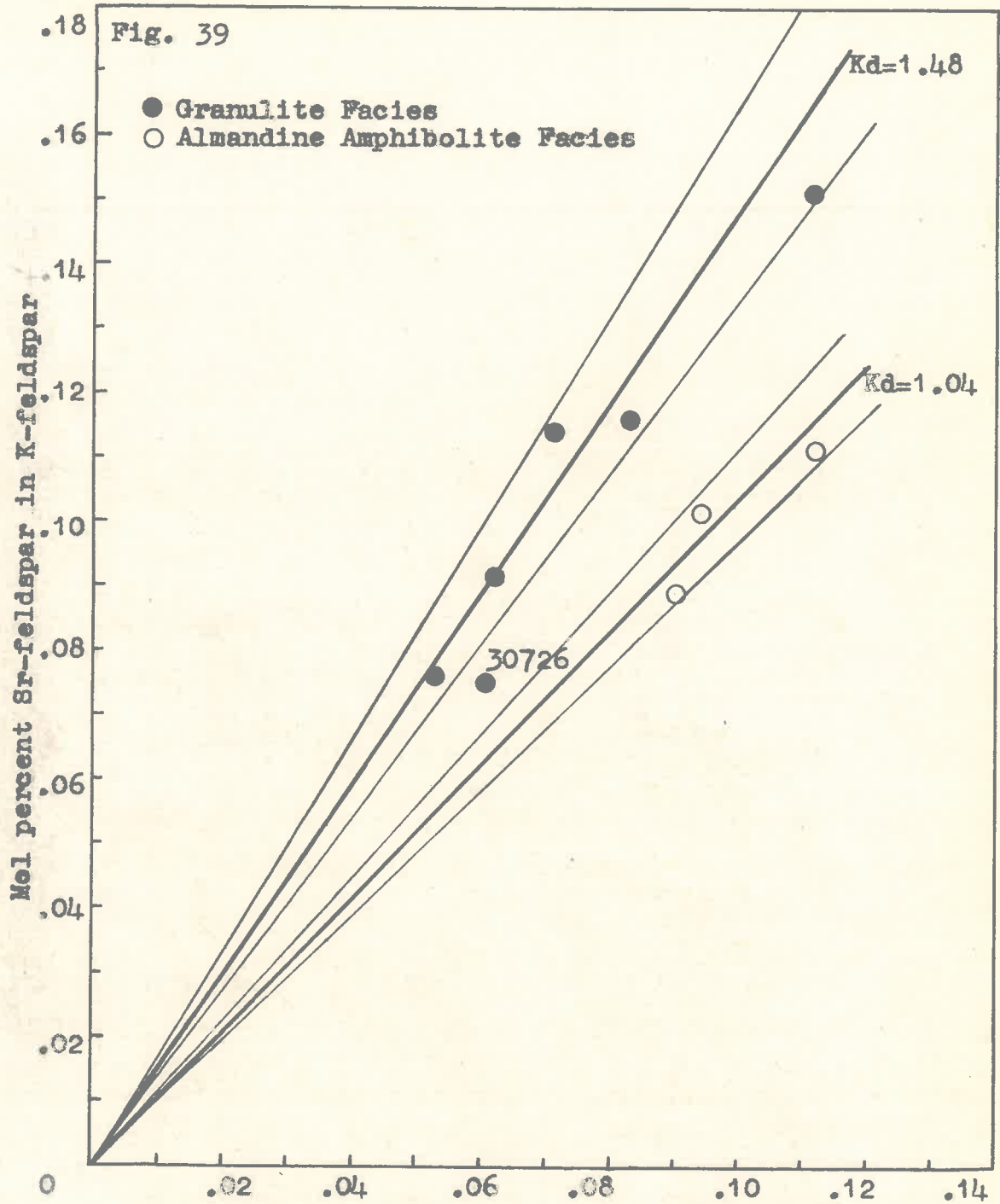
Data from the Musgrave Range, Broken Hill, Ceylon and Langby areas are given in Figures 39, 40, 41, and 45 respectively. It has been stated before (p. 14) that for uniform

---

\* The distribution coefficient  $Kd_{SrF}$  equals

$$\frac{\text{Mol percent Sr-feldspar in K-feldspar}}{\text{Mol percent Sr-feldspar in Plagioclase}}$$


---

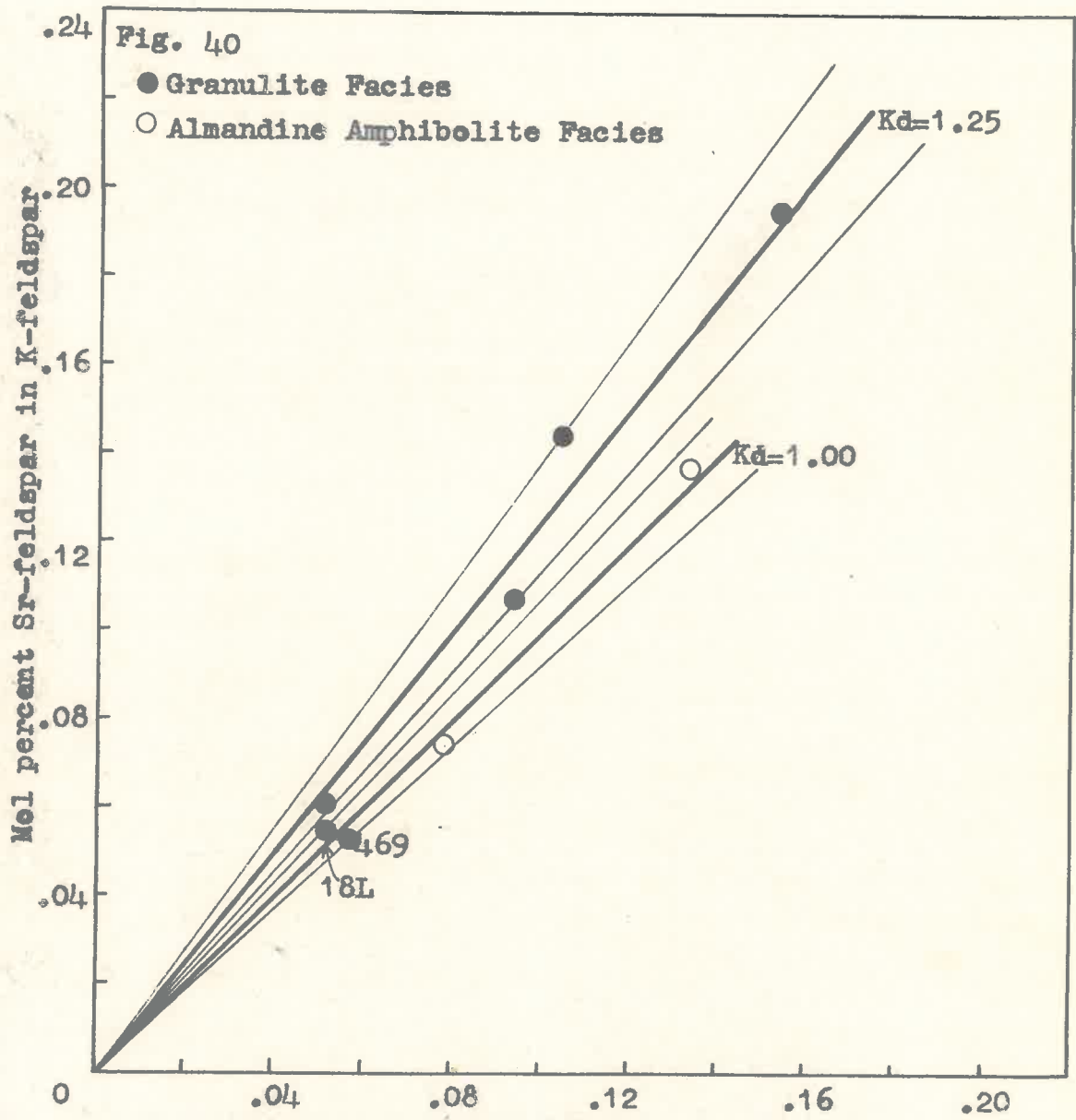


Mol percent Sr-feldspar in Plagioclase

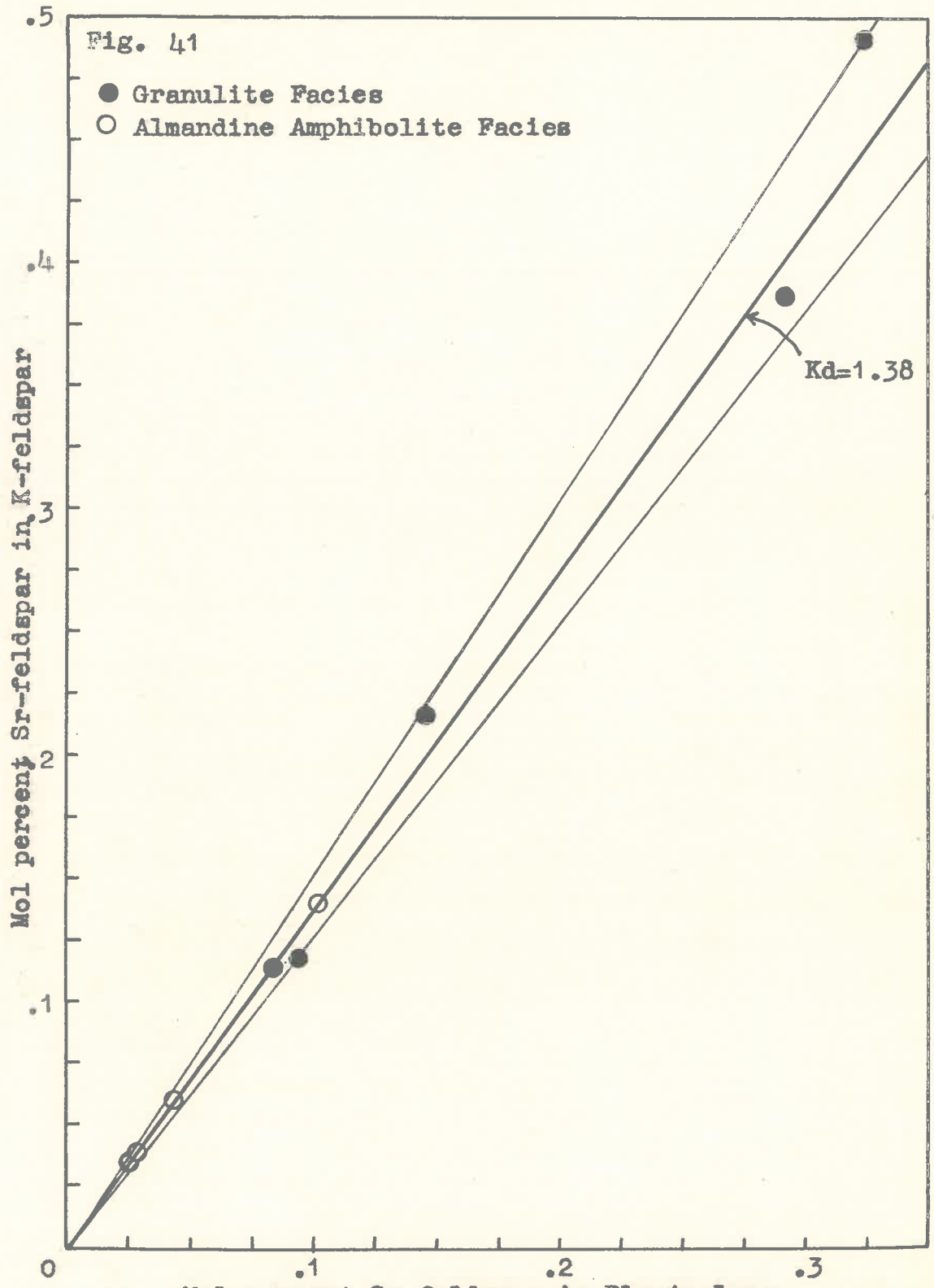
Distribution of strontium-feldspar  
between K-feldspar and Plagioclase

Musgrave Range area.



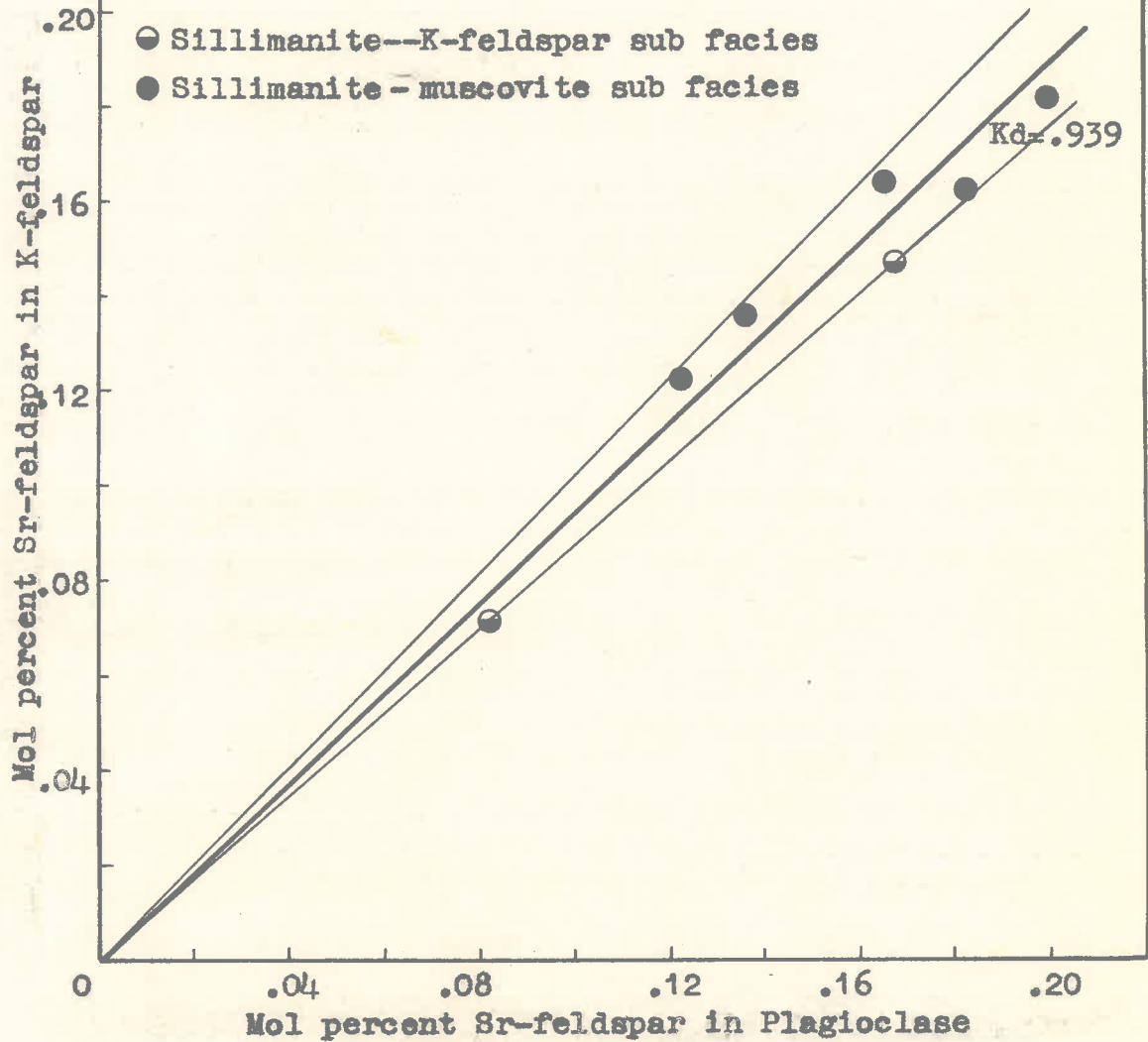


Mol percent Sr-feldspar in Plagioclase  
Distribution of strontium-feldspar  
between K-feldspar and Plagioclase  
Broken Hill area



Distribution of strontium-feldspar  
between K-feldspar and Plagioclase  
Ceylon area.

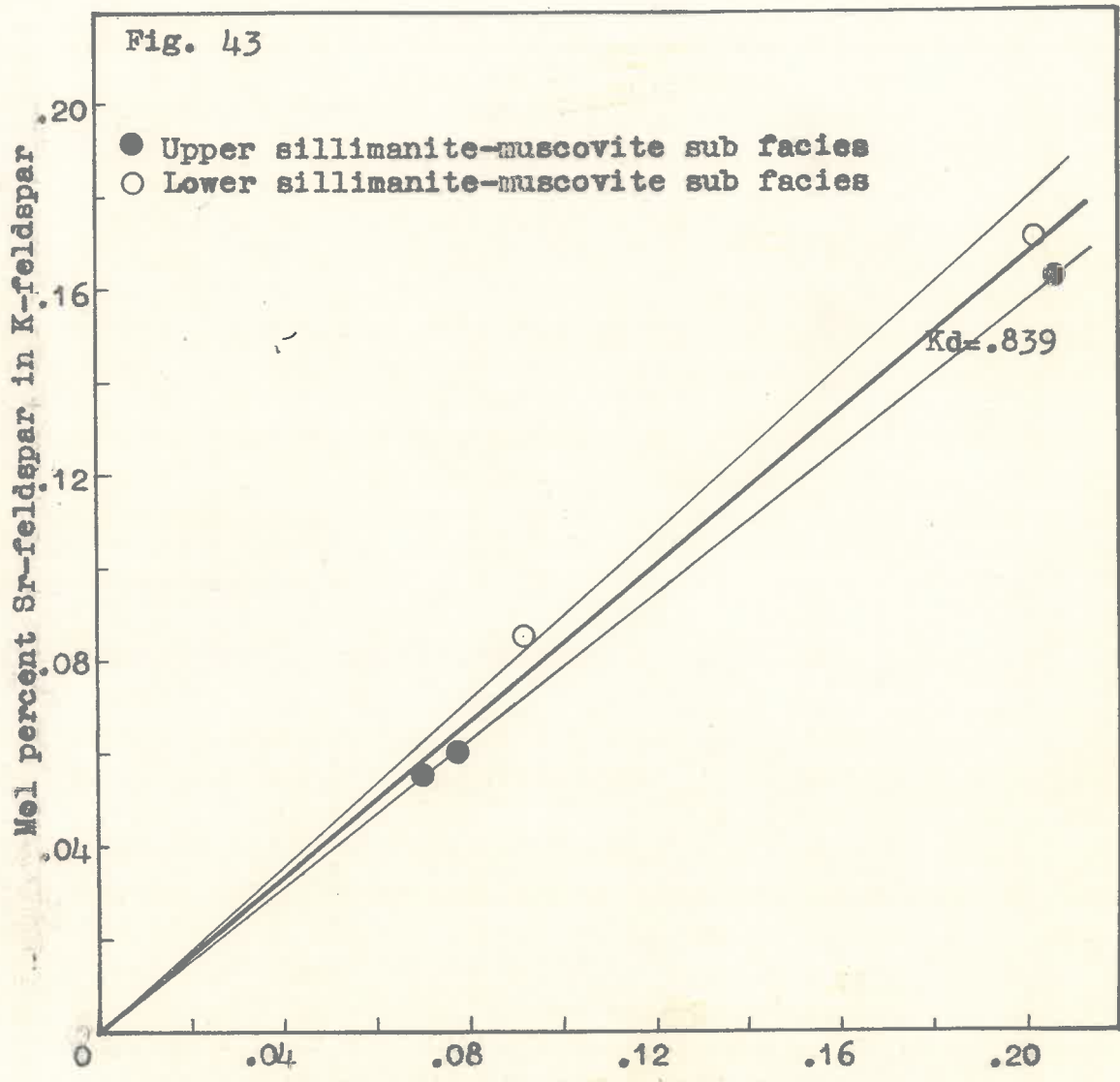
Fig. 42



Mol percent Sr-feldspar in Plagioclase

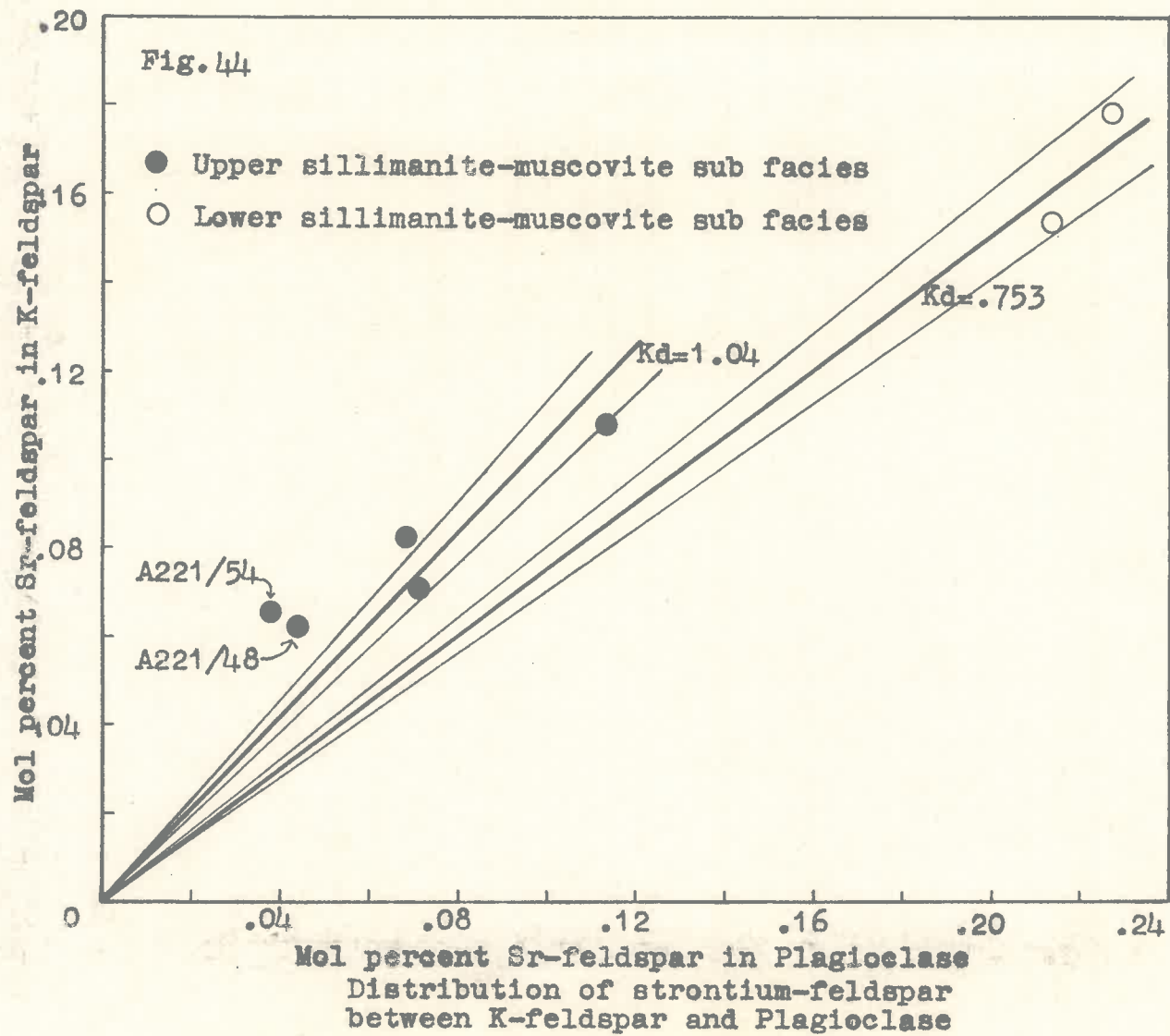
Distribution of strontium-feldspar  
between K-feldspar and Plagioclase

Pewsey Vale area.

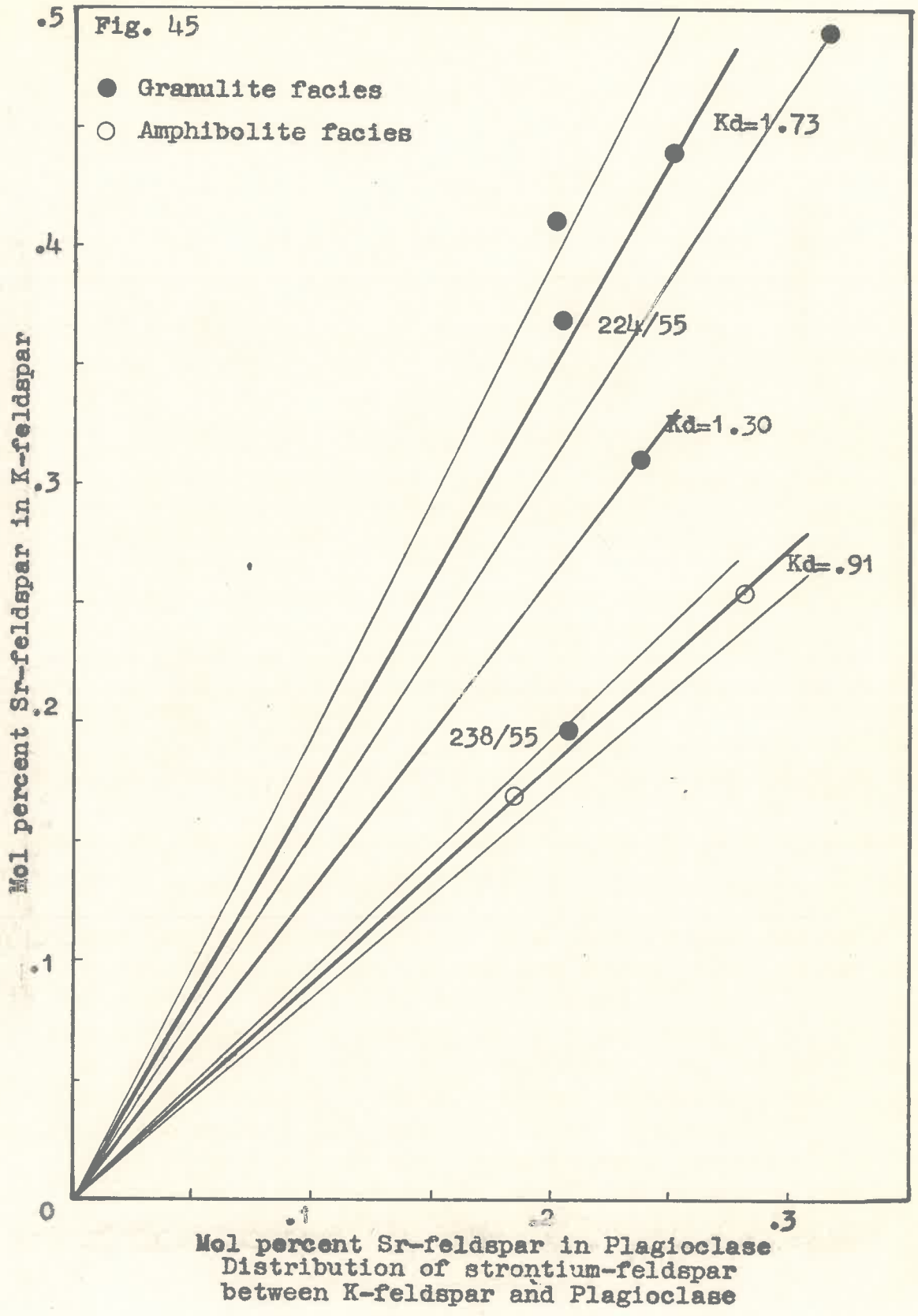


Mol percent Sr-feldspar in Plagioclase  
Distribution of strontium-feldspar  
between K-feldspar and Plagioclase

Palmer area.



Springton area.



pressure - temperature conditions and in the absence of any compositional effects (see also discussion of Na, Ba and Rb distributions) a constant distribution coefficient  $Kd_{SrF}$  should exist for the distribution of strontium between the coexisting feldspar pairs. On each diagram an average distribution coefficient and also a  $\pm 5$  percent range in  $Kd$  is indicated for isofacial rocks. Inasmuch as  $Kd$  is the ratio of two separate ratios an estimated precision of  $\pm 2$  percent in each determination of Sr would result in a  $\pm 4$  percent combined error. The estimated total error is increased due to a larger error in the Sr-feldspar content of the plagioclase. This is so because of the necessity to correct the determined Sr-feldspar component of the plagioclase concentrate to 100 percent feldspar due to unavoidable quartz contamination: in this correction procedure an error in the total feldspar components of the plagioclase concentrate due mainly to errors in the determined Ab, Or and An contents will increase the error in the Sr-feldspar content for pure plagioclase. For this reason a calculated total error of  $\pm 5$  percent in the average  $Kd_{SrF}$  is used. From these figures, the following generalizations can be made concerning iso-facial rocks:

- (a) the points fall close to a straight line that passes through the origin of the graphs.
- (b) the deviation of points from a straight line but still

within the  $\pm 5$  percent range in  $K_d$  are considered to be due to analytical errors alone. Those outside this range of error are discussed below.

It follows from (a) and (b) that:

- (c) The distribution of points about each line can be taken as a graphic expression of the Nernst distribution law. Also if the Nernst distribution law is applicable it is highly probable that Henry's law (i.e. a linear relationship between the activity of Sr and the concentration of Sr) is also realized in the plagioclase and potassium feldspars.
- (d) The regularity of Sr partitioning is a strong indication that chemical equilibrium has been attained between the coexisting phases.

Samples 30726 and 469 and 18L from the Musgrave Range and Broken Hill areas respectively are not consistent with the above generalizations, however, and some explanation is therefore necessary. In the Musgrave Range area, the  $K_d$  value for 30726 (equals 1.24) is significantly lower than the average  $K_d_{SrF}$  value for the other granulite facies samples (viz. 1.48). Mineralogical studies indicate that this sample is consistent with the highest grade of metamorphism in the area except for the triclinicity of the K-feldspar. Triclinicities measured according to the method of Goldsmith and Laves (1954) are consistently low for the K-feldspars



from the Musgrave Range granulite facies rocks (a single  $131/1\bar{3}1$  peak slightly broadened at the base) whereas the K-feldspars from the amphibolite facies rocks are all cross hatched twinned microclines having  $\Delta = .76 - .96$  but with a single well defined monoclinic peak between the triclinic peak. In contrast to both the above states the structural state of K-feldspar 30726 is randomly disordered (a broad diffuse hump is obtained in the  $131/1\bar{3}1$  region). It is reasonable to suggest that this departure from equilibrium is associated with the different distribution of strontium between the feldspars in 30726.

Some explanation of the genesis of randomly disordered feldspars is given by Smithson (1962), Christie et al. (1965), amongst others. Such factors as different temperature conditions, deformation, growth rates, presence of volatiles have been mooted to explain the transitional disequilibrium structural states represented by random order. In the Broken Hill area, samples 469 and 18L give distribution coefficients lower (1.04 and .94 respectively) in contrast to the average  $Kd_{SrF}$  value for the other granulite samples (1.25) of that area. Sample 18L occurs within the lode horizon and it is noted that the grains are fractured and seritized suggesting a later period of retrogressive metamorphism (Binns, 1963). Its lower Kd value is therefore probably due to these later changes. Sample 469 is

from the Alma Platy gneiss (Andrews 1922, King and Thompson, 1953) and thought to be of igneous origin because of its field relationships, chemical composition and angular inclusions of metasediment (Browne, 1922). Binns (1964) suggests that this unit in contrast to others may not have been completely recrystallized in the Willyama metamorphism and the Kd values are thus likely to be anomalous. Data from Taylor and Heier (1960), Heier (1962) and Taylor (1965a) indicate that K/Rb and Ba/Rb ratios in K-feldspars are sensitive indicators of geological processes and that these ratios decrease with increasing fractionation. In Table 20 the also anomalous K/Rb and Ba/Rb ratios from the K-feldspars of 469 (and also 18L) suggest in the light of postulations by the above workers that these rocks have crystallized from a different source than that of the other samples and therefore may represent different equilibrium states.

In the Langöy rocks the unaltered granulites and the amphibolite facies samples lie respectively on two separate lines (Figure 45) and a sample from a transitional metamorphic zone is in between. Samples 224/55 and 238/55 show retrogressive effects, particularly 238/55, and this may be the reason for its relatively low Kd.

With the advance from almandine - amphibolite facies to granulite facies the following changes in strontium distribution are noted:

Table 20. K/Rb and Ba/Rb ratios of K-feldspars from the Broken Hill area:

Sample number	K/Rb	Ba/Rb
642	280	9.63
466	284	12.00
462	303	17.09
465	314	15.94
447	303	15.39
410	352	11.12
469	231	3.68
18L	171	2.74

- (a) In the Musgrave Range, Broken Hill, and Langöy areas,  $Kd_{SrF}$  changes from 1.04 → 1.48; 1.00 → 1.25; .91 → 1.73, respectively.
- (b) In the Ceylon area  $Kd_{SrF}$  is similar for rocks of both facies and equal to 1.38

2. Almandine - amphibolite facies areas.

Data from the Pewsey Vale, Palmer and Springton areas are plotted in Figures 42, 43 and 44 respectively. In the Pewsey Vale area similar  $Kd$ 's are indicated for all samples (average  $Kd_{SrF} = .94$ ). These include migmatites and schists belonging to the sillimanite-almandine sub facies and pelites of the sillimanite orthoclase zone\*. In the Palmer area schists from the lower sillimanite-almandine muscovite sub facies and gneisses and migmatites from the upper sillimanite-almandine muscovite zone\*\* give the same  $Kd$ 's but lower than those from the Pewsey Vale area (average  $Kd_{SrF} = .84$ ). In the Springton area samples from the

---

\* In this zone muscovite is unstable and has presumably broken down completely according to the following reaction:  
 Muscovite + quartz  $\rightleftharpoons$  sillimanite + K-feldspar + H<sub>2</sub>O ... (1)

\*\* In the upper part of this zone, muscovite occurs, but in disequilibrium with sillimanite. This implies that the above reaction (1) has taken place but has not proceeded to completion. A zone in which sillimanite and K-feldspar only are stable (without muscovite) is not formed.

---

lower sillimanite-muscovite zone give an average  $Kd_{SrF}$  value of .75: higher grade samples from this area show wide scatter. It is thought that samples 221/54 and 221/48 are anomalous because the plagioclases are particularly heavily kaolinized and for this reason these rocks are ignored in the positioning of the average  $Kd_{SrF}$  of 1.04 in Figure 44; this is within the range of  $Kd$ 's for almandine-amphibolite facies rocks from elsewhere (approximately equal to or less than unity). Summarizing the data from the Kanmantoo group of sediments:

- (a) For isofacial rocks generalizations (a) - (d)<sub>A</sub><sup>p. 79</sup> above are applicable.
- (b) The transition from lower to upper sillimanite muscovite zone is characterized by an increase of  $Kd$  from .75 to 1.04 in the Springton area and uniform  $Kd$ 's (equal to .84) in the Palmer area.
- (c) Within the sillimanite muscovite zone samples from different areas give different  $Kd$ 's viz. .94, .84, .75 and 1.04.

B. FACTORS RESPONSIBLE FOR THE OBSERVED SYSTEMATIC CHANGES IN  $Kd_{SrF}$

The most likely variables controlling the strontium distribution are pressure, temperature and compositional factors (see Chapter II).

### 1. Compositional effects

Kretz (1959, 1960) found that the partitioning of an element between two coexisting phases is affected by the presence of certain chemical species in either mineral phase. Examples of this effect have been demonstrated in the partitioning of Rb and Ba between coexisting feldspars where  $Kd_{BaF}$ ,  $Kd_{RbF}$  are controlled partly by the K content of the plagioclase (see Chapter VI p.73). With regard to  $Kd_{SrF}$ , however, it is evident from the bulk compositions (in terms of Ab, An, Or contents given in Appendix VI) that there are no systematic differences in the composition of either phase in those instances where the average  $Kd_{SrF}$  value is different. In other instances even substantial variation of Si and Al content in plagioclase corresponding to different alkali concentrations can be ignored because in such instances where the rocks are isofacial,  $Kd$  is constant.

The length of the distribution line for each group of samples, to a first approximation, represents the range of absolute amounts of Sr in the rock samples; these lengths overlap extensively and the amount of Sr in an environment is therefore immaterial. That the absolute amounts of each feldspar phase can also be ignored is obvious. Of particular note is sample A200/27 (Figure 42) which contains < 5 volume percent of K-feldspar, but the  $Kd_{SrF}$  is consistent with the other samples which have greater volumes of

### K-feldspars.

Albee (1965b) showed that the presence of a third phase which readily accepts the partitioning element can alter the distribution coefficient. The present writer has previously noted that the presence of biotite can alter Rb partitioning between coexisting feldspars. The likely minerals to affect Sr partitioning are pyroxenes, hornblendes, garnets and biotites. Analyses of these minerals for Sr (Turekian and Phinney, 1962; Moxham, 1965; White (b), and others) indicate that their Sr content is very small and even allowing for the largest volumes of these minerals found in some of the writer's rocks, their presence can be safely ignored. The writer has found < 20 p.p.m. Sr in coexisting Ca rich hastingsites in A185/706 and A185/784 (Figure 44). It can be concluded that the presence of other phases in samples used in this study has no effect on Sr partitioning between coexisting feldspar phases.

### 2. Temperature effects

Elemental exchange experiments involving Ca, Na, K and Sr exchange between coexisting feldspars are being carried out in the writer's department by Mr. P. Slade. A brief discussion of these experiments is given in Chapter V. Mr. Slade has found that, for absolute concentrations of Sr in the synthetic feldspars similar to that determined in natural coexisting feldspars by the present writer, strontium

distributions between the coexisting feldspars in systems of similar bulk composition is temperature dependent. For example  $Kd_{SrF}^*$  at 520, 660 and 770°C (experiments 10, 8 and 7 in Table 15) is .655, .801 and .960, respectively. It is not possible at this stage of Mr. Slade's work to explain different  $Kd$ 's at the same temperature in systems of different bulk composition and certainly this effect is not consistent with the writer's data from natural systems. It is believed that this is not principally a function of the bulk composition. For this reason it is not possible, yet, to equate the experimentally determined  $Kd$ 's at particular temperatures with the naturally determined distribution coefficients. It is important however that a trend with temperature is obtained, and that this trend viz. with increasing temperature  $Kd_{SrF}$  changes such that more strontium is taken into the K-feldspar in preference to the plagioclase, is in the same sense as observed in natural systems corresponding to different grades of metamorphism (e.g. see Figures 39, 40, 44 and 45).

### 3. Pressure effects

The effect of pressure on elemental partitioning between coexisting feldspars is generally insignificant in comparison to temperature and compositional effects. This is supported by data from some mineral systems: e.g. Ramberg

---

\* See footnote on p. 78

---



and DeVore (1951), Kretz (1961), and Albee (1965a), who have examined this effect in a theoretical way (see Chapter II p. 13); more positive data are provided by the experimental work of Eugster (1955) (see Chapter II, p. 13).

It is concluded therefore from the foregoing discussion that temperature is the sole variable affecting the distribution of Sr between feldspar phases in such a way that with increasing temperature more Sr is taken into the coexisting K-feldspar phase. Theoretical considerations predict that an increase in the distribution coefficient can be associated with either an increase in temperature or a decrease in pressure (the converse will also be true). It is unlikely, however, that an increase in temperature in metamorphic systems is always accompanied by a decrease in total pressure. Therefore a decrease in pressure is an improbable alternative to the above hypothesis.

### C. DISCUSSION

The following postulations can be made in the light of the temperature dependence of  $Kd_{SrF}$ :

- (a) for isofacial rocks uniform horizontal temperature gradients are likely for comparatively large areas of regional metamorphism e.g. the Musgrave Range, Pewsey Vale areas.
- (b) in a single area uniformly higher temperatures of crystallization are indicated by granulite facies rocks

in comparison to almandine - amphibolite facies rocks. This also applies when data from all areas are compared. The almandine - amphibolite facies rocks from Ceylon are an exception which is discussed below.

- (c) Different temperatures are indicated for different granulite facies areas (cf. Kd's from the high grade rocks in Ceylon, Broken Hill, Musgrave Range and Langöy areas).
- (d) Within the sillimanite zone\* of the almandine - amphibolite facies from the Springton area, significantly lower temperatures of recrystallization are indicated by samples from the lower part of this zone than by samples of higher grade in this zone and these latter temperatures are lower than those corresponding to granulite facies conditions.
- (e) In different areas rocks from the sillimanite-muscovite zone have been uniformly metamorphosed† within the

---

\* This corresponds to the sillimanite-almandine-muscovite and the sillimanite-almandine orthoclase sub facies defined by Turner and Verhoogen, (1960).

† Some confirmatory evidence of this in the Palmer area, is indicated in Figure 46. In this figure, data from White (b) relating to Ba and Rb exchange between coexisting biotite and K-feldspar phases in samples from the upper sillimanite-muscovite zone are plotted. Conformity of points about a straight line passing through the origin indicates that chemical equilibrium between the coexisting

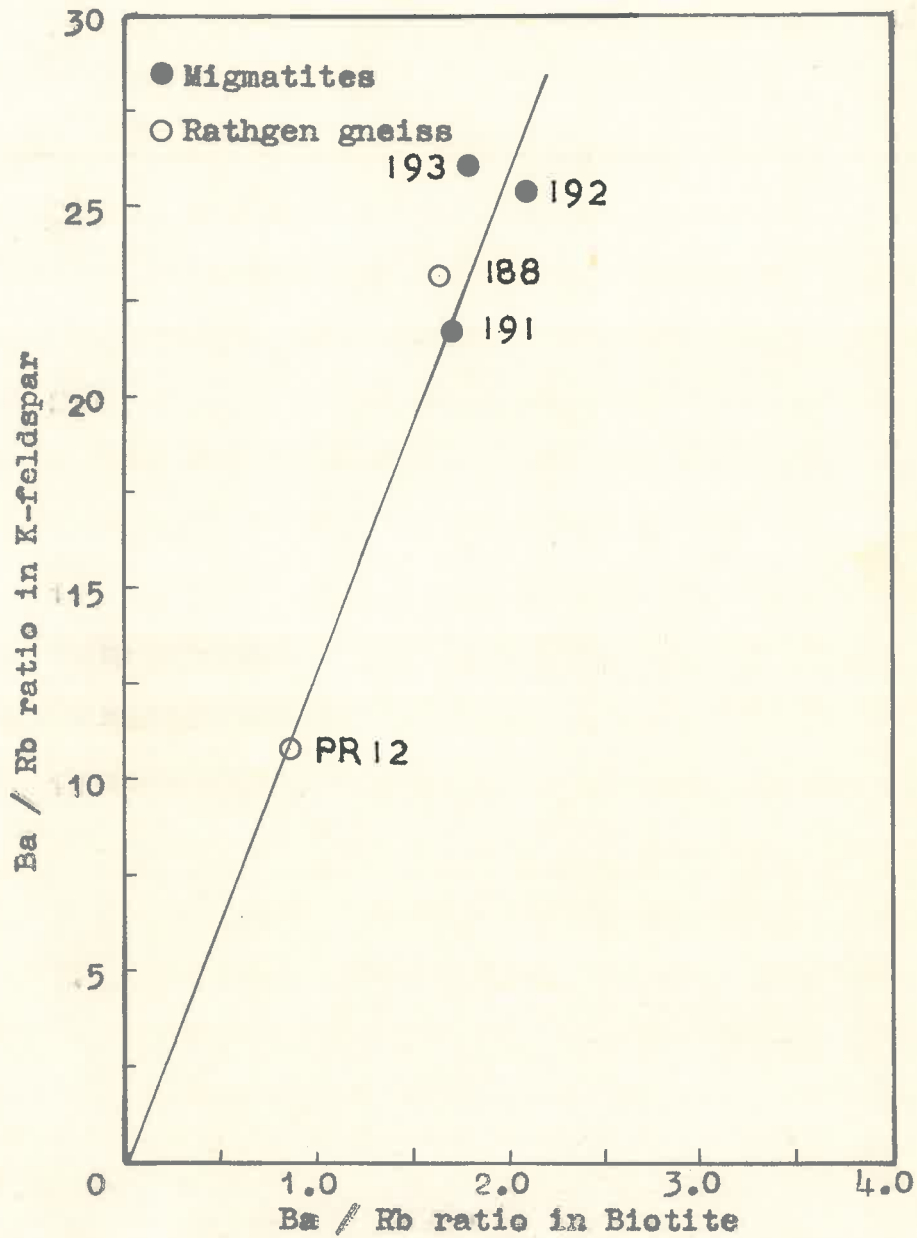


Fig. 46. Distribution of Ba / Rb ratio between coexisting K-feldspar and Biotite. Palmer area.

temperature range indicated by the Springton area\*.

- (f) The transition granulite - amphibolite facies corresponds to a comparatively small temperature range (when all data are considered  $Kd_{SrF}$  approaches unity for this metamorphic transition).

Some further ideas relating to the uniform temperature conditions in each of the granulite facies areas of Broken Hill and Musgrave Ranges and also relating to the difference between the average temperatures for these areas and the granulite facies in Ceylon are as follows. Uniform temperature conditions within the granulite facies samples from the Musgrave Range and Broken Hill areas are reflected in the compositions (inferred from R.I. measurements) of coexisting ortho- and clino-pyroxenes from basic granulites (Figure 47, Binns 1962, Figure 2). These rocks are closely associated phases and uniform  $P_T$ -T conditions of equilibration have been achieved for these samples of migmatites and gneisses. Similar data from samples close to DVH2 and AJWH6 (see location map Figure 9) were not available.

\* Also sample A221/104 (Appendix VI), taken from the migmatite zone in the Reedy Creek area gives a  $Kd_{SrF}$  value equal to 1.00 which is consistent with the relative temperatures for the highest grade rocks in the sillimanite zone.

---

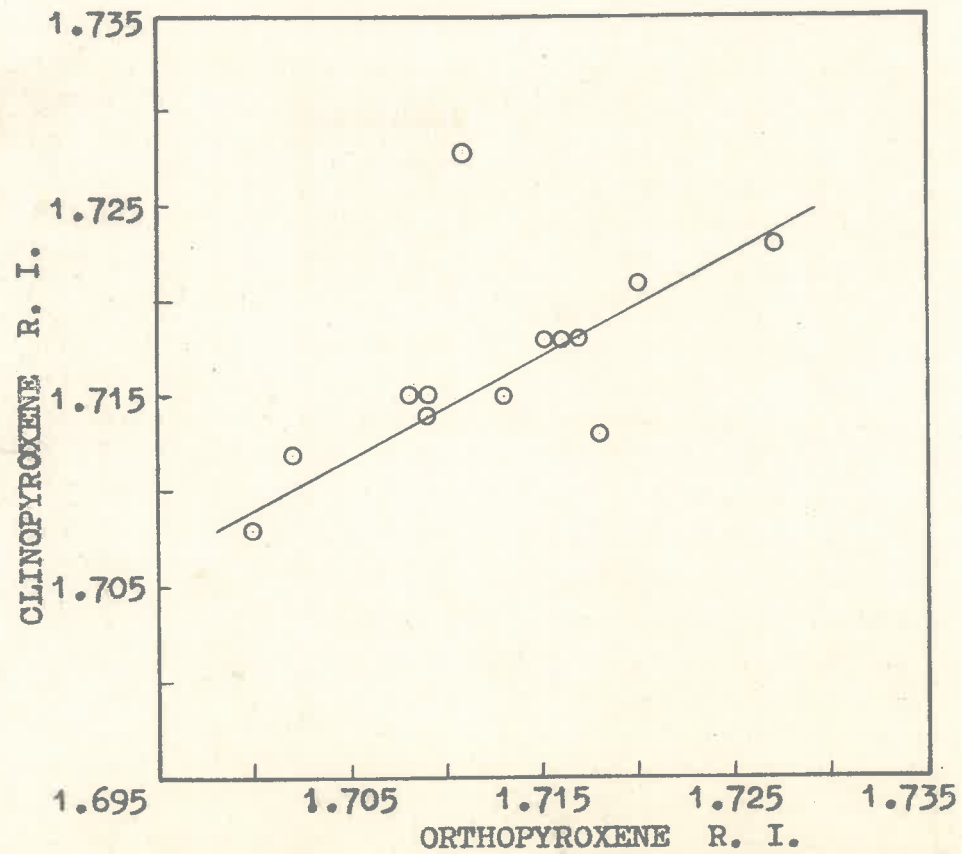


Figure 47. Plot of refractive index of orthopyroxene against of coexisting clinopyroxene (both  $\pm .001$ ) from the Musgrave Range area (Data taken from Wilson, 1960).

in the field with the acidic rocks containing the feldspars which have been studied from these areas. Furthermore from Binns (op. cit. Figure 7) it is likely that the linear plots of optical properties represent an orderly arrangement of  $\text{Fe}^{2+}$  and  $\text{Mg}^{2+}$  between the coexisting pyroxenes under specific environmental conditions. In this connection Kretz (1961) indicated that the distribution of iron ( $\text{Fe}^{2+}$ ) and magnesium between coexisting pyroxenes is mainly temperature dependent such that with increasing temperature the  $\frac{\text{Fe}^{2+}}{\text{Mg}}$  ratio increases in the clinopyroxene in preference to the coexisting orthopyroxene. In Figure 48 the writer has plotted  $\frac{\text{Fe}}{\text{Mg}}$  ratios of coexisting pyroxenes from Broken Hill (Binns, 1962), Musgrave Range (Wilson, 1960b) and Madras area, India (Howie, 1955). From the conclusions of Kretz (1961) and Binns (1962), the intercepts of the lines on the orthopyroxene axis can be regarded as a function of metamorphic grade such that line D represents the highest temperatures of crystallization. Comparison of data in Figures 39 and 40, and Figure 48 indicates that the relative temperatures of crystallization for the granulites from the Musgrave Range and Broken Hill areas deduced from the strontium feldspar distribution coefficient are in agreement with the relative temperatures indicated by the coexisting pyroxene data (cf. lines D and A in Figure 48). Also plotted in Figure 48 are data from the Madras district India which indicate a grade

Figure 48.

In Figure 48, data relating to the Musgrave Range area are optically derived (RI & 2V) composition whilst the data from the other areas are taken from chemical analyses: data from the Broken Hill and Madras areas are from Binns (1962) and Howie (1955) respectively.

Lines A and B refer to lower and intermediate grades of metamorphism within the granulite facies from the Broken Hill area, line C to the granulites from India and line D to the granulites from the Musgrave Range area.





of metamorphism between that of the Musgrave Range and Broken Hill areas. This is in approximate agreement with the relationship between the temperature of crystallization indicated by the  $Kd_{SrF}$  values, for the granulites in Ceylon, and the indicated temperatures for the Musgrave Range and Broken Hill areas (cf. Fig. 41 with Figs. 39 and 40). This latter comparison may be entirely fortuitous however, since the samples from India have been taken from a much larger area than in either the Musgrave Range or Broken Hill areas and also the granulites from the Madras district may not be of the same grade of metamorphism as the Highland Series rocks in Ceylon. In the Broken Hill and Musgrave Range areas the coexisting pyroxene rocks occur intermixed with the rocks from which the coexisting feldspars have been analysed. A comparison between these areas is justified.

Data from Ceylon are in contrast to the general pattern of Sr partitioning viz. higher temperatures of metamorphism for granulite facies rocks in comparison to almandine - amphibolite facies material. Strontium partitioning between coexisting feldspars in the Vijayan Series (almandine - amphibolite facies, Cooray 1962) is indicative of chemical equilibrium but the average  $Kd_{SrF}$  is 1.38 and the same as that for the Highland Series (granulite facies) rocks. Similar temperatures (and furthermore temperatures consistent with granulite facies conditions) are therefore inferred for the

recrystallization of both facies rocks.

These findings are somewhat inconsistent with the interpretations of the metamorphism by other workers in Ceylon as discussed also in Chapter III p. 20. For the purpose of convenience some generalizations are repeated in the following text. Cooray (1961, 1962) derives the Vijayan Series by retrogressive metamorphism from Highland Series type rocks. He also suggests that water has played an important role in the conversion to almandine - amphibolite facies rocks. Oliver (in press) suggests that different garnet compositions in Vijayan and Highland Series rocks may reflect different  $P_T$ -T conditions though his evidence from the composition of a single phase must be treated with caution in the light of data from Kretz (1959); Albee (1965a and b); Evans (1965) and Atherton (1965).

An alternative interpretation of the writer's data is that Sr has not partitioned according to differences of temperature, though the sensitivity of Sr to temperature changes as indicated elsewhere renders this unlikely. The writer's preferred interpretation is that both the Highland and Vijayan Series have been metamorphosed under uniform granulite temperature conditions and the different mineralogical compositions of the two Series are primarily a function of different bulk compositions, particularly water. The occurrence of microcline in the Vijayan rocks (in comparison

to orthoclase in the Highland Series) is probably the result of transformation of original monoclinic K-feldspar in the presence of a high fluid content with slow cooling during which there has been no change of the already established, respective Highland and Vijayan Series chemical equilibrium compositions and mineralogical compositions. The ease with which feldspars can be ordered has been noted by various authors (Heier 1957, 1962; Nilssen et al. 1965) and implies that such processes can take place without affecting chemical compositions of coexisting mineral phases. The writer's data can be taken as support that the strontium feldspar distribution coefficient reflects the near maximum temperatures which the rocks have subjected to (cf. criticism by Dietrich, 1961 p. 16).

There is left now to examine the changes in temperature at metamorphic grades lower than the granulite - amphibolite facies transition. As previously noted lower temperatures of crystallization are indicated for these rocks by the lower  $Kd_{SrF}$  values. In the Springton area differences in temperatures of recrystallization are indicated between samples from the lower sillimanite-muscovite zone (.8 - 2.1 km. upgrade from the sillimanite isograd) and samples from the upper part of this zone (>3.3 km. upgrade from the sillimanite isograd). It is apparent that a horizontal temperature gradient has existed within the upper part of this zone

during regional metamorphism. This contrasts with the uniform temperatures of equilibrium obtained in the Palmer area for samples from close to the sillimanite isograd and also samples from assumed higher parts of this zone (migmatite zone). The migmatite zones in the Palmer and Springton areas form the western and eastern margins respectively of an elongate high grade node (see Figure 7). Sufficient detailed mapping within the Kanmantoo group of sediments has not been done to delineate isotherms about this node although the grade of metamorphism everywhere increases towards it. The close proximity of the sillimanite isograd in the Springton area to this high grade zone in comparison to the Palmer area (see Figure 7) is perhaps in support of the steeper temperature gradient indicated by the  $Kd_{\text{Srf}}$  values in the Springton area.

Data from the sillimanite - muscovite zone in the <sup>area</sup> Pewsey Vale indicates that uniform temperatures of metamorphism have been reached over a comparatively large area including migmatized and non migmatized rocks. In this area pelites (A200/124A and A200/887) consistent mineralogically with the sillimanite - K-feldspar sub facies, and occurring as isolated lenses within the migmatitic rocks in which muscovite is stable, indicate the same temperature of recrystallization. In order to explain the close proximity

of these two mineralogical facies, Offler (1966 and pers. comm.) suggests that the pelites have been metamorphosed under lower  $P_{H_2O}$  conditions in which case muscovite will break down while still occurring in adjacent migmatites. This obviates the necessity for a steep temperature gradient between the two rock types. As noted previously, data from the Pewsey Vale and Palmer areas indicate a grade of metamorphism within the range shown by the Springton area.

It can be concluded then that over the range of metamorphic grade examined in this study viz. middle almandine - amphibolite facies to high grade granulite facies, continuous, systematic, and significant temperature dependent changes in Sr partitioning occurs between coexisting feldspars.

#### D. STRONTIUM PARTITIONING IN TERMS OF THE FELDSPAR STRUCTURES AND ATOMIC PROPERTIES.

Strontium partitioning between feldspars can be explained satisfactorily in structural terms. The relevant details of the two feldspar lattices have been summarized by Taylor (1965b) but some discussion important to this study is given below.

The group of oxygen atoms around the cation positions (K, Na or Ca) is irregular but is comparatively constant for most of the feldspar structures. The K-cation environment in K-feldspars is similar in sanidine, orthoclase and microcline and is made up of nine nearest oxygen atoms at

distances less than about  $3.1\text{\AA}$  although one of the K-O bonds ( $\text{K-O}_{A2}$ ) is much shorter than the rest and only slightly smaller ( $2.698\text{\AA}$  in orthoclase) than the sum of the accepted ionic radii ( $\text{K}^+ = 1.33\text{\AA}$ ;  $\text{O}^{2-} = 1.40\text{\AA}$ ). In low albite the sodium cation is surrounded by seven nearest oxygen atoms ( $< 3.0\text{\AA}$ ), whereas in high albite other oxygen atoms are also closer and a higher co-ordination is probably possible. Also, in anorthite the calcium atom is bounded by 7 nearest oxygen atoms ( $< 3.1\text{\AA}$ ) but in bytownite two of the four sites are in seven fold co-ordination whereas the other two are in 6-fold co-ordination. Again in the plagioclase lattices the cation - oxygen bond ( $\text{Na-O}_{A2}$ ;  $\text{Ca-O}_{A2}$ ) is exceptionally shorter than the other cation bonds. As the ionic radius\*\* of  $\text{Sr}^{2+}$  ( $1.18\text{\AA}$ ) is close to all three cations,  $\text{K}^+ = (1.33\text{\AA})$ ,  $\text{Na}^+ = (.98\text{\AA})$  and  $\text{Ca}^{2+} = (.99\text{\AA})$  it can be suggested then that suitable co-ordination of strontium is achieved in both feldspar lattices; strontium preferring K and probably Ca sites in the K-feldspar and plagioclase lattices respectively. However an important difference between the cation environment of the respective feldspars exists: the plagioclase sites are much smaller than in the K-feldspars and this is due to collapse of the Si and Al tetrahedral framework around the smaller cations. This

---

\* Radii from Ahrens, 1953. \*\* Strontium radius from Heier and Taylor, 1959.

---

means in effect that both calcium and sodium are tightly co-ordinated in the plagioclase lattice. Comparison between the calculated Sr-O inter-ionic distance (using the above accepted ionic radii) and the observed Na-O, Ca-O and K-O distances suggests that acceptance of strontium into the plagioclase lattice will involve a certain pushing apart of the oxygen anions in order that a void of requisite size is formed. It might therefore be expected that, in terms of purely geometrical considerations, strontium would substitute preferentially into the K-site of the K-feldspars at any given temperature.

It is evident however, from the writer's work that temperature is the most important single factor in controlling changes in Sr partitioning between the coexisting feldspars. This is also supported by data from an experimental system (see Chapter V p. 59). These data show that with increasing temperature, strontium is preferentially taken into the K-feldspar lattice in comparison to the coexisting plagioclase.

Certain atomistic effects are likely in the advent of elevated temperatures:

- (a) Increased openness of the cation environment due to increased thermal agitations.
- (b) Increase in the "effective radius"\* of the Sr atom due

---

\* Donnay and Donnay, 1952.

---

to increased thermal vibrations.

- (c) Increase in the entropy of both feldspar lattices due to disordering of Si and Al.

The degree of ordering in the K-feldspar has no observable effect on the Sr partitioning e.g. K-feldspars from the almandine-amphibolite and granulite facies rocks in the Musgrave Range and Ceylon areas have respectively triclinic and monoclinic states but in the former case the  $K_d$ 's are different whereas in the latter they are the same. The relative magnitude of effects (a) and (b) above cannot be stated definitely but the reason that with increasing temperature, strontium will be preferentially taken into the K-feldspar lattice is perhaps because the larger effective radius of the Sr atom excludes this element from the plagioclase sites. At significantly lower temperatures the better fit of strontium in the plagioclase sites seems to be the more important factor despite the larger size of strontium in comparison to calcium and sodium sites.

#### E. SUMMARY

The hypothesis, that there should be a regular partitioning of elements between coexisting minerals, provided equilibrium is established in the absence of compositional influences has been confirmed for strontium. The positive results indicate that the partitioning can be described by the Nernst distribution equation of the type: Sr-feldspar



component in the K-feldspar / Sr-feldspar component in the plagioclase = constant. Further it has been shown that the Sr partitioning varies with the varying metamorphic grade (equal P - T conditions) in a regular manner. There is evidence from experimental studies to suggest that this partitioning depends solely on temperature.

In conclusion then the writer suggests that strontium - feldspar distribution coefficients can be used reliably as geothermal indicators. It is inferred that if all data are taken into consideration the Sr-feldspar coefficient closely represents the maximum temperatures to which the rocks have been subjected. Furthermore it is of interest to note that mineralogical metamorphic facies can be misleading in terms of inferred temperatures of recrystallization viz. Ceylon area.

More conclusive indications of the temperature dependence of Sr partitioning in terms of feldspar structures and atomic properties must await future experimental work.



BIBLIOGRAPHY

- AHRENS, L. H. (1953), The use of ionization potentials - I. Ionic radii of the elements. Geochim. et Cosmochim. Acta 2, 155-169.
- ALBEE, A. L. (1965a), Distribution of Fe, Mg, and Mn between garnet and biotite in natural mineral assemblages. J. Geol. 73, 155 - 164.
- ALBEE, A. L. (1965b), Phase equilibria in three assemblages of kyanite-zone pelitic schists, Lincoln Mountain Quadrangle, Central Vermont. J. Petrology 6, 246 - 301.
- ANDREWS, E.A. (1922), The geology of the Broken Hill District. Mem. geol. Surv. N.S.W., Geol. 8, 1 - 432.
- ATHERTON, M. P. (1965), The chemical significance of isograds. In PITCHER, W. S.: Controls of Metamorphism p. 169 - 202. Edinburgh; Oliver and Boyd.
- BAIRD, A.K. (1961), A pressed-specimen die for the Norelco vacuum-path X-ray spectrograph. Norelco Repr. 8, 108 - 109.
- BARTH, T.F.W. (1956), Studies in gneiss and granite. I. Relation between temperature and the composition of the feldspars. Norske Vid. Akad. Skr. no. 1.
- BARTH, T.F.W. (1961), The feldspar lattices as solvents of foreign ions. Curs. y. confs. Fasc. VIII, 3 - 8.
- BINNS, R.A. (1962), Metamorphic pyroxenes from the Broken Hill District, New South Wales. Minerolog. Mag. 33, 320 - 338.
- BINNS, R.A. (1963), Some observations on metamorphism at Broken Hill, N.S.W. Proc. Australas. Inst. Min. Metall. 207, 239 - 261.
- BINNS, R.A. (1964), Zones of progressive regional metamorphism in the

- Willyama Complex, Broken Hill District, New South Wales.  
J. geol. Soc. S. Aust. XI, 283 - 330.
- BIRKS, L.S. (1959), X-ray spectrochemical analysis. New York:  
 Interscience Publishers.
- BOWEN, N.L. and SCHAIRER, J.F. (1935), The System MgO-FeO-SiO<sub>2</sub>.  
Am. J. Sci. 5th ser., 29, 151 - 217.
- BROWNE, W.R. (1922), Report on the petrology of the Broken Hill  
 region, excluding the great lode and its immediate vicinity.  
 Appendix I. Mem. geol. surv. N.S.W. Geol. 8, 245 - 353.
- CHINNER, G.A. (1955), The granite gneisses of the Barossa Ranges,  
Unpublished M.Sc. Thesis, University of Adelaide.
- COORAY, P.G. (1961), The geology of the country around Rangala.  
Ceylon Dept. Minerology Mem. 2.
- COORAY, P.G. (1962), Charnockites and their associated gneisses in  
 the pre-cambrian of Ceylon. Quart. J. geol. Soc. Lond. 118,  
 239 - 273.
- DEER, W.A. et al. (1963), Rock-forming minerals. Vol. 4 - Framework  
silicates. London: Longmans.
- DEVORE, G.V. (1955), Crystal growth and the distribution of elements.  
J. Geol. 63, 471 - 494.
- DIETRICH, R.V. (1961), Comments on the "two-feldspar geothermometer"  
 and K-feldspar obliquity. Curs. y confs. Fasc. VIII, 15-20.
- DONNAY, G. and DONNAY, J.D.H. (1952), The symmetry change in the high-  
 temperature alkali-feldspar series. AM. J. Sci. Bowen vol.,  
 115 - 132.
- ENGEL, A.E.J. and ENGEL, C.G. (1958), Progressive metamorphism and

- granitization of the major paragneiss, Northwest Adirondack Mountains, New York. Part I: total rock. Bull. geol. Soc. Am. 69, 1369 - 1413.
- ENGEL, A.E.J. and ENGEL, C.G. (1960), Progressive metamorphism and granitization of the major paragneiss, Northwest Adirondack Mountains, New York. Part II: mineralogy. Bull. geol. Soc. Am. 71, 1 - 57.
- EUGSTER, H.P. (1955), The cesium-potassium equilibrium in the system sanidine-water. Carnegie Inst. Wash. Yearbook no. 54, 112-3.
- EVANS, B.W. (1965), Pyrope garnet-piezometer or thermometer. Bull. geol. Soc. Am. 76, 1295 - 1300.
- GOLDSMITH, R. and LAVES, F. (1954), The microcline-sanidine stability relations. Geochim. et Cosmochim. Acta. 5, 1 - 19.
- HEIER, K.S. (1957), Phase relations of potash feldspar in metamorphism. J. Geol. 65, 468 - 479.
- HEIER, K.S. (1960), Petrology and geochemistry of high-grade metamorphic and igneous rocks on Langoy, Northern Norway. Norg. geol. Unders. no. 207.
- HEIER, K.S. (1962), Trace elements in feldspars - a review. Norsk geol. Tidsskr. Bind 42.2, 415 - 454.
- HEIER, K.S. and TAYLOR, S.R. (1959), Distribution of Li, Na, K, Rb, Cs, Pb and Tl in southern Norwegian pre-Cambrian alkali feldspars. Geochim. et Cosmochim. Acta. 15, 284 - 304.
- HOPKINS, B. McD. (1950), Report on Monarto-Summerfield area; Unpublished Honours Thesis, University of Adelaide.
- HOSSELD, P. (1925), The Tanunda Creek granite and its field relations. Trans. Soc. S. Aust. 49, 191 - 197. Trans. R. Soc. S. Aust.

- HOWER, J. (1961), The determination of Sr/Rb ratios by an X-ray spectrographic technique. U.S. Atomic Energy Commission NYO-3942, Ninth Annual Progress Report for 1961. 179 - 191.
- HOWIE, M.A. (1955), The geochemistry of the charnockite series of Madras, India. Trans. R. Soc. Edinb., 62, 725 - 768.
- JOHNS, R.K. and KRUGER, J.M. (1949), The Murray Bridge and Monarto granites and associated rocks of the metamorphic aureole. Transactions of the Royal Soc. of South Australia. 73, 122-136.
- KING, H.F. and THOMPSON, B.P. (1953), Geology of the Broken Hill District. In Geology of Australian Ore deposits. Proc. 5th Emp. Min. Metall. Congr. I, 533 - 577.
- KRETZ, R. (1959), Chemical study of garnet, biotite, and hornblende from gneisses of southwestern Quebec, with emphasis on distribution of elements in coexisting minerals. J. Geol. 67, 371 - 402.
- KRETZ, R. (1960), The distribution<sup>of</sup> certain elements among coexisting calcic pyroxenes, calcic amphiboles and biotites in skarns. Geochim. et Cosmochim. Acta 20, 161 - 191.
- KRETZ, R. (1961), Some applications of thermodynamics to coexisting minerals of variable composition. Examples: orthopyroxene-clinopyroxene and orthopyroxene-garnet. J. Geol. 69, 361 - 387.
- LIEBHAFSKY, H.A. et al. (1960), X-ray absorption and emission in analytical chemistry. New York: John Wiley and Sons.
- LORENTZ, R. and ERBE, F. (1929), Das Verteilungsgleichgewicht von Silber zwischen Blei und Aluminium, ein Beitrag zur Prüfung des

- Verteilungssatzes für kondensierte Systeme. Zeitschr. anorg. Chemie, 183, 311 - 339.
- MILLS, K.J. (1964), The structural petrology of an area east of Springton, South Australia. Unpublished Ph.D. Thesis, University of Adelaide.
- MOXHAM, R.L. (1965), Distribution of minor elements in coexisting hornblendes and biotites. Can. Mineralogist, 8, 204 - 240.
- MUELLER, R.F. (1960), Compositional characteristics and equilibrium relations in mineral assemblages of a metamorphosed iron formation. Am. J. Sci. 258, 449 - 97.
- MUELLER, R.F. (1961), Analysis of relations among Mg, Fe and Mn in certain metamorphic minerals. Geochim. et. Cosmochim. Acta. 25, 267 - 96.
- NICKEL, E.H. (1954), Distribution of major and minor elements among coexisting ferro-magnesian silicates. Am. Miner. 39, 486 - 493.
- NILSSEN, B. and SMITHSON, S.B., Studies of the pre-cambrian Herefoss granite. I. K-feldspar obliquity Norsk geol. Tidsskr. Bind 45, 1965 p. 367 - 396.
- NOCKOLDS, S.R. and MITCHELL, R.L. (1948), The geochemistry of some Caledonian plutonic rocks; a study in the relationship between the major and trace elements of igneous rocks and their minerals. Trans.<sup>R.</sup> Soc. Edinb. 61, 533 - 575.
- OFFLER, R. (1966), The structure and Metamorphism of the Pewsey Vale area, North East of Williamstown, S.A. Unpublished Ph.D. Thesis, University of Adelaide.
- OLIVER, B.L. (1957), The geological structure of Ceylon. Ceylon

Geographer XI, 9 - 16.

- OLIVER, R.L. (In prep.), Note on some garnetiferous rocks from Ceylon.
- OLIVER, R.L. and ERB, D.K. (1957), Reconnaissance study of the geology of the Kirinda Oya basin. Ceylon Geographer. XI, 25 - 9.
- ORVILLE, P.M. (1962), Comments on the two-feldspar geothermometer Norsk Geol. Tidsskr. Bind 42.2, 340 - 348.
- RAMBERG, H. (1952), The origin of metamorphic and metasomatic rocks. Chicago: University of Chicago Press.
- RAMBERG, H. and DEVORE, G.W. (1951), The distribution of  $Fe^{++}$  and  $Mg^{++}$  in coexisting olivines and pyroxenes. J. Geol. 59, 193 - 210.
- RATTIGAN, J.H. and WEGENER, C.F. (1951), Granites of the Palmer area and associated granitized sediments. Trans. R. Soc. S. Aust. 74, 149 - 164.
- REYNOLDS, R.C. (1963), Matrix corrections in trace element analysis by X-ray fluorescence: estimation of the mass absorption coefficient by Compton scattering. Am. Miner. 48, 1133-1143.
- SANDO, M. (1957), The granitic and metamorphic rocks of the Reedy Creek area, Mannum, South Australia. Unpublished M.Sc. Thesis, University of Adelaide.
- SMITHSON, S.B. (1962), Symmetry relations in alkali feldspars of some amphibolite-facies rocks from the Southern Norwegian Precambrian. Norsk geol. Tidsskr. Bind 42.2 586 - 599.
- STEUHL, H.H. (1960), Die experimentelle Metamorphose und anatexis

- eines Parabiotitgneises aus dem Schwarzwald. Diss. Marburg.  
 Referred to in Winkler, 1961.
- TAYLOR, S.R. (1965a), The application of trace element data to  
 problems in petrology. Physics and chemistry of the earth.  
6, 133 - 213. Oxford: Pergamon Press.
- TAYLOR, W.H. (1965b), Framework silicates: the feldspars. In BRAGG, L:  
Crystal structure of minerals. 293 - 339. London: G. Bell  
 and Sons.
- TAYLOR, S.R. and HEIER, K.S. (1960), The petrological significance of  
 trace element variations in alkali feldspars. Int. Geol.  
Congr. XXI Norden Part XIV, 47 - 61.
- TAYLOR, S.R. and KOLBE, P. (1964), Geochemical standards. Geochim. et  
Cosmochim. Acta. 28, 447 - 454.
- TUREKIAN, K.K. and PHINNEY, W.C. (1962), The distribution of Ni, Co,  
 Cr, Cu, Ba and Sr between biotite-garnet pairs in a metamorphic  
 sequence. Am. Miner. 47, 1434 - 41.
- TURNER, F.J. and VERHOOGEN, J. (1960), Igneous and metamorphic petrology.  
 2nd ed. New York: McGraw-Hill.
- VITANAGE, P.W. (1959), The geology of the country around Polonnaruwa.  
Ceylon Dept. Min. Mem. 1.
- WHITE, A.J.R. (1956), Granites and associated metamorphic rocks of  
 Palmer, South Australia. Unpublished Ph.D. Thesis, University  
of London.
- WHITE, A.J.R. (b) (In preparation), Genesis of migmatites from the  
 Palmer Region of South Australia.
- WHITE, A.J.R. (a) (In preparation), Petrology and structure of the



## Rathjen Granitic Gneiss of South Australia.

- WHITE, A.J.R. et. al (In prep.), The Palmer Granite - a study of granite within a regional metamorphic environment.
- WILSON, A.F. (1947a), The Musgrave Ranges. Walkabout 14, 8 - 16.
- WILSON, A.F. (1947b), The charnockitic and associated rocks of north-western South Australia, pt. 1: the Musgrave Ranges - an introductory account. Trans. R. Soc. S. Aust. 71, 195 - 211.
- WILSON, A.F. (1948), The charnockitic and associated rocks of north-western South Australia, pt. 2: dolerites from the Musgrave and Everard Ranges. Trans. R. Soc. S. Aust. 72, 178-200.
- WILSON, A.F. (1950a), Some unusual alkali-feldspars in the Central Australian charnockitic rocks. Mineralog. Mag. 29, 215-224.
- WILSON, A.F. (1950b), Fluorescent feldspar and Zircon as petrological aids. Mineralog. Mag. 29, 225-233.
- WILSON, A.F. (1952), The charnockite problem in Australia. Sir D. Mawson Anniv. Vol. p. 203-224. Adelaide: University of Adelaide.
- WILSON, A.F. (1953), The significance of lineation in Central Australia. Aust. J. Sci. 16, 47 - 50.
- WILSON, A.F. (1954a), The significance of lineation in Central Australia - a reply. Aust. J. Sci. 16, 242 - 243.
- WILSON, A.F. (1954b), Studies on Australian charnockitic rocks and related problems: Vol. 2 - The charnockitic granulites and associated gneisses of the Musgrave Ranges, Central Australia. Vol. 3 - The charnockitic granites and associated granites of Central Australia. Unpublished D.Sc. Thesis, University of Western Australia.

- WILSON, A.F. (1955), Charnockitic rocks in Australia - a review. Proc. Pan-Ind. Ocean Sci. Congr. Perth, 1954, p. 10 - 17.
- WILSON, A.F. (1960a), The charnockitic granites and associated granites of Central Australia. Trans. R. Soc. S.Aust. 83, 36 - 76.
- WILSON, A.F. (1960b), Co-existing pyroxenes: some causes of variation and anomalies in the optically derived compositional tie-lines, with particular reference to charnockitic rocks. Geol. Mag. 97, 1 - 17.
- WINKLER, H.G.F. (1961), On coexisting feldspars and their temperature of crystallization. Curs. y. confs. Fasc. VIII, 9 - 13.
- YODER, H.S., STEWART, D.B. and SMITH, J.R. (1957), Ternary feldspars. Carnegie Inst. Wash. Yearbook, no. 56, 1956. p. 206-214.
- ZEN, E. (1963), Components, phases, and criteria of chemical equilibrium in rocks. Am. J. Sci. 261, 929-942.

APPENDIX I

List of mineralogical compositions of all rock samples from which the coexisting feldspars used in this investigation have been extracted.

A 1.

Quartz, plagioclase and K-feldspar occur in all samples and are therefore not included in the following lists. Abbreviations used below are: C = cordierite; Orp = orthopyroxene; Clp = clinopyroxene; G = garnet; B = biotite; M = muscovite; Sp = sphene; S = sillimanite; H = hornblende.

Accessory minerals including apatite, zircon, rutile, and Fe ores are not included; (r) denotes rare (generally 1 volume per cent).

---

MUSGRAVE RANGE AREA

Sample number<sup>\*</sup>

30829 Clp(r), Orp, B(r).  
 30726 Clp(r), Orp(r), H, B(r).  
 30674 Orp, H(r), B(r).  
 34611 G, S, B(r).  
 34504 Orp, B(r).  
 30652 Orp, H, B(r).  
 30577 H, B, Sp.  
 30573 H, B, Sp.  
 30575 H, B, Sp.

BROKEN HILL AREA

Sample number<sup>†</sup>

469 B.  
 466 B, G.  
 465 B, G.  
 462 B, G.  
 642 C, S, B(r), G.  
 18L G, S, B.  
 410 B.  
 447 G, B.

---

\* Specimen numbers refer to those housed in the Geology Department, University of Adelaide.

† Specimen numbers apply to the same specimens referred to by Bians (1964), with the exception of 18L which is a specimen collected by Mr. P. Slade, Geology Department, University of Adelaide.

---

CEYLON AREASample number\*

A152/79	Orp, B(r)
A152/630	G, B(r)
E23 518A	G, Orp, B(r)
A152/794	Orp, H
OL 584	Orp, G
SOL 166	B, H
SOL 164	H, B(r)
SOL 158	B
SOL 181	B, G

PEWSEY VALE AREASample number†

A200/124A	S, B, G
A200/887A	S, B
A200/670B	B, M
A200/27	B, M
A200/430	B, M
A200/871A	B, M
A200/561	B, M

---

\* Specimen numbers refer to samples from Ceylon collected by Dr. R. L. Oliver, Geology Department, University of Adelaide.

† Specimen numbers refer to those housed in the Geology Department, University of Adelaide.

---

SPRINGTON AREASample number\*

A221/57 B, M  
 A221/58 B, M(r)  
 A221/52 B  
 A221/54 B, M(r)  
 A221/48 B, M(r)  
 A185/706 H  
 A185/784 H

PALMER AREASample number

PR12<sup>†</sup> B  
 8308\* B  
 DVH2\* B, M  
 AJWH6<sup>†</sup> B, M  
 221/41\* B, M

REEDY CREEK AREASample number\*

A221/35 B, Sp  
 A221/104 B, M

\* Specimen numbers refer to those housed in the Geology Department,  
 University of Adelaide.

† Specimen numbers apply to the same specimens referred to by  
 A. J. R. White, (pers. comm.).

APPENDIX II

Comparison of Ca, Sr and Ba results from X-ray spectrographic, wet chemical and optical spectrographic techniques.

A. INTRODUCTION

Prior to obtaining X-ray spectrographic equipment in the writer's department the writer investigated the use of d.c. arc spectrographic techniques for the analysis of Ba, Sr and Ca in feldspar samples. This work was carried out at the Australian Mineral Development Laboratories, Adelaide under the supervision of Mr. A. B. Timms. Methods of analysis for the above mentioned elements, giving results of high relative accuracy and precision, had not been previously established in this laboratory and therefore considerable preliminary work was necessary in order that suitable calibration curves could be constructed. In this appendix, a brief description of the methods used is given and some results are compared with X-ray spectrographic analyses for Sr and Ba and wet chemical results for Ca.

B. EXPERIMENTAL TECHNIQUE

This work was carried out using a Baird 3 metre grating spectrograph: instrumental details can be obtained from the Australian Mineral Development Laboratories. Previously ground samples were diluted (50, 100 and 200 fold dilutions were used) with a flux containing equal weights ammonium sulphate and anhydrous ferric sulphate, the latter prepared from spec pure iron rods and A.R. concentrated acids. The mixing was carried out in glass phials ( $3/4$  inches in length x  $3/8$  inches diameter) containing 4 stainless steel balls (diameter  $1/16$ " in a Spex Mill for 5 - 7 minutes. From



this mix small pellets (3mm. diameter x 1mm. thickness) weighing approximately 12mgms. were made with the use of a special jig. These pellets were arced between Cu electrodes. Lines used were Ca 4425, Sr 4607, Ba 4554.03 with Fe 4321.8 as the internal standard line.

Standards used include G1, W1, NBS99 and numerous feldspar standards obtained from the Department of Geophysics and Geochemistry, Australian National University, and the Geology Department, University of Adelaide.

### C. RESULTS

Some results for Ba, Sr and Ca obtained from this technique are compared with X-ray spectrographic and wet chemical techniques in the following Table:

Sample number	CaO*		Sr**		Ba**	
	EDTA method	dc arc spect.	X-ray fluor.	dc arc spect.	X-ray fluor.	dc arc spect.
A221/35 P	5.78	6.11	830	1148	455	533
30829 P	5.43	5.59	136	118	159	67
34611 P	1.12	1.12	69	72	137	108
A221/104 P	3.71	3.02	327	311	469	525
A221/35 KF	0.17	0.32	659	717	2.2%	1.82%
30829 KF	0.49	0.52	243	216	2991	2500
34611 KF	0.31	0.35	476	398	4150	4300
A221/104 KF	0.13	0.28	355	248	6418	5016

\* These results are in weight percents.

\*\* These results except as indicated are p.p.m.

P and KF refers to plagioclase and K-feldspar respectively.

### D. DISCUSSION

On the assumption that the wet chemical and X-ray

spectrograph analyses are correct, it is evident that the optical spectrographic technique used by the writer yields results which are both significantly different and non systematic, in some cases. Generally the optical spectrographical technique used by the writer suffered from several disadvantages:

- (a) lack of reproducibility in the intensity measurements.
- (b) in order to remove matrix differences between the non feldspar and feldspar samples, it was found necessary to use comparatively large dilutions of the samples. For this reason some errors in mixing obviously contributed to (a) above.
- (c) the instrumental method involved use of a 3 step sector (ratio of the graded intensities were 1:1/2:1/4). Measurement of the intensity ratios necessitated establishing a calibration curve for each of the intensity steps. In some cases lack of standards of suitable intensity increased the uncertainty in the slope of the calibration curves.
- (d) some reliable standards deviated from the calibration line, for no accountable reason. Matrix effects were not thought to be the cause, in view of the comparatively large dilutions.

Discussion of these above disadvantages of this technique with Dr. K. Nerrish (C.S.I.R.O. Soils Division,

A 7.

Adelaide) and Dr. J. B. Jones (Geology Department, University of Adelaide) led the writer to use the more reliable X-ray fluorescent techniques of analyses, discussed in the text, Chapter IV.

APPENDIX III

Basic X-ray spectrographic equipment.

A. PHILIPS EQUIPMENT

X-ray generator PW1010

Power supply PW4029/01

Linear amplifier PW4072/01

Discriminator PW4082

High voltage supply for counters PW4025/10 (this replaced the H.V. and amplifier unit of the EKCO rate meter, type N624A).

Electronic counter PW4032

Electronic timer PW4062

Universal vacuum spectrograph PW1540

Proportional counter PW1965/10

Scintillation counter PW1964/10

B. EKCO ELECTRONICS LTD.

Ratemeter type N624A

APPENDIX IV

Instrumental conditions for analyses  
of feldspars by X-ray spectrography.

Element	Characteristic radiation	Target excitation	Analysing crystal	Vacuum	Window volts P.H.A.*	Entrance collimator	Counter**
Rb, Sr	K <sub>α</sub>	Mo 50kv 18ma	LiF	-	10 - 24	180μ spacing	Scintillation
Ba	La <sub>1</sub>	Cr 44kv 20ma	LiF	~5mm. Hg	10 - 24	160μ spacing	Proportional
Ca	K <sub>α</sub>	Mo 50kv 18ma	LiF	~5mm. Hg	10 - 24	160μ spacing	Proportional

\* Optimum window settings of 10-24 volts (based upon suitable Peak/Background ratios and maximum counting rates) were chosen for all elements investigated.

\*\* Using the above mentioned pulse height analyser settings and fixed amplification factors, the Dead-time for both the scintillation and proportional counters (and associated electronic circuitry) were determined. The most reliable method was one using foils of known attenuation factors which had been previously measured by Dr. K. Norrish (C.S.I.R.O. Soils Division, Adelaide). The Dead-time was accurately determined up to about 80,000 counts/sec for both counters. Although the Dead-time was found to differ slightly at both high and low counting rates, average values were chosen. These were:

Scintillation counter —  $5.31 \times 10^{-6}$  secs.

Proportional counter —  $4.91 \times 10^{-6}$  secs.

APPENDIX V

Measurement of mass-absorption coefficients  
using the Compton scattering technique.



A. INTRODUCTION

Reynolds (1963) discussed the theoretical considerations of this method. Briefly he proposed that the intensity of the Compton scattering associated with the incident Mo K-characteristic lines could be used in an empirical way to allow for matrix differences between samples (viz.  $A_2$  in equations (2) - (4), Chapter IV). Reynolds showed that a linear relationship existed between the reciprocal of the Compton scattering intensity and the calculated mass absorption coefficient of samples of pure compounds, mixtures of compounds, pure elements, and the standard rocks G1 and W1. The mass absorption coefficients were calculated from elemental mass absorption coefficients tabled in Liebhafsky et al. (1960).

This method was tested by the writer using samples of granites, norites, potassium and plagioclase feldspars of known bulk composition.

B. EXPERIMENTAL

The intensity of the Compton scattering peak was determined using the instrumental conditions given in Appendix IV for Rb and Sr analyses (pulse height analysis was not used, however). A fixed count method was employed and at least  $2 \times 10^5$  counts accumulated. Samples were prepared as discussed in Chapter IV p. 34. The mass absorption coefficients of the samples were calculated using elemental absorption data from the "International Tables for X-ray Crystallography".

Sample Number	Compton Intensity Avg. time for $4 \times 10^4$ cts.	Calculated A2 $\lambda = .700\text{\AA}$	Time Calculated A2	Measured A2* $\lambda = .709$	Time Measured A2
Sitting-Bull plagioclase	87.7	3.57	$2.46 \times 10$	3.58	$2.45 \times 10$
Boolcoomatta K-feldspar	117.4	4.50	$2.61 \times 10$	4.86	$2.42 \times 10$
Crystal Bay plagioclase	124.1	5.14	$2.41 \times 10$	5.11	$2.43 \times 10$
Mannum tonalite	130.7	5.00	$2.61 \times 10$	5.37	$2.43 \times 10$
Black Hill norite	172.4	6.90	$2.50 \times 10$	7.12	$2.42 \times 10$
G1	119.2	4.58	$2.62 \times 10$	-	

\* These measurements were made using equipment of the C.S.I.R.O. Soils Division, Adelaide.

Vol. III" at  $\lambda = .700\text{\AA}$ . The mass absorption coefficients were also measured at  $\lambda = .709\text{\AA}$  using the technique given in Chapter IV p. 37.

C. RESULTS

Compton scattering intensities and measured and calculated  $A_2$  values are given in the following Table, (see opposite page).

D. DISCUSSION

The constancy of the ratio  $\frac{\text{"Time"}}{A_2}$  in column 4 of the above table indicates that the Compton scattering intensity can be used as reliable measure of the mass absorption coefficient of silicate bearing powders, in a relative manner.

Data in column 6 indicates the improved reliability when the  $A_2$  values are measured (the relative deviation of data in columns 5 and 6 are 1.4 and .4 percents respectively).

The scatter of data using calculated  $A_2$  values results partly from errors in the bulk chemical analyses and also from errors in the elemental mass absorption coefficient data.

APPENDIX VI

Coexisting Feldspar compositions in terms of elemental concentrations (weight percent) and theoretical feldspar components (weight and molecular percents).

1(a) Musgrave Range area - K-feldsparsChemical analyses ( $K_2O$ ,  $Na_2O$ ,  $CaO$  in weight percent; Ba, Sr, Rb in p.p.m.)

Sample number	$K_2O$	$Na_2O$	$CaO$	Ba	Sr	Rb
30829	13.38	2.10	.49	2991	243	440
30726	12.68	2.68	.52	2705	244	495
30674	13.58	2.00	.39	3427	371	549
34611	13.15	2.16	.305	4153	476	609
34504	13.78	1.69	.33	4885	358	404
30652	14.00	1.86	.22	3608	295	546
30577	14.51	1.72	.14	4137	289	503
30575	13.38	2.16	.15	4464	324	594
30573	13.02	2.30	.27	4658	351	462

Calculated theoretical feldspar components (weight percent)

Sample number	Or	Ab	An	BaF	SrF	RbF	Total
30829	79.0718	17.7698	2.4301	.8176	.0903	.1672	100.3468
30726	74.9350	22.6776	2.5798	.7395	.0907	.1880	101.2106
30674	80.2537	16.9490	1.9348	.9368	.1379	.2086	100.4208
34611	77.7126	18.2521	1.5131	1.1353	.1769	.2313	99.0213
34504	81.4356	14.3004	1.6372	1.3354	.1331	.1535	98.9952
30652	82.7358	15.7389	1.0914	.9863	.1097	.2074	100.8695
30577	85.7497	14.5543	.6945	1.1309	.1074	.1906	102.4274
30575	79.0718	18.2775	.7445	1.2204	.1204	.2256	99.6601
30573	76.9266	19.4621	1.3395	1.2733	.1305	.1755	99.3075

Calculated theoretical feldspar components (molecular percent)

Sample number	Or	Ab	An	BaF	SrF	RbF
30829	78.1414	18.6394	2.4025	.5991	.0762	.1417
30726	73.1989	23.5126	2.5213	.5356	.0756	.1574
30674	79.3253	17.7819	1.9133	.6867	.1164	.1766
34611	77.8757	19.4130	1.5171	.8438	.1515	.1986
34504	81.8549	15.2572	1.6462	.9955	.1144	.1323
30652	81.4841	16.4530	1.0754	.7204	.0921	.1752
30577	83.2632	15.0002	.6746	.8143	.0892	.1586
30575	78.7429	19.3195	.7417	.9012	.1026	.1924
30573	76.8270	20.6307	1.3382	.9429	.1112	.1501

1(b) Musgrave Range area - PlagioclasesChemical analyses (K<sub>2</sub>O, Na<sub>2</sub>O, CaO in weight percent; Ba, Sr, Rb in p.p.m.)

Sample number	K <sub>2</sub> O	Na <sub>2</sub> O	CaO	Ba	Sr	Rb
30829	.29	5.94	5.43	159	136	-
30726	.44	5.78	3.85	158	141	11
30674	.47	6.06	5.09	179	218	7
34611	.14	1.47	1.12	137	69	-
34504	.43	5.59	5.10	310	174	8
30652	.24	5.21	4.18	119	136	-
30577	.92	6.90	4.73	342	260	28
30575	.81	7.08	4.56	324	269	28
30573	.53	5.02	3.22	238	228	-

Calculated theoretical feldspar components (weight percent)

Sample number	Or	Ab	An	BaF	SrF	RbF	Total
30829	1.7138	50.2631	26.9388	.0435	.0506	-	79.0098
30726	2.6003	48.8754	19.1002	.0432	.0525	.0042	70.6758
30674	2.7775	51.2700	25.2520	.0489	.0810	.0026	79.4320
34611	.8214	12.4135	5.5713	.0375	.0257	-	18.8694
34504	2.5412	47.3015	25.3016	.0847	.0647	.0032	75.3255
30652	1.4183	44.0859	20.7374	.0325	.0506	-	66.3247
30577	5.4546	58.3610	23.4660	.0935	.0967	.0106	87.4824
30575	4.7868	59.9095	22.6226	.0886	.1000	.0106	87.5181
30573	3.1380	42.4782	15.9747	.0651	.0848	-	61.7409

Calculated theoretical feldspar components (molecular percent)Corrected for 100 percent feldspar

Sample number	Or	Ab	An	BaF	SrF	RbF
30829	2.0877	64.9896	32.8310	.0391	.0525	-
30726	3.5295	70.4202	25.9392	.0435	.0609	.0048
30674	3.3638	65.9084	30.5974	.0439	.0838	.0026
34611	4.1864	67.1529	28.4080	.1419	.1116	-
34504	3.2492	64.1979	32.3672	.0802	.0708	.0035
30652	2.0546	67.7917	30.0567	.0348	.0623	-
30577	5.9914	68.0441	25.7880	.0760	.0907	.0099
30575	5.2504	69.7489	24.8252	.0719	.0938	.0099
30573	4.8781	70.0900	24.8446	.0748	.1125	-

2(a) Broken Hill area - K-feldsparsChemical analyses ( $K_2O$ ,  $Na_2O$ , CaO in weight percent; Ba, Sr, Rb in p.p.m.)

Sample number	$K_2O$	$Na_2O$	CaO	Ba	Sr	Rb
466	15.35	1.27	.08	5294	196	449
465	14.37	1.29	.10	6065	598	378
462	14.65	1.39	.13	6981	342	409
469	14.75	1.31	.18	1956	165	531
18L	15.14	1.07	.12	2015	173	735
642	13.60	1.48	.14	3880	435	403
410	14.76	1.60	.14	3874	242	349
447	14.38	1.24	.08	6065	421	391

Calculated theoretical feldspar components (weight percent)

Sample number	Or	Ab	An	BaF	SrF	RbF	Total
466	90.7139	10.7465	.3969	1.4472	.0729	.1706	103.5479
465	84.9224	10.9157	.4961	1.6579	.2238	.1447	98.3607
462	86.5771	11.7619	.6449	1.9084	.1271	.1554	101.1749
469	87.1681	11.0850	.8930	.5347	.0613	.2017	99.9438
18L	89.4800	9.0500	.6000	.5508	.0643	.2792	100.0243
642	80.3719	12.5235	.6946	1.0607	.1617	.1531	94.9654
410	87.2272	13.5389	.6946	1.0590	.0899	.1324	102.7420
447	84.9815	10.4926	.3969	1.6580	.1565	.1485	97.8340

Calculated theoretical feldspar components (molecular percent)

Sample number	Or	Ab	An	BaF	SrF	RbF
466	87.3942	10.9891	.3824	1.0335	.0601	.1408
465	86.1730	11.8571	.5036	1.2470	.1940	.1257
462	85.4131	12.3164	.6365	1.3956	.1071	.1313
469	86.7731	11.7126	.8892	.3946	.0521	.1784
18L	89.1393	9.5693	.5978	.4004	.0546	.2384
642	84.2342	13.9314	.7281	.8241	.1447	.1374
410	84.4666	13.9156	.6728	.7606	.0744	.1099
447	86.7104	11.3636	.4050	1.2548	.1363	.1299

2(b) Broken Hill area - PlagioclasesChemical analyses ( $K_2O$ ,  $Na_2O$ ,  $CaO$  in weight percent; Ba, Sr, Rb in p.p.m.)

Sample number	$K_2O$	$Na_2O$	CaO	Ba	Sr	Rb
466	.43	6.80	7.44	160	164	7
465	.47	7.11	6.38	158	478	5
462	.43	6.65	7.25	192	293	7
469	.23	3.11	1.61	91	67	8
18L	.41	.73	18.03	115	163	52
642	.25	7.74	4.15	122	257	7
410	.23	3.25	.91	142	87	-
447	.31	2.95	4.30	118	208	8

Calculated theoretical feldspar components (weight percent)

Sample number	Or	Ab	An	BaF	SrF	RbF	Total
466	2.5412	57.5402	36.9106	.0437	.0610	.0024	97.0991
465	2.7539	60.1633	31.6518	.0432	.1777	.0017	94.7917
462	2.5116	56.2710	35.9680	.0525	.1089	.0027	94.9146
469	1.3592	26.3162	7.9874	.0249	.0250	.0031	35.7159
18L	2.4200	6.1500	89.4500	.0314	.0606	.0197	98.1317
642	1.4774	38.3989	35.0742	.0333	.0955	.0026	75.0819
410	1.3592	27.5432	4.5146	.0388	.0325	-	33.4883
447	1.8320	24.9623	21.3327	.0323	.0773	.0028	48.2395

Calculated theoretical feldspar components (molecular percent)Corrected for 100 percent feldspar

Sample number	Or	Ab	An	BaF	SrF	RbF
466	2.5252	60.6921	36.6965	.0322	.0518	.0022
465	2.7968	64.8550	33.1604	.0324	.1541	.0013
462	2.5536	60.7245	36.5855	.0395	.0945	.0024
469	3.6390	74.7860	21.3953	.0492	.0572	.0073
18L	2.4561	6.6245	90.8254	.0236	.0521	.0172
642	1.8903	52.1416	44.8933	.0321	.1043	.0027
410	3.8365	82.2524	12.7494	.0812	.0784	-
447	3.6799	53.2204	42.8699	.0480	.1327	.0049



3(a) Ceylon area - K-feldsparsChemical analyses ( $K_2O$ ,  $Na_2O$ ,  $CaO$  in weight percent; Ba, Sr, Rb in p.p.m.)

Sample number	$K_2O$	$Na_2O$	$CaO$	Ba	Sr	Rb
A152/794	13.69	1.88	.21	7277	688	321
E23518A	13.50	1.89	.20	8678	1218	371
A152/79	13.00	2.14	.30	6433	1537	308
OL584	14.25	1.49	.16	6698	374	425
152/630	14.81	1.61	.22	3869	375	339
OL181	14.50	1.41	.17	2742	446	394
OL166	14.95	1.41	.14	1452	195	481
OL164	15.09	1.30	.11	3970	129	224
OL158	14.66	1.64	.11	418	120	438

Calculated theoretical feldspar components (weight percent)

Sample number	Or	Ab	An	BaF	SrF	RbF	Total
A152/794	80.9038	15.9082	1.0418	1.9893	.2558	.1219	100.2208
E23518A	79.7809	15.9928	.9922	2.3723	.4528	.1409	99.7320
A152/79	76.8261	18.1083	1.4834	1.7586	.5714	.1170	98.8648
OL584	84.2132	12.6081	.7938	1.8310	.1390	.1615	99.7466
152/630	87.5226	13.6066	1.0914	1.0577	.1394	.1288	103.5465
OL181	85.6906	11.9311	.8434	.7496	.1658	.1497	99.5302
OL166	88.3736	11.9311	.6945	.3969	.0725	.1827	101.6515
OL164	89.1715	11.0000	.5457	1.0853	.0479	.0851	101.9354
OL158	86.6362	13.8773	.5457	.1143	.0446	.1664	102.8820

Calculated theoretical feldspar components (molecular percent)

Sample number	Or	Ab	An	BaF	SrF	RbF
152/794	80.3983	16.7798	1.0356	1.4660	.2171	.1037
E23518A	79.7694	16.9727	.9924	1.7592	.3866	.1208
152/79	77.2721	19.3322	1.4927	1.3119	.4911	.1008
OL584	84.2096	13.3819	.7941	1.3580	.1189	.1383
152/630	84.0993	13.8776	1.0489	.7534	.1145	.1062
OL181	85.6703	12.6608	.8435	.5554	.1416	.1283
OL166	86.4328	12.3860	.6795	.2878	.0607	.1533
OL164	87.1558	11.4118	.5349	.7862	.0399	.0713
OL158	83.1252	14.1328	.5237	.0813	.0366	.1368

3(b) Ceylon area - PlagioclasesChemical analyses ( $K_2O$ ,  $Na_2O$ ,  $CaO$  in weight percent; Ba, Sr, Rb in p.p.m.)

Sample number	$K_2O$	$Na_2O$	$CaO$	Ba	Sr	Rb
A152/794	.55	5.36	4.45	275	340	7.5
E23518A	.48	5.25	4.28	306	659	9.5
A152/79	.22	4.65	3.23	100	605	-
OL584	.34	6.24	6.32	139	265	-
152/630	.24	3.00	2.05	96.5	101	-
OL181	.81	8.05	3.56	130	305	35
OL166	.22	4.29	2.24	71.2	71.2	-
OL164	.31	9.34	1.96	154	85	-
OL158	.31	8.90	1.98	54.2	75.7	-

Calculated theoretical feldspar components (weight percent)

Sample number	Or	Ab	An	BaF	SrF	RbF	Total
A152/794	3.2503	45.3553	22.0769	.0752	.1263	.0029	70.8868
E23518A	2.8130	44.4244	21.2335	.0836	.2450	.0036	68.8032
A152/79	1.3001	39.3474	16.0392	.0273	.2249	-	56.9389
OL584	2.0093	53.0555	31.3542	.0380	.0985	-	86.5548
152/630	1.4360	25.3854	10.1703	.0264	.0374	-	37.6299
OL181	4.7868	68.1175	17.6615	.0355	.1134	.0134	90.7281
OL166	1.3001	36.3011	11.1129	.0195	.0264	-	48.7599
OL164	1.8497	79.0332	9.7238	.04210	.0316	-	90.6804
OL158	1.8320	75.3439	9.8230	.0148	.0281	-	87.0418

Calculated theoretical feldspar components (molecular percent)Corrected for 100 percent feldspar

Sample number	Or	Ab	An	BaF	SrF	RbF
A152/794	4.4135	65.3697	29.9916	.0756	.1466	.0032
E23518A	3.9352	65.9630	29.7176	.0868	.2928	.0046
A152/79	2.1915	70.4012	27.0496	.0339	.3238	-
OL584	2.2372	62.7079	34.9299	.0314	.0936	-
152/630	3.7194	69.7919	26.3554	.0505	.0828	-
OL181	5.0443	76.1934	18.6207	.0277	.1019	.0119
OL166	2.5499	75.5718	21.8059	.0282	.0442	-
OL164	1.9369	87.8187	10.1863	.0326	.0283	-
OL158	1.9984	87.2427	10.7208	.0119	.0262	-

4(a) Pewsey Vale area - K-feldsparsChemical analyses (K<sub>2</sub>O, Na<sub>2</sub>O, CaO in weight percent; Ba, Sr, Rb in p.p.m.)

Sample number	K <sub>2</sub> O	Na <sub>2</sub> O	CaO	Ba	Sr	Rb
A200/423	14.48	1.13	.12	4760	376	321
A200/871A	15.75	.90	.05	6095	440	252
A200/561	15.02	1.14	.07	7697	524	287
A200/670B	15.05	.87	.05	11108	569	237
A200/27	15.05	1.12	.10	10417	520	247
A200/124A	13.84	1.47	.08	9705	454	199
A200/887A	15.09	.98	.05	3703	224	211

Calculated theoretical feldspar components (weight percent)

Sample number	Or	Ab	An	BaF	SrF	RbF	Total
A200/423	85.5724	9.5618	.6102	1.3012	.1398	.1219	97.3073
A200/871A	93.0778	7.6156	.2381	1.6662	.1636	.0957	102.8570
A200/561	88.7637	9.6465	.3572	2.1041	.1948	.1090	101.1753
A200/670B	88.9410	7.3448	.2481	3.0289	.2115	.0903	99.8647
A200/27	88.9410	9.4772	.4961	2.8477	.1933	.0938	102.0492
A200/124A	81.7607	12.4050	.3721	2.6531	.1689	.0756	97.4353
A200/887A	89.1774	8.3180	.2481	1.0123	.0833	.0802	98.9191

Calculated theoretical feldspar components (molecular percent)Corrected for 100 percent feldspar

Sample number	Or	Ab	An	BaF	SrF	RbF
A200/423	87.7483	10.4073	.6259	.9896	.1224	.1070
A200/871A	90.4931	7.8588	.2317	1.2013	.1359	.0798
A200/561	87.7286	10.1197	.3532	1.5422	.1645	.0924
A200/670B	89.3935	7.8354	.2496	2.2578	.1816	.0778
A200/27	87.3230	9.8763	.4873	2.0734	.1621	.0789
A200/124A	83.8784	13.5078	.3818	2.0186	.1479	.0665
A200/887A	89.9459	8.9049	.2502	.7572	.0716	.0693

4(b) Pewsey Vale area - PlagioclasesChemical analyses ( $K_2O$ ,  $Na_2O$ ,  $CaO$  in weight percent; Ba, Sr, Rb in p.p.m.)

Sample number	$K_2O$	$Na_2O$	$CaO$	Ba	Sr	Rb
A200/423	.22	7.59	2.47	138	315	-
A200/871A	.34	9.39	2.89	221	431	-
A200/561	.30	9.48	2.27	191	501	-
A200/670B	.26	9.21	3.01	200	624	-
A200/27	.32	6.93	1.86	221	421	-
A200/124A	.13	6.06	5.69	163	440	-
A200/887A	.46	9.51	2.13	165	254	7.4

Calculated theoretical feldspar components (weight percent)

Sample number	Or	Ab	An	BaF	SrF	RbF	Total
A200/423	1.3000	64.2251	12.2539	.0376	.1171	-	77.9337
A200/871A	2.0093	79.4563	14.3376	.0604	.1602	-	96.0238
A200/561	1.7611	80.2179	11.2617	.0522	.1863	-	93.4792
A200/670B	1.5365	77.9332	14.9329	.0600	.2320	-	94.6946
A200/27	1.8911	58.6403	9.2276	.0604	.1565	-	69.9759
A200/124A	.7683	51.2785	28.2287	.0446	.1635	-	80.4835
A200/887A	2.7185	80.4717	10.5820	.0450	.0944	.0028	93.9144

Calculated theoretical feldspar components (molecular percent)  
Corrected for 100 percent feldspar

Sample number	Or	Ab	An	BaF	SrF	RbF
A200/423	1.5882	83.2791	14.9767	.0340	.1222	-
A200/871A	1.9917	83.6078	14.2203	.0445	.1357	-
A200/561	1.8222	88.1330	11.6623	.0401	.1648	-
A200/670B	1.5450	83.1869	15.0238	.0448	.1993	-
A200/27	2.5713	84.6329	12.5529	.0609	.1819	-
A200/124A	.9747	65.0603	33.7585	.0394	.1671	-
A200/887A	2.7504	86.4207	10.7114	.0339	.0815	.0024

5(a) Springton area - K-feldsparChemical analyses ( $K_2O$ ,  $Na_2O$ ,  $CaO$  in weight percent; Ba, Sr, Rb in p.p.m.)

Sample number	$K_2O$	$Na_2O$	$CaO$	Ba	Sr	Rb
A221/52	15.60	.58	-	4441	216	265
A221/54	15.33	.98	-	4250	208	337
A221/58	15.13	.98	.10	7102	263	201
A221/57	15.32	1.04	.09	4357	338	191
A185/706	15.72	.72	.16	4374	570	524
A185/784	15.57	.88	.14	6069	496	416
A221/48	15.20	.99	.05	4377	195	130

Calculated theoretical feldspar components (weight percent)

Sample number	Or	Ab	An	BaF	SrF	RbF	Total
A221/52	92.1913	4.9332	-	1.2140	.0803	.1007	98.5196
A221/54	90.5957	8.2503	-	1.1618	.0774	.1278	100.2130
A221/58	89.4138	8.2926	.5110	1.9415	.0978	.0764	100.3329
A221/57	90.5366	8.8003	.4564	1.1911	.1257	.0726	101.1826
A185/706	92.9004	6.0925	.7938	1.1957	.2119	.1991	101.3934
A185/784	92.0140	7.4464	.6945	1.6591	.1840	.1573	102.1553
A221/48	89.8274	8.3687	.2580	1.1965	.0725	.0494	99.7725

Calculated theoretical feldspar components (molecular percent)Corrected for 100 percent feldspar

Sample number	Or	Ab	An	BaF	SrF	RbF
A221/52	93.6121	5.3170	-	.9143	.0695	.0876
A221/54	90.2440	8.7229	-	.8584	.0660	.1092
A221/58	89.1334	8.7741	.5094	1.4354	.0832	.0652
A221/57	89.2985	9.2129	.4503	.8711	.1060	.0612
A185/706	91.6187	6.3774	.7832	.8746	.1784	.1683
A185/784	89.9547	7.8784	.6792	1.2028	.1537	.1317
A221/48	89.8639	8.8863	.2581	.8877	.0621	.0423

5(b) Springton area - PlagioclasesChemical analyses ( $K_2O$ ,  $Na_2O$ ,  $CaO$  in weight percent; Ba, Sr, Rb in p.p.m.)

Sample number	$K_2O$	$Na_2O$	$CaO$	Ba	Sr	Rb
A221/52	.43	10.57	.83	170	222	8.8
A221/54	.63	10.92	.61	229	129	15.3
A221/58	.32	7.11	1.43	372	156	-
A221/57	.41	9.64	1.52	227	346	-
A185/706	.20	8.53	4.70	216	729	-
A185/784	.24	5.49	3.12	208	444	-
A221/48	.67	9.66	.62	259	131	-

Calculated theoretical feldspar components (weight percent)

Sample number	Or	Ab	An	BaF	SrF	RbF	Total
A221/52	2.5234	89.4412	4.1073	.0463	.0823	.0033	96.2040
A221/54	3.7408	92.4029	3.0312	.0626	.0479	.0051	99.2905
A221/58	1.8911	60.1634	7.0795	.1017	.0580	-	69.2937
A221/57	2.4230	81.5718	7.5409	.0621	.1286	-	91.7263
A185/706	1.1997	72.1792	23.3171	.0589	.2706	-	97.0255
A185/784	1.4124	46.4553	15.4786	.0568	.1669	-	63.5700
A221/48	3.9550	81.7410	3.0759	.0709	.0487	-	88.8914

Calculated theoretical feldspar components (molecular percent)Corrected for 100 percent feldspar

Sample number	Or	Ab	An	BaF	SrF	RbF
A221/52	2.5376	95.5044	4.1337	.0345	.0708	.0027
A221/54	3.5645	93.4584	2.8898	.0442	.0390	.0042
A221/58	2.5918	87.5289	9.7082	.1034	.0679	-
A221/57	2.5055	89.5321	7.8012	.0475	.1135	-
A185/706	1.1829	75.5438	23.0022	.0431	.2280	-
A185/784	2.1273	74.2699	23.3248	.0634	.2148	-
A221/48	4.2123	92.4100	3.2775	.0559	.0443	-

6(a) Palmer Area - K-feldspars.Chemical analyses ( $K_2O$ ,  $Na_2O$ ,  $CaO$  in weight percent; Ba, Sr, Rb in p.p.m.)

Sample number	$K_2O$	$Na_2O$	$CaO$	Ba	Sr	Rb
A221/41	15.00	1.01	.03	9940	515	256
AU8308	15.42	1.06	.07	4080	195	nd
AJWH6	14.86	.80	.07	7462	524	224
PR12	15.43	1.04	.06	3690	176	376
DVH2	15.06	.86	.10	4907	267	292

Calculated theoretical feldspar components (weight percent)

Sample number	Or	Ab	An	BaF	SrF	RbF	Total
A221/41	88.6455	8.5464	.1240	2.7172	.1915	.0973	100.3218
AU8308	91.1276	8.9695	.3473	1.1154	.0725	-	101.6322
AJWH6	87.8181	6.7694	.3622	2.0399	.1948	.0851	97.2695
PR12	91.1867	8.8003	.2877	1.0087	.0654	.1428	101.4917
DVH2	88.9764	7.2772	.4713	1.3414	.0993	.1109	99.1698

Calculated theoretical feldspar components (molecular percent)Corrected for 100 percent feldspar

Sample number	Or	Ab	An	BaF	SrF	RbF
A221/41	88.3260	9.0386	.1236	2.0132	.1630	.0832
AU8308	89.4424	9.3443	.3410	.8119	.0609	-
AJWH6	90.4251	7.3986	.3732	1.5577	.1714	.0751
PR12	89.6259	9.1810	.2829	.7354	.0550	.1204
DVH2	89.7761	7.7934	.4758	1.0038	.0855	.0961

6(b) Palmer area - PlagioclasesChemical analyses ( $K_2O$ ,  $Na_2O$ ,  $CaO$  in weight percent; Ba, Sr, Rb in p.p.m.)

Sample number	$K_2O$	$Na_2O$	$CaO$	Ba	Sr	Rb
A221/41	.46	8.03	1.81	529	548	8.7
AU8308	.26	7.94	3.37	133	218	-
AJWH6	.66	9.55	1.90	314	634	23
PR12	.44	6.74	2.64	192	169	10.6
DVH2	.45	9.50	2.68	238	295	-

Calculated theoretical feldspar components (weight percent)

Sample number	Or	Ab	An	BaF	SrF	RbF	Total
A221/41	2.7185	67.9483	8.9796	.1446	.2037	.0033	79.9979
AU8308	1.5600	67.1700	16.7200	.0364	.0809	-	85.5673
AJWH6	3.9004	80.8102	9.4261	.0858	.2357	.0087	94.4669
PR12	2.6003	57.0325	13.1221	.0524	.0628	.0040	72.8741
DVH2	2.6594	80.3871	13.4126	.0651	.1097	-	96.6338

Calculated theoretical feldspar components (molecular percent)Corrected for 100 percent feldspar

Sample number	Or	Ab	An	BaF	SrF	RbF
A221/41	3.2312	85.7231	10.6778	.1276	.2070	.0034
AU8308	1.7395	79.5007	18.6527	.0300	.0770	-
AJWH6	3.9252	86.3112	9.4895	.0640	.2027	.0074
PR12	3.4052	79.2770	17.1924	.0507	.0703	.0045
DVH2	2.6189	84.0270	13.2145	.0475	.0922	-



7(a) Reedy Creek area - K-feldsparsChemical analyses (K<sub>2</sub>O, Na<sub>2</sub>O, CaO in weight percent; Ba, Sr, Rb in p.p.m.)

Sample number	K <sub>2</sub> O	Na <sub>2</sub> O	CaO	Ba	Sr	Rb
A221/104	14.32	1.80	.13	6418	355	235
A221/35	13.91	1.73	.17	2.20	659	166

Calculated theoretical feldspar components (weight percent)

Sample number	Or	Ab	An	BaF	SrF	RbF	Total
A221/104	84.6269	15.1889	.6449	1.7545	.1319	.0892	102.5308
A221/35	82.2039	14.6389	.8235	6.0141	.2449	.0631	103.9884

Calculated theoretical feldspar components (molecular percent)Corrected for 100 percent feldspar

Sample number	Or	Ab	An	BaF	SrF	RbF
A221/104	82.2543	15.6697	.6271	1.2648	.1096	.0744
A221/35	79.5860	15.0432	.7977	4.3182	.2027	.0523

7(b) Reedy Creek area - PlagioclasesChemical analyses (K<sub>2</sub>O, Na<sub>2</sub>O, CaO in weight percent; Ba, Sr, Rb in p.p.m.)

Sample number	K <sub>2</sub> O	Na <sub>2</sub> O	CaO	Ba	Sr	Rb
A221/104	.78	8.29	3.71	469	327	-
A221/35	.40	8.05	5.78	455	830	-

Calculated theoretical feldspar components (weight percent)

Sample number	Or	Na <sub>2</sub> O	CaO	Ba	Sr	Rb	Total
A221/104	4.6096	70.1483	18.4057	.1282	.1216	-	93.4133
A221/35	2.3697	68.1174	28.6752	.1244	.3086	-	99.5953

Calculated theoretical feldspar components (molecular percent)Corrected for 100 percent feldspar

Sample number	Or	Na <sub>2</sub> O	CaO	Ba	Sr	Rb
A221/104	4.7189	76.2258	18.8517	.0974	.1062	-
A221/35	4.2847	69.7113	27.6586	.0890	.2542	-

APPENDIX VII

Mass - absorption coefficient measurements of K-feldspars and Plagioclases

K-feldspars			Plagioclases	
Sample number	$\lambda = .875$	$\lambda = 2.75$	$\lambda = .875$	$\lambda = 2.75$
30829	9.26	229.60	7.67	197.29
30726	9.04	226.54	7.29	189.83
30674	9.29	228.71	7.54	194.21
34611	9.46	227.79	6.94	183.64
34504	9.37	230.85	7.57	188.13
30652	9.42	231.21	7.42	191.55
30577	9.44	233.48	7.64	194.77
30573	9.32	227.13	7.45	189.93
30575	9.32	228.26	7.64	194.35
469	9.41	234.03	7.03	184.36
466	9.47	237.33	7.83	202.55
465	9.70	232.30	7.64	198.32
462	9.59	234.02	8.05	201.91
642	9.41	228.65	7.91	206.08
18L	9.61	235.51	9.84	240.02
410	9.45	234.90	6.88	182.33
447	9.59	231.92	7.45	194.56
A152/79	9.45	227.50	7.26	189.18
A152/630	9.47	239.32	7.10	185.92
B23518A	9.60	231.62	7.67	193.25
A152/794	9.60	230.53	7.71	193.68
OL584	9.58	232.13	7.82	198.96
OL166	9.34	233.90	7.02	185.49
OL164	9.53	235.86	7.04	179.91
OL158	9.30	233.02	6.83	180.01
OL181	9.39	232.49	7.23	186.85
A200/124A	9.59	230.89	7.52	188.91
A200/887A	9.50	235.32	6.99	181.03
A200/670B	9.83	236.75	7.04	183.98
A200/27	9.93	237.02	6.97	181.69

K-feldspars			Plagioclases	
Sample number	$\lambda = .875$	$\lambda = 2.75$	$\lambda = .875$	$\lambda = 2.75$
A200/423	9.54	232.35	6.92	184.72
A200/871A	9.45	239.10	7.03	182.61
A200/561	9.82	236.74	6.93	181.57
A201/57	9.88	235.78	6.82	179.49
A221/58	9.72	235.50	6.85	178.35
A221/52	9.75	237.50	6.69	172.19
A221/54	9.64	236.39	6.65	169.72
A221/48	9.35	236.03	6.77	177.81
A185/706	9.76	238.96	7.50	191.13
A185/784	9.79	237.88	7.71	188.27
PR12	9.81	237.08	7.13	185.57
AU8308	9.63	-	7.16	-
DVH2	9.77	235.54	7.06	182.71
AJWH6	9.77	235.01	7.08	181.96
A221/41	9.82	236.18	6.90	180.04
A221/35	10.27	234.88	7.67	195.93
A221/104	9.48	233.08	7.23	187.69

### APPENDIX VIII

Coexisting feldspar compositions recalculated, from data given in Appendix VI, in terms of Or and Ab end-members for the K-feldspar, and Ab and An end-members for the Plagioclase: calculated distribution coefficients ( $K_{Ab} = \frac{\text{Mol percent Ab in K-feldspar}}{\text{Mol percent Ab in Plagioclase}}$ ) and deduced temperatures of equilibrium crystallization from the "Barth geothermometer" are given.

Table 21. Broken Hill area, New South Wales.

Sample number	Granulite Facies						Almandine - Amphibolite Facies	
	462	466	469	465	18L	642	410	447
<u>K-feldspar</u>								
Mol percent Ab	12.60	11.17	11.89	12.01	9.69	14.20	14.14	11.59
Mol percent Or	87.40	88.83	88.11	87.99	90.31	85.80	85.86	88.41
<u>Plagioclase</u>								
Mol percent Ab	62.40	62.32	77.76	66.85	6.78	53.73	86.58	55.39
Mol percent An	37.60	37.68	22.24	33.15	93.22	46.27	13.42	44.61
Distribution coefficient $K_{d_{Ab}}$	.202	.179	.153	.179	1.426	.264	.163	.209
Temperature °C	480	450	430	450	-	540	444	488

Table 22. Musgrave Range area, South Australia.

Sample number	Granulite Facies						Almandine- Amphibolite Facies		
	30726	34611	30652	30674	30829	34504	30575	30577	30573
<u>K-feldspar</u>									
Mol percent Ab	23.30	19.96	16.80	18.31	19.26	15.71	19.70	21.17	15.27
Mol percent Or	76.70	80.04	83.20	81.69	80.74	84.29	80.20	78.83	84.63
<u>Plagioclase</u>									
Mol percent Ab	73.08	70.27	69.28	68.30	66.44	66.48	73.75	73.83	72.52
Mol percent An	26.92	29.73	30.72	31.70	34.56	33.52	26.25	26.17	27.48
Distribution coefficient $K_{d_{Ab}}$	.333	.284	.242	.268	.289	.236	.267	.287	.210
Temperature °C	599	554	514	539	559	510	538	557	486



Table 23. Ceylon area.

Sample number	Granulite Facies					Almandine-Amphibolite Facies			
	A152/630	E23518A	A152/79	A152/794	OL584	SOL166	SOL164	SOL158	SOL181
<u>K-feldspar</u>									
Mol percent Ab	14.16	17.54	20.01	17.27	13.71	12.53	11.58	14.53	12.88
Mol percent Or	85.84	82.46	79.99	82.73	86.29	87.47	88.42	85.47	87.12
<u>Plagioclase</u>									
Mol percent Ab	72.59	68.94	72.24	68.55	64.23	77.61	89.61	89.06	80.36
Mol percent An	27.41	31.06	27.76	31.45	35.78	23.39	10.39	10.94	19.63
Distribution coefficient $K_{d_{Ab}}$	.195	.254	.277	.252	.214	.161	.129	.163	.160
Temperature °C	472	526	547	526	490	440	400	443	440

Table 24. Adirondack Lowlands area, New York (Engel and Engel, 1960).

	Almandine - Amphibolite Facies										
	Granulite Facies		Sillimanite-Almandine-K-feldspar sub facies			Sillimanite-Almandine Muscovite sub facies					
Sample number	Bgn18	Bgn21	Qb100	Qb100G1	Qb100G2	Bgn26	Bgn27	Qb228	Qb236	Qb236G1	Qb236G2
<u>K-feldspar</u>											
Mol percent Ab	22.3	20.5	15.3	20.6	18.4	8.9	19.3	19.0	16.6	19.3	16.6
Mol percent Or	77.7	79.5	84.7	79.4	81.6	91.1	80.7	81.0	81.6	80.7	83.4
<u>Plagioclase</u>											
Mol percent Ab*	64	65	68	70	70	68	75	71	73	75	77
Distribution coefficient $K_{d_{Ab}}$	.348	.315	.225	.294	.263	.13	.257	.267	.227	.257	.215
Temperature °C	610	590	500	560	540	400	540	550	530	540	490

\* Plagioclase composition determined using refractive index techniques.

Table 25. Langøy area, Northern Norway.

	Granulite Facies				Retrograde gneisses Granulite to Almandine-Amphibolite Facies.		Rocks transitional between Granulite Facies and Almandine-Amphibolite Facies.			Upper Almandine- Amphibolite Facies.					Lower Almandine- Amphibolite Facies.				
	Group III		Group V		Group IV		Group VII		Group VIII					Group IX					
	Sample number	251/55	255/55	293/55	271/55	348/55	an12	224/55	238/55	318/55	150/56	25/55	an1	37/55	35/55	3/56	147/56	E(vatn)	99/56
<u>K-feldspar</u>																			
Mol percent Ab	21.9	20.5	22.4	26.0	16.8	15.8	19.1	24.1	27.2	20.7	18.3	9.7	13.8	15.0	16.1	11.9	9.6	16.5	9.0
Mol percent Or	78.1	79.5	77.6	74.0	83.2	84.2	80.9	75.9	72.8	79.3	81.7	90.3	86.2	85.0	83.9	88.1	90.4	83.5	91.0
<u>Plagioclase</u>																			
Mol percent Ab*	70	70	70	70	72	70	68	70	77	72	69	75	74	80	72	72	100	67	70
Distribution coefficient $K_{d,Ab}$	.313	.293	.320	.371	.233	.226	.281	.344	.353	.288	.265	.129	.186	.188	.224	.165	.09	.246	.129
Temperature °C	585	570	590	625	515	510	560	605	610	565	545	400	465	470	505	440	300	525	400

\* Plagioclase composition determined using refractive index techniques.

Table 26. Kanmantoo Group, Mt. Lofty Ranges South Australia - Pewsey Vale area.

	Almandine - Amphibolite Facies						
	Sillimanite-Almandine K-feldspar sub facies		Sillimanite-Almandine Muscovite sub facies				
	A200/124A	A200/887	A200/423	A200/871A	A200/561	A200/670B	A200/27
<u>Sample number</u>							
<u>K-feldspar</u>							
Mol percent Ab	13.12	9.01	10.60	7.99	10.34	10.16	8.06
Mol percent Or	86.49	90.98	89.40	92.01	98.66	89.84	91.94
<u>Plagioclase</u>							
Mol percent Ab	65.84	88.97	84.76	85.46	88.31	87.08	84.70
Mol percent An	34.16	11.03	15.24	14.54	11.69	12.92	15.30
Distribution coefficient $Kd_{Ab}$	.199	.101	.125	.094	.117	.117	.095
Temperature °C	475	360	390	<360	383	383	<360

Table 27. Kanmantoo Group, Mt. Lofty Ranges South Australia - Springton area.

	Almandine - Amphibolite Facies						
	Upper Sillimanite-Almandine Muscovite sub facies					Lower Sillimanite Almandine Muscovite subfacies	
Sample number	A221/57	A221/58	A221/52	A221/54	A221/48	A185/706	A185/784
<u>K-feldspar</u>							
Mol percent Ab	8.96	9.35	5.37	8.81	8.99	7.91	6.51
Mol percent Or	91.04	90.65	94.63	91.19	91.00	92.09	93.49
<u>Plagioclase</u>							
Mol percent Ab	90.02	91.99	95.85	97.00	96.56	76.10	76.66
Mol percent An	9.98	8.01	4.15	3.00	3.43	23.90	23.34
Distribution coefficient $K_{d_{Ab}}$	.099	.102	.056	.091	.093	.104	.085
Temperature °C	<360	362	<360	<360	<360	363	<360

A 34.

Table 28. Kanmantoo Group, Mt. Lofty Ranges, South Australia - Palmer area.

	Almandine - Amphibolite Facies				
	Upper Sillimanite-Almandine Muscovite sub facies			Lower Sillimanite Almandine Muscovite subfacies	
Sample number	PR12	AU8308	DVH2	AJWH6	A221/41
<u>K-feldspar</u>					
Mol percent Ab	9.29	9.45	7.99	10.63	9.26
Mol percent Or	90.71	90.55	92.01	89.37	90.74
<u>Plagioclase</u>					
Mol percent Ab	82.18	80.06	86.41	90.09	88.92
Mol percent An	17.82	19.94	13.59	9.90	11.08
Distribution coefficient $Kd_{Ab}$	.113	.118	.092	.118	.104
Temperature °C	375	380	<360	380	362

Table 29. Kanmantoo Group, Mt. Lofty Ranges, South Australia - Reedy Creek area.

<u>Sample number</u>	Upper Almandine Amphibolite Facies	
	A221/104	A221/35
<u>K-feldspar</u>		
Mol percent Ab	16.00	15.9000
Mol percent Or	83.99	84.10
<u>Plagioclase</u>		
Mol percent Ab	80.17	71.59
Mol percent An	19.83	28.41
Distribution coefficient $K_{d_{Ab}}$	.1999	.222
Temperature °C	478	500